Humboldt-Universität zu Berlin – Geographisches Institut

Understanding land use and land cover change in Inner Mongolia using remote sensing time series

DISSERTATION

Zur Erlangung des akademischen Grades
doctor rerum naturalium
(Dr. rer. nat.)

Im Fach Geographie

eingereicht an der
Mathematisch-Naturwissenschaftlichen Fakultät II
der Humboldt-Universität zu Berlin
von

M.Sc. He Yin

Präsident der Humboldt-Universität zu Berlin
Prof. Dr. Jan-Hendrik Olbertz
Dekan der Mathematisch-Naturwissenschaftlichen Fakultät II
Prof. Dr. Elmar Kulke

Gutachter:
Prof. Dr. Patrick Hostert
Prof. Dr. Thomas Udelhoven
Prof. Dr. Tobias Kümmerle

Eingereicht: 06. Juni 2014
Tag der Verteidigung: 05. September 2014

Abstract

Monitoring land use and land cover change (LULCC) support better interpretation about how land surfaces are impacted by human decisions. The overall aim of this thesis is to gain a better understanding about LULCC in Inner Mongolia using remote sensing under consideration of China's land use policies. With the largest scale land restoration programs in the world, China aims to reduce human pressure on lands and promote sustainable land use. As a hot-spot of environmental change, Inner Mongolia received the heaviest investment from the central government for land restoration. Yet the effectiveness and consequences of China's land use policies in Inner Mongolia remain unclear. Remote sensing is an effective tool for monitoring land use and land cover change across broad scales, yet data limitations and a lack of available change detection methods hampers the capacity of researchers to apply remote sensing techniques for LULCC monitoring. To reliably map LULCC in Inner Mongolia, the opportunities and limitations of using coarse resolution imagery time series for monitoring long-term land changes was first examined. Second, an approach detecting annual changes between multiple land categories was developed and applied in Inner Mongolia. Results indicate that China's land use policies effectively preserved and recovered forest ecosystems in Inner Mongolia after the year 2000. The decreasing trends of deforestation and forest gain are obvious in the regions that implement China's land use policies, which reflect the positive influence of the policy. Cropland retirement was mostly found in ecologically fragile areas where climate and topographic conditions are unsuitable for cultivation, suggesting that China's land use policies support local farmers who use their vulnerable lands in a more adaptive way. Strong political influences were reflected by the drastic change in forest re-generation and cropland retirement in 2004, when the land restoration program was largely reduced due to worries about food security. This thesis reveals how political factors and other underlying social-economic drivers impact a country's land surface, and highlights the values of using coarse resolution imagery and time series analysis for LULCC monitoring across large areas.

Zusammenfassung

Das Monitoring des Landnutzungswandels trägt dazu bei, die Auswirkungen des menschlichen Handelns auf die Landoberflächen besser zu verstehen. Ziel dieser Dissertation war es, mittels Fernerkundung ein besseres Verständnis der Folgen des Landnutzungswandels in der Inneren Mongolei unter der Berücksichtigung der Landnutzungspolitik Chinas zu erlangen. Mittels umweltpolitischer Programme von weltweit einzigartigem Ausmaß versucht China sowohl den menschlichen Druck auf die Landbedeckung zu mindern als auch eine nachhaltige Landnutzung zu fördern. Als Hotspot globaler Umweltveränderungen wurden insbesondere für die Innere Mongolei erhebliche Investitionen zur Renaturierung von Landoberflächen von der chinesischen Zentralregierung getätigt. Die Wirksamkeit und Auswirkungen dieser Landnutzungspolitik Chinas innerhalb der Inneren Mongolei sind jedoch unklar. Die Fernerkundung ist ein effektiver Ansatz für ein flächendeckendes Monitoring des Landnutzungswandels. Jedoch erschweren die limitierte Datenverfügbarkeit und das Fehlen verfügbarer Veränderungsanalysemethoden die Anwendung fernerkundlicher Techniken zum Monitoring von Landnutzung und ihrer Veränderungen. Um den Landnutzungswandel in der Inneren Mongolei verlässlich zu kartieren, wurden daher in einem ersten Schritt Möglichkeiten und Grenzen von Zeitreihen räumlich grob aufgelöster Fernerkundungsdaten für das Monitoring von Langzeitveränderungen der Landbedeckung untersucht. Im zweiten Schritt wurde ein Ansatz zur Erfassung von jährlichen Veränderungen zwischen mehreren Landnutzungsklassen entwickelt und angewandt. Die Ergebnisse zeigen, dass die chinesische Landnutzungspolitik seit dem Jahr 2000 wirksam zum Erhalt und zur Regenerierung von Waldökosystemen in der Inneren Mongolei beiträgt. Abnehmende Entwaldung und ein Zuwachs von Waldflächen sind insbesondere in jenen Regionen zu finden, in welchen die landnutzungspolitischen Maßnahmen umgesetzt wurden. Dies bestätigt den positiven Einfluss politischen Handelns. Die Konvertierung von Ackerland zu Grasland wurde zumeist innerhalb anfälliger, klimatisch und topographisch ungeeigneter Gebiete beobachtet. Dies deutet auf die Wirksamkeit der chinesischen Landnutzungspolitik bei der Unterstützung von lokalen Bauern hin, welche Anpassungsstrategien für ihre anfälligen Landflächen entwickelt haben. Der starke Einfluss der Politik spiegelt sich im Jahre 2004 in den drastischen Veränderungen der Waldregenerierung und Ackerlandkonvertierung wider. Diese sind auf Kürzungen der umweltpolitischen Programme zurückzuführen, welche aufgrund von Sorgen bezüglich der Nahrungsmittelverfügbarkeit beschlossen wurden. Die vorliegende Dissertation veranschaulicht sowohl den Einfluss politischer Maßnahmen und zugrunde liegender sozio-ökonomischer Treiber auf die Landoberfläche als auch die Bedeutung von grob aufgelösten Fernerkundungsdaten und Zeitreihenanalysen für das Monitoring des Landnutzungswandels in großräumigen Gebieten.

Contents

List of Figures

List of Tables

Chapter I:
Introduction

1 Global environmental change and land system

Humans are currently influencing the global environmental system in unprecedented ways (MEA 2005b). During the early stages of human civilization, the Earth was altered through hunting and fishing, fiber and other material extraction, as well as land clearing for farming and housing to meet human's demand for food, medicine, clothing and shelter (Ruddiman 2003; Ellis et al. 2013). Since the industrial revolution, however, human impact on the environment has profoundly accelerated (Jelinski et al. 1992; Vitousek et al. 1997). To address the spatial extent and temporal changes of the human influences on the Earth, the term *Anthropocene* was established to describe the new geological era (Crutzen 2002; Zalasiewicz et al. 2011). Since the 18th century, Earth's population has increased 10-fold, from 600 million people to currently 6.9 billion (US Census Bureau 2014). Most of this increase occurred in the 20th century, largely due to advances in food production and distribution, and improvements in public health and medical technology (UN 2013). With this population increase and accompanying technological innovation, the environment has been fundamentally transformed at both local and global scales (Tilman and Lehman 2001; Vörösmarty et al. 2004; Cardinale et al. 2012).

As the core component of the biosphere, the land surface has experienced the longest and most extensive changes by humans (Steffen 2005; Ramankutty et al. 2006). Characterized by the arrangements, activities and inputs people undertake in a certain land type, land use reflects the purpose for which humans exploit land cover (Di Gregorio and Jansen 1998; Lambin et al. 2004). Throughout the emergence and development of human civilization, the use of land provides material support and was in turn reshaped by humans. While land was already significantly used in Asia and Europe by 3000 B.C., and in most other regions by A.D. 1000 (Ellis et al. 2013), only during the last three centuries have changes in land (i.e., changes in land use and land cover) rapidly sped up globally (Goldewijk 2001; Ramankutty et al. 2006). The most significant land change is rapid agricultural expansion, which has come at the expense of natural habitats such as forest, grassland and wetland, and has been driven by the increasing demand for resources (Ramankutty and Foley 1999). Indeed, the total area of cultivated land worldwide increased by 466% from 1700 to 1980 (Meyer and Turner 1992; Matson et al. 1997).

As fertile and cultivatable land is becoming scarcer, land-based production has to rely on increases of output per unit area rather than on the expansion of land use (Lambin and Meyfroidt 2011; Erb et al. 2013; Kuemmerle et al. 2013). Land use intensification (i.e.,

using high-yielding species, irrigation, fertilization, mechanization and labor input to increase land output), for example, has substantially contributed to the tremendous improvements in food production since the 1960s (Matson et al. 1997; Foley et al. 2011). To address the complexity of land use and land cover change (LULCC), two forms of the changes are conceptualized: land conversion and land modification (Meyer and Turner 1992; Turner et al. 1994; Lambin et al. 2003). Land conversion refers to the changes between different land categories, exemplified by cropland encroachment at the expense of forests or grasslands. Land modification is a more subtle change that occurs within the same land category without changing the overall land attribute, such as higher levels of inputs and increased output of cropland per unit area and time (Lambin et al. 2003).

LULCC has both beneficial and unfavorable impacts to human society and the Earth's environment. Indeed, land use underpinned ecosystems' ability to sustain human population and thus promotes the evolution of civilization. However, land change at the expense of natural ecosystems is often linked to a high environmental cost and in turn can affect human well-being. In the mid-1970s, the scientific community became aware of regional climate change due to the alteration of energy-water budge caused by land cover change (Otterman 1974; Charney et al. 1975). Deforestation, for instance, has been widely recognized as a mechanism that releases CO_2 into the atmosphere and reduces carbon storage in trees and soils (Woodwell et al. 1983; DeFries et al. 2002). Roughly 35% of the anthropogenic emission of CO_2 equivalents since 1850 can be directly traced to the totality of land cover change (Foley et al. 2005; Turner et al. 2007). The impacts of land use on the biotic environment are also visible and pervasive. Habitat loss and fragmentation, especially caused by agricultural expansion, have greatly degraded biological diversity from regional to global scales (Harding et al. 1998; Sala et al. 2000). The negative environmental consequences that land use causes become clear when considering regions with fragile ecological settings, such as arid and semi-arid areas (Reynolds and Stafford Smith 2002). The limited water resource and interannual variability in precipitation makes drylands particularly vulnerable to human exploitation. It has been estimated that 10-20% of the Earth's drylands are already degraded, and 250 million people in the developing world are directly affected (MEA 2005a).

Confronting the challenges outlined above, trade-offs have to be considered to meet the increasing demand for food and to maintain the structure and function of ecosystems in the future (DeFries et al. 2004b; Foley et al. 2005). Under the umbrella of "sustainable development" (WCED 1987), sustainable land use has been identified as an important

objective to address the challenges of the 21st century (UN 1996). Land use policy, in this sense, is an important tool for regulating land management and thus land use and land cover change (Reid et al. 2006). Aiming for reconciling human requirements and environmental protection, land use policies are often designed to preserve ecologically valuable landscapes, promote sustainable land use practices and restore degraded ecosystems (Zhang et al. 2000; Chazdon 2008). Establishing nature reserves, for example, is one of the typical approaches to ecosystem conservation through national and sometimes cross-border political interventions. Recently, land use policies that primarily target environmental issues have become more prevalent in developing countries with fast-growing economies because they often face severe environmental deterioration. One of the most prominent examples is China, which implemented a series of policies for fostering sustainable land use in the early 2000s to address the devastating environmental crises that the country was and is facing (Liu et al. 2008).

In this context, monitoring LULCC is crucial for policy making. Spatially explicit, timely information on land use and land cover change is a prerequisite for interpreting ecosystem status (Foster et al. 2003; Mustard et al. 2004). Information about land conversion and land modification provides valuable references to policy makers for defining their objectives. While policy makers need land use change information to address, for instance, pressing policy issues, policy can also cause changes in land use (Reid et al. 2006). Indeed, land use change information is often used as one of the most important indicators for assessing the effectiveness of current land use policy (Ellis and Porter-Bolland 2008; Sieber et al. 2013). Therefore, land use and land cover change information are needed and should be conveyed to policy makers for them to understand the impacts of the current policy and to create more effective ones (Goetz et al. 2004; Reid et al. 2006).

Driven by multiple factors across various spatial and temporal scales (Lambin et al. 2001), the temporal pathway of land change is often complex. Evidence has shown that land change is not always progressive and gradual. Rather, abrupt social or economic factors such as institutional changes, conflicts or land use policies can introduce non-linear change (Lambin and Meyfroidt 2010; Hostert et al. 2011). Such “shocks” may trigger the change of land use decisions in a short period and influence land use patterns in the long-run. On the other hand, the drastic influence of a “shock” on land system, however, can only be addressed by continuous monitoring in space and time (Lambin and Linderman 2006). Unfortunately, until now we still cannot fully understand how and when land system responds to “shocks” or other drivers (Ramankutty et al. 2006).

In summary, we are witnessing unprecedented changes on Earth, and these processes have radically accelerated over the past 50 years, largely driven by the social-economic development of human society. Land surface, as the core component of the biosphere, was extraordinarily altered by humans through land conversion and land modification. The overuse of land resources, together with other human activities, however, have deeply affected the function of global ecosystems and have led to profound environmental deterioration in many areas across the globe. To meet human demand and maintain ecosystem functioning, sustainable land use is therefore needed to address the challenges of the future. Land use policy, as one of the most important and effective tools in this regard, is often employed to regulate territorial land use and promote sustainable practices. Monitoring land use and land cover changes helps one to better understand the mechanism of land response to multiple drivers and provide valuable references for policy makers to revise and make more effective land use policies for sustainable land use.

2 Inner Mongolia and China's land restoration program

The Inner Mongolia Autonomous Region is located in the north of the People's Republic of China, and is bordered by Mongolia and Russia (Figure I-1). As the third-largest provincial subdivision, Inner Mongolia covers an area of 1.18 million km^2, or 12% of the nation's territory. Inner Mongolia is a relatively sparsely populated area, with 24.7 million people in 2010, which constituted 1.84% of the population in China (IMARBS 2000-2013). Primarily divided into 12 prefecture-level divisions (Leagues or Primate City, Chinese: 盟市), Inner Mongolia includes 101 county-level administrative divisions (Banner, County or District, Chinese: 旗, 县或区).

Listed as one of the International Geosphere-Biosphere Programme (IGBP) terrestrial transects (Steffen et al. 1992; Canadell et al. 2002), Inner Mongolia is characterized as a climate-ecological transitional zone. Monsoons, and a semi-arid continental climate with cold, dry winters and warm, relatively wet summers characterize Inner Mongolia (Barthold et al. 2013). The annual precipitation gradually decreases from 570 mm in the east to 10 mm in the west, and inter-annual variation is relative high. Corresponding to the climatic gradient, Inner Mongolia consists of a forest-steppe ecotone where various types of forests in the northeast are gradually replaced by grasslands, which require less rainfall, in the central region (Liu et al. 2000). The vegetation cover of the grassland decreased along the precipitation gradient and desert occupies the extremely dry west. In the south and

southeast areas neighboring the surrounding provinces, cropland replaces grassland and forms China's largest farming-pastoral zone.

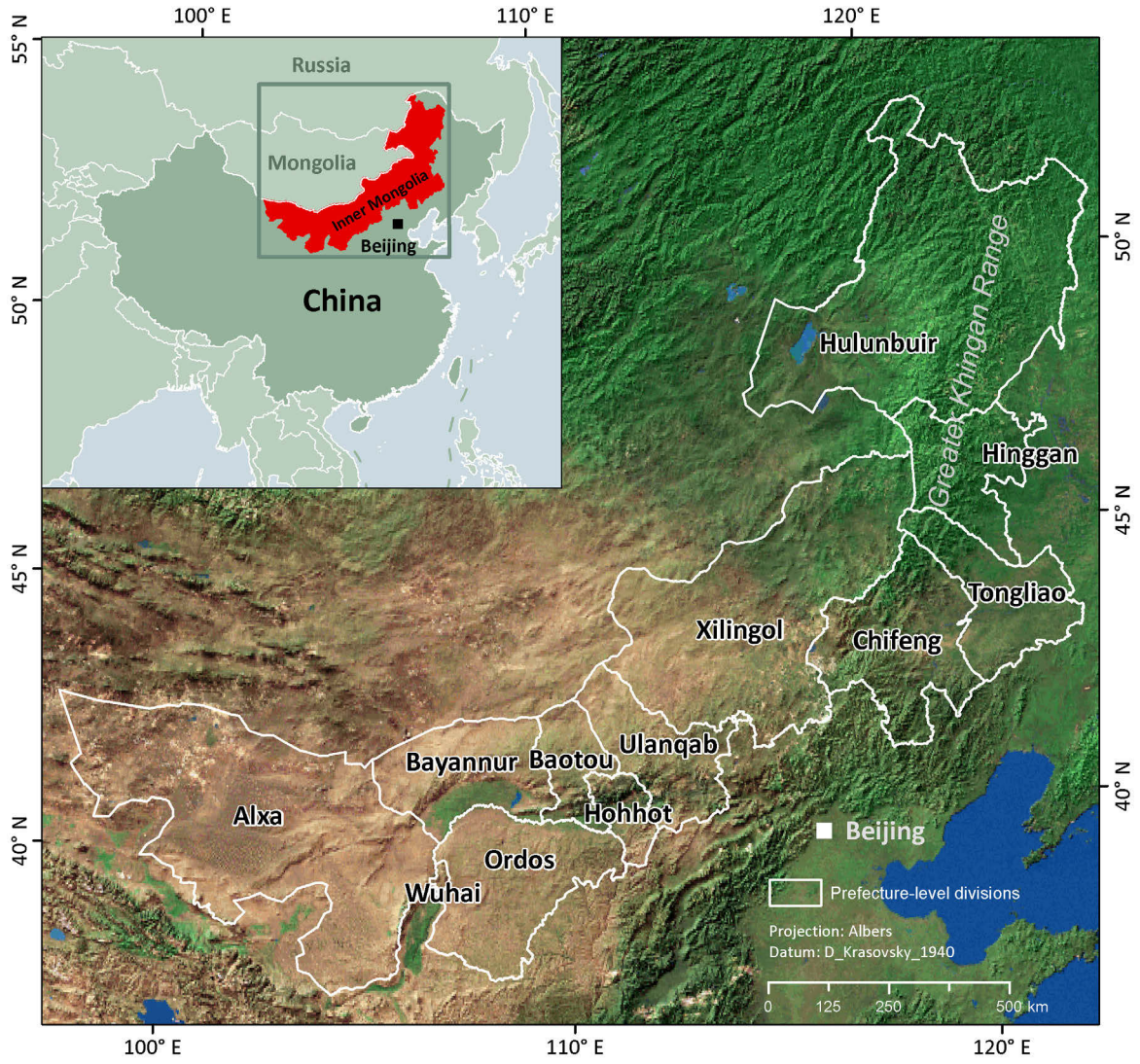

Figure I-1: Location of Inner Mongolia and its administrative divisions. Data source: ESRI Data and Maps Kit, Data Sharing Infrastructure of Earth System Science of China (http://www.geodata.cn).

Covered by 0.14 million km^2 of forest (11.9% of the entire region), Inner Mongolia is home to China's largest forest ecosystem in terms of area and living forest stock volume (SFA 2000-2013). Constituted mostly by deciduous needle-leaf forests and deciduous broadleaf forests in the Greater Khingan Range, the tree species of Inner Mongolia are mainly Dahurian Larch (*Larix gmelinii*), Mongolian Scots Pine (*Pinus sylvestris*), Chinese Pine (*Pinus armandii*), Mongolian Oak (*Quercus mongolica*) and Birch (*Betula platyphylla*) (Li et al. 2014). Inner Mongolia's forests not only provide timber products but also play an important role for watershed regulation (Wang et al. 2010a; Li et al. 2012b; Tang et al. 2012), carbon sequestration (Tan et al. 2007; Piao et al. 2009; Li et al. 2014), and wildlife habitat (Wang et al. 2000; Wang et al. 2002; Zhang et al. 2007a).

Grassland and cropland account for more than half (58.1%) of the area in Inner Mongolia. Including natural prairie and anthropogenically-managed types such as pasture and hay lands, grassland forms the largest land cover class, stretching across an area of 0.46 million km^2 (45.3% of the entire territory). The diverse grasslands in Inner Mongolia are highly valued for livestock grazing (Longworth and Williamson 1993; Yu et al. 2004), wildlife habitat (Wang et al. 1997; Luo et al. 2014), and for maintaining natural areas and watershed protection (Zhao et al. 2006). Historically, nomadism was the main practice of land use in Inner Mongolia (Li et al. 1993). However, during the late period of the Qing dynasty (1840-1912), grasslands in southern and eastern Inner Mongolia were gradually cultivated and converted to cropland for grain production by the Han immigration from surrounding provinces (Bayaer et al. 2005; Ye and Fang 2014). By the end of the 1990s, cropland occupied nearly 12.6% of Inner Mongolia. Maize (36.6%), soybean (13.6%) and wheat (8.0%) were the dominant crop speceis in terms of sown area.

The present land use and land cover pattern is, to a major degree, a result of drastic social-economic changes that have taken place since the late 1940s in Inner Mongolia (Sneath 1998; Bayaer et al. 2005). Three sub-periods with different land use policies and social environments influenced the land system prior to 2000: 1) Moderate land use (1949-1957); 2) Land use intensification and cropland expansion (1958-1977); 3) Post-socialism land use (1978-1999) (Table I-I).

Table I-1: Land use and land cover change in Inner Mongolia during various periods. The orange colors in the cells indicate area loss and the green colors indicate area gain. Higher levels of change magnitude are illustrated in deeper-color tones.

	1949-1957	1958-1977	1978-1999
Forests			
Croplands			
Grasslands			

Shortly before and after the foundation of the People's Republic of China in 1949, socialism was adopted and land reform was conducted in the Communist Party-controlled Inner Mongolia (Chaogemandula 2012). Private cropland was taken away and equally redistributed to individuals, while most grasslands and forests remained under the previous commune's ownership (Qinggeletu 1998). During this period, grasslands were well protected under regional policies between 1949 and 1957 (Jiang 2005). For instance, a regional regulation was authorized in 1951 to maintain grasslands and prohibit land

reclamation (Chinese: 保护牧场, 禁止开荒) (Zhang et al. 2008). To reduce wind and water erosion, forests were well-protected in Inner Mongolia, as well as in China as a whole (Richardson 1990).

The moderate use of land in Inner Mongolia prior to 1957 was interrupted by social and political changes. With an aim of rapidly transforming the country from an agrarian economy into an advanced communist society, drastic industrialization and collectivization was taken in the "Great Leap Forward" campaign (Chinese: 大跃进, 1958-1961) (Eckstein 1977; Chan 2001). Private lands were taken away again and managed by communes under a collective farming regime. Land use was gradually intensified to meet the increasing material needs of industry. Encouraged by the national policy "grain-first" (Chinese: 以粮为纲), large-scale cropland expansion on grasslands or forests spread out in Inner Mongolia (Song and Zhang 2006). It is estimated that more than two million hectares of grasslands or forests have been converted to cropland between 1958 and 1976 in Inner Mongolia (Enkhee 2000; Bayaer et al. 2005).

The end of political turmoil in 1976 developed into a period of profound political-economic reform that marked the beginning of the Chinese era of "Reform and Opening Up" (Chinese: 改革开放) (Song 1985). After 1978, the economy was put ahead of politics and a series of economic reform initiatives were implemented, including the expansion of free markets, diminishing state control over enterprises, decollectivization of agriculture, and opening up of the country to foreign investment and so forth (Brogaard and Zhao 2002). The reforms reached every economic sector and greatly influenced the agricultural sector in Inner Mongolia. The implementation of the Households Production Responsibility System (HPRS), for instance, contracts farmers and stimulates their incentives for choosing more profitable means of land management. As a result, the number of livestock rapidly increased and exacerbated wide-spread grassland degradation (Thwaites et al. 1998; Su et al. 2005; Li et al. 2007). Meanwhile, cultivation continued to encroach on grasslands, resulting in a new wave of cultivation from 1986 to 1996 (Bao et al. 1998; Jiang 2005). Contrary to the semi-privatization reforms in the agricultural sector, the forestry sector in Inner Mongolia remained mostly state-controlled, although small parcels of forested land were leased to individuals. The government's intense exploitation of timber has caused forests to rapidly shrink in Inner Mongolia; the forest stock volume in the Greater Khingan Range was estimated to have decreased by 28.7% between 1962 and 2000 (Wang 2005; Wang 2013).

The overuse of land resources before the 2000s resulted in severe ecological consequences in the ecologically fragile area of Inner Mongolia. Desertification (Wu and Ci 2002; Zhao et al. 2005; Ci and Yang 2010), frequent sandstorms (Xu 2006; Han et al. 2008; Wang et al. 2013), increasing floods (Lv and Zhang 1999) and biodiversity loss (Li 1995; Zhou et al. 2006; Tian et al. 2009) have been widespread in Inner Mongolia, which pushed the Chinese central government to rethink how land is used (Liu and Diamond 2005). To mitigate negative ecological outcomes and ensure a more sustainable method of development, in the late 1990s the Chinese central government launched a series of nationwide land restoration programs to preserve natural ecosystems, regenerate forests and reduce human pressure in ecologically fragile regions (Liu et al. 2008). Most of the national land restoration programs were implemented in Inner Mongolia, which makes it the province with the heaviest investment (SFA 2013).

The Natural Forest Conservation Program (NFCP, Chinese: 天然林保护工程), approved by the State Council in 2000, is a prominent land restoration program. Spanning nearly half a century (1999-2050), the NFCP intends to preserve natural forests and to increase the productivity of forest plantations (Zhang et al. 2000). Complementing NFCP, another notable land use policy titled Returning Farmlands to Forest and Grassland Project (also known as "Grain to Green Program", GGP, Chinese: 退耕还林还草工程) plans to spend 325 billion yuan (1 Euro = 8.6 yuan in April 2014) to convert 147 million ha of farmland on steep slopes (≥15° in northwestern China and ≥25° elsewhere) or with low yield, and 173 million ha of grassland into forest between 1999 and 2010 (Uchida et al. 2005; Wang et al. 2007a). To reduce the sources of sandstorms that affect Beijing and its neighboring Tianjin Municipality, 145 billion yuan have been invested into vegetation re-generation in phase I (2001-2012) of the Beijing and Tianjin Sandstorm Source Treatment Project (BTSST, Chinese: 京津风沙源治理工程), and an additional 88 billion yuan will be invested into the phase II program (2013-2022) (Li and Zhang 2004; Zhang et al. 2012).

The land restoration programs in China are implemented through several policy instruments. On the one hand, administrative means were adopted and the overall goals were sub-tasked and assigned to the local governments each year. Vegetation regenerations, including mountain enclosure or tree plantations, were conducted in the state-owned land directly (Hyde et al. 2003). Further, the local governments were requested to create off-land jobs and re-train the labor in the forestry and agricultural sectors for re-settlement (Zhang et al. 2000). On the other hand, subsidies higher than the opportunity costs were

offered to farmers to encourage conversion from marginal cropland to forest or grassland (Gauvin et al. 2010). Based on the choice of land use, farmers receive contracts with different time limits and compensation levels. For instance, farmers can obtain 8-year subsidies if the cropland is converted to ecological forests (i.e., forests serving to alleviate soil erosion and sandstorms) (SFA 2008) while compensation is carried out over 5 years if economic tree species such as fruit trees are used for afforestation (Yan and Yan 2004).

Yet land use and land cover change in Inner Mongolia after 2000 has not been completely known. Beyond China's land use policies, other social-economic factors may influence land use decisions in Inner Mongolia as well. One of the underlying drivers is the increasing demand for agricultural and timber products during the past decade. Inner Mongolia has been experiencing the most rapid economic development in its history, and the Gross Domestic Product (GDP) has increased more than 10-fold between 2000 and 2012 (IMARBS 2000-2013). Correspondingly, the consumption of timber and agricultural products has reached all-time highs in Inner Mongolia since the late 2000s (Zhu 2008; Wang 2009; Xiao 2012). The increasing price of commodities may stimulate land use intensification and reduce the willingness of farmers to join governmental land restoration plans. Unfortunately, by now we still do not clearly know how land use and land cover in Inner Mongolia was changed under the background of Chinese land use policies and other interacting factors.

3 Monitoring land use and land cover change using remote sensing

Remote sensing has proven to be a valuable tool for land surface monitoring, as it provides a synoptic perspective and periodic view of the Earth's surface. The reflected or emitted electromagnetic energy can be captured through sensors and can then be translated into physical properties of the land surface (Loveland and Defries 2004b). The repeated observation of remote sensing makes it possible to investigate changes by comparing the imagery acquired at several points in time. Since the late 1970s, imagery taken from remote sensing has been employed for the purpose of land cover mapping and change detection (Tardin et al. 1979; Tardin et al. 1980).

The great abundance of earth-observing sensors available today has greatly improved the capacities for land monitoring from local to global scales (Kenneny et al. 2014). In 1972, the Landsat satellites were launched to monitor land surfaces, making them the longest consecutively running remote sensing program. However, the relatively narrow swath that

they encircle (ca. 185 km) hampers the utility of Landsat for large-scale mapping (Clark et al. 2012). With wide-field-of-view (henceforth: coarse resolution) satellite data, land monitoring at the continental or global scale becomes feasible for the first time (Tucker et al. 1985; Defries and Townshend 1994). Since the launch of National Oceanic and Atmospheric Administration (NOAA)-6 in 1979, the Advanced Very High Resolution Radiometer (AVHRR) has provided global coverage imagery that has been successfully used for continental and global land cover mapping at coarse spatial resolution (i.e., 8x8 km, (Townshend 1994; Loveland et al. 2000)). Several more recent satellite missions have tremendously improved monitoring capabilities, specifically with regard to improved spatial resolution and radiometric calibration. Among others, Système Probatoire d'Observation de la Terre VEGETATION (SPOT VGT), launched in 1998, and Moderate-Resolution Imaging Spectroradiometer (MODIS), in operation since 2000, have increased the utilities of remote sensing for wall-to-wall large scale land cover monitoring (Friedl et al. 2002; Huete et al. 2002) (Table I-2).

Table I-2: Characteristics of the AVHRR, SPOT-VGT, and MODIS and the respective Normalized Difference Vegetation Index (NDVI) datasets, adopted from Tarnavsky et al (2008).

	AVHRR	SPOT-VGT	MODIS
NDVI product	AVHRR GIMMS	SPOT-VGT S10	MOD13Q1
Platform	NOAA-7/9/11/14/16	SPOT- 4/5	MODIS Terra
Wavebands used for NDVI calculation	Red = 580-680 µm NIR = 725-1100 µm	Red = 610-680 µm NIR = 780-890 µm	Red = 620-670 µm NIR = 841-876 µm
Time period	06/1981 to - 12/2006	04/1998 to -	03/2000 to -
Nadir pixel size	5 km	1 km	250 m
Nominal pixels size	8 km	1 km	250m
Off-nadir view angle (degree)	55.4	50.5	65
Radiometric quantization	10-bit	8-bit	12-bit
Compositing, cloud removal	15-day MVC NDVI	10-day MVC NDVI	16-day CV-MVC NDVI

MVC = maximum value composite; CV–MVC = constrained maximum value composite.

Another advantage of the coarse resolution data is the capacity of observing the Earth at high frequency intervals. Compared to the 16-day satellite revisits of Landsat, AVHRR and other coarse resolution sensors provide a daily repeat observation, which is crucial for monitoring seasonal and inneranual variation in land surface driven by climatic variability or land use change (Linderman et al. 2005). The advantage provided by daily observation is particularly acute in drylands, which are highly influenced by large seasonal variations in precipitation. Thus, to be able to separate subtle land use and land cover change (i.e., land modification) from fluctuations in land cover conditions caused by climatic

variability, a long-term time series of coarse resolution imagery is required for land change monitoring across broad scales (Brown et al. 2007; Redo and Millington 2011).

To be able to rely on the changes detected from integrated time series from multiple sensors, it is crucial to ensure consistency across products and over time. While state-of-the-art remote sensing instruments provide higher quality data, their relatively short record compared to AVHRR has been a limiting factor for long-term surface monitoring. Integrating imagery from different sensors provides an option to extend the higher quality dataset acquired from SPOT VGT or MODIS back to the 1980s (Brown et al. 2008; Liu et al. 2012).

However, combining imagery from various sensors and platforms remains a challenging task and related uncertainties are not well understood (van Leeuwen et al. 2006; Baldi et al. 2008; Beck et al. 2011). In addition to the different bandwidths and calibration techniques, temporal inconsistency due to sensor replacement and degradation means that AVHRR is not easily combined with imagery from other advanced sensors (Latifovic et al. 2012; Yu et al. 2013). During the past 30 years, three AVHRR instruments have been operated on more than ten NOAA satellite platforms, and orbital drift often resulted in inconsistent time-sampling of clouds and other geophysical variables (Price 1991; Gleason et al. 2002; Devasthale et al. 2012). Therefore, examining the temporal consistency of long-term satellite records is a prerequisite for robust change detection (Fensholt et al. 2009; Stellmes et al. 2010).

Methodologically, developing cost-effective, accurate, and automated methods for monitoring land use and land cover change is a growing area of research (Mas 1999; Turner et al. 2007). Depending on the forms of land use and land cover change, methods utilized for change detection are diverse (Singh 1989; Lu et al. 2004). As a simple and robust approach, trend analysis has frequently been applied to characterize land cover change processes from multi-temporal imagery, using, for example, Normalized Difference Vegetation Index (NDVI) time series (Eklundh and Olsson 2003; Vogelmann et al. 2012; Jamali et al. 2014). Trend analysis of biophysical land properties can capture the magnitude and direction of land changes (Hostert et al. 2003; Verbesselt et al. 2010b), yet it does not provide detailed information about land change processes. For instance, without other auxiliary information, it is difficult to label land conversion directly from the results of trend analysis (Lasanta and Vicente-Serrano 2012). Nevertheless, trend analysis is still a useful tool for screening land changes, especially ones that are related to subtle land

modifications such as land use intensification or land degradation (Hill et al. 2008; Hilker et al. 2014).

While trend analysis supports the detection of gradual land modification, there is a strong need to develop a method that can reliably map land cover conversions at frequent time intervals. Though annually updated land cover maps have been produced for many regions (Friedl et al. 2002; Clark et al. 2010), automated methods and standards for mapping land cover change across multiple land cover types at annual intervals are not readily available. This disparity has consequences for land change analyses. Comparing land cover maps from multiple dates is one of the most traditional approaches for land conversion mapping; however, annual land cover conversion cannot be accurately inferred from the existing annual land cover products due to the large inter-annual variation in heterogeneous areas (Friedl et al. 2010; Fritz et al. 2011). Recently, trajectory-based techniques have emerged for detailed change detection (Huang et al. 2010; Kennedy et al. 2010). However, the trajectory approach mostly focused on changes between two conditions within the scope of forest monitoring. If changes between multiple land cover classes are of interest, the change attribution becomes difficult to map.

4 Objectives, research questions and method design

The overall aim of this thesis is to gain a better understanding of land use and land cover change in Inner Mongolia after 2000 using remote sensing and considering China's land restoration programs. The study area of Inner Mongolia is a hotspot for global environmental change research. The ecosystems there are vulnerable and past anthropogenic disturbances have caused a series of environmental disasters that have caught wide public attention (Liu et al. 2013). While great efforts and massive investments have targeted land restoration, little knowledge has been gained regarding *how* and *when* land surface was altered in Inner Mongolia. Coarse resolution imagery provides the potential for monitoring land changes across broad scales, yet it suffers from uncertainty due to temporal consistency. Moreover, to capture complex land change processes, we need a robust approach to detect changes across multiple land classes at frequent intervals (e.g., annual). Therefore, a comprehensive examination of data consistency and the development of robust methods for annual land cover change mapping are prerequisites.

The first objective of this thesis is to examine the utility of coarse resolution imagery time series for long-term land change monitoring. The second objective is to develop a method

for land use and land cover change mapping at frequent time intervals to improve the capabilities of remote sensing to capture changes across multiple land cover categories. The final aim is to investigate how the land changed in Inner Mongolia under the background of national land restoration programs since the year 2000. Consequently, this thesis investigates these questions in three separate research chapters (Chapter II-IV):

Research question I (Chapter II): How do time series from global satellite archives compare across Inner Mongolia, and how do trends derived from time series relate to land change?

To investigate this question, this chapter used a trend analysis to examine the temporal consistency of AVHRR GIMMS data – the longest NDVI time series record against the latest state-of-the-art sensors SPOT VGT and MODIS Terra. This chapter compared the trend from NDVI time series, as well as the derived phenological indicators to investigate the utility of different sensor-based NDVI archives for land monitoring. The results of the trend analysis were interpreted to learn about the land modification process in Inner Mongolia.

Research question II (Chapter III): How can land use and land cover change be reliably mapped at an annual interval using hyper-temporal satellite imagery?

To address the complexly of land surface dynamics, wall-to-wall land change monitoring at frequent time intervals is needed. This chapter tested the utility of a trajectory-based change detection approach applied to MODIS data to map annual land use and land cover change using time series of land cover class probabilities for multiple land cover class trajectories. The approach developed in this chapter was applied to Inner Mongolia to address research question III.

Research question III (Chapter IV): How was the land changed in Inner Mongolia considering national land restoration programs?

Three processes that are mostly related to China's land restoration programs are the main foci in this chapter: deforestation, forest regeneration (i.e., afforestation and reforestation) and conversion from cropland to grassland (cropland retirement). This chapter mapped the spatial and temporal pattern of these three processes in Inner Mongolia after 2000, when the various land restoration programs were initially implemented.

5 Structure of this thesis

This thesis comprises five chapters. Following this introduction three core chapters (Chapters II - IV) address each research question. Chapter V provides a synthesis of the thesis by summarizing the answers to the research questions, and concludes by providing an outlook for future research. The core chapters were written as stand-alone documents in the format of an article that can be published in peer-reviewed journals. Nevertheless, these chapters fit the framework of this thesis well. The three core chapters were published (Chapter II), submitted (Chapter III), or is under preparation (Chapter IV) as follows:

Chapter II: Yin, H., Udelhoven, T., Fensholt, R., Pflugmacher, D., & Hostert, P. (2012). How Normalized Difference Vegetation Index (NDVI) trends from Advanced Very High Resolution Radiometer (AVHRR) and Système Probatoire d'Observation de la Terre VEGETATION (SPOT VGT) time series differ in agricultural areas: An Inner Mongolian case study. *Remote Sensing*, *4*, 3364-3389.

Chapter III: Yin, H., Pflugmacher, D., Kennedy, R.E., Sulla-Menashe, D., & Hostert, P. Mapping annual land use and land cover changes using MODIS time series. (in revision). *IEEE Journal of Selected Topics in Applied Earth Observation and Remote Sensing*.

Chapter IV: Yin, H., Pflugmacher, D., Li, A., Li, Z.G., & Hostert, P. (in preparation). Land use and land cover change in Inner Mongolia - understanding the effects of China's re-vegetation programs.

Chapter II:
How NDVI trends from AVHRR and SPOT VGT time series differ in agricultural areas: An Inner Mongolian case study

Remote Sensing 4 (2012) 33364-3389

He Yin, Thomas Udelhoven, Rasmus Fensholt, Dirk Pflugmacher and Patrick Hostert

Abstract

Detailed information from global remote sensing has greatly advanced our understanding of Earth as a system in general and of agricultural processes in particular. Vegetation monitoring with global remote sensing systems over long time periods is critical to gain a better understanding of processes related to agricultural change over long time periods. This specifically relates to sub-humid to semi-arid ecosystems, where agricultural change in grazing lands can only be detected based on long time series. By integrating data from different sensors it is theoretically possible to construct NDVI time series back to the early 1980s. However, such integration is hampered by uncertainties in the comparability between different sensor products. To be able to rely on vegetation trends derived from integrated time series it is therefore crucial to investigate whether vegetation trends derived from NDVI and phenological parameters are consistent across products. In this paper we analyzed several indicators of vegetation change for a range of agricultural systems in Inner Mongolia, China, and compared the results across different satellite archives. Specifically, we compared two of the prime NDVI archives – AVHRR Global Inventory Modeling and Mapping Studies (GIMMS) and SPOT Vegetation (VGT) NDVI. Because a true accuracy assessment of long time series is not possible, we further compared SPOT VGT NDVI with NDVI from MODIS Terra as a benchmark. We found high similarities in interannual trends, and also in trends of the seasonal amplitude and integral between SPOT VGT and MODIS Terra ($r > 0.9$). However, we observed considerable disagreements in NDVI-derived trends between AVHRR GIMMS and SPOT VGT. We detected similar discrepancies for trends based on phenological parameters, such as amplitude and integral of NDVI curves corresponding to seasonal vegetation cycles. Inconsistencies were partially related to land cover and vegetation density. Different pre-processing schemes and the coarser spatial resolution of AVHRR GIMMS introduced further uncertainties. Our results corroborate findings from other studies that vegetation trends derived from AVHRR GIMMS data not always reflect true vegetation changes. A more thorough understanding of the factors introducing uncertainties in AVHRR GIMMS time series is needed, and we caution against using AVHRR GIMMS data in regional studies without applying regional sensitivity analyses.

1 Introduction

Remote sensing data have provided unique insights for global environmental change research during the past decades (Tucker et al. 1985; MEA 2005b; Turner et al. 2007). Global data archives such as those based on imagery acquired by the Moderate-Resolution Imaging Spectroradiometer (MODIS), Système Probatoire d'Observation de la Terre VEGETATION (SPOT VGT) or the National Oceanic and Atmospheric Administration (NOAA) Advanced Very High Resolution Radiometer (AVHRR) are key to understanding ecosystem changes from regional to global scales(Cracknell 1997; van Leeuwen et al. 1999; Friedl et al. 2002; Fensholt et al. 2009; Ganguly et al. 2010). Without detailed information from global remote sensing systems, global environmental change research would be hampered from understanding Earth as a system (Townshend et al. 1991; Gutman et al. 2004; Turner et al. 2008).

Monitoring agricultural change trajectories over long time periods is critical to gain a better understanding of the Earth System's carrying capacities (Matson et al. 1997; Rasmussen et al. 1998; Barnosky et al. 2012). Gradual or long-term change processes, such as ecosystem degradation due to agricultural over-use, can only be detected and characterized with confidence from time series. However, extracting trends from time series can be challenging due to short-term (e.g. phenological) variations in the data or overall low signal-to-noise-ratios (Verbesselt et al. 2010a; Verbesselt et al. 2010b; Samanta et al. 2011; de Jong et al. 2012). It is hence necessary to establish long enough time series to reliably capture vegetation trends in agricultural ecosystems (Tucker et al. 1991; Reed and Brown 2005; Udelhoven et al. 2009). In this paper, we strive to better understand how time series from global satellite archives compare across one of China's prime agricultural areas and how trends derived from time series relate to agricultural change.

Among the various remote sensing-based vegetation measures utilized in agricultural monitoring, the Normalized Difference Vegetation Index (NDVI) is the most widely used proxy for vegetation cover and production (Tucker 1979; Myneni et al. 1997; Field et al. 1998; Pettorelli et al. 2005; Panda et al. 2010). There is a strong relationship between NDVI and agricultural yield (Labus et al. 2002; Boschetti et al. 2009). Vegetation properties, such as length of growing season, onset date of greenness, and date of maximum photosynthetic activity are often derived from NDVI time series for monitoring changes in agricultural systems (Lee et al. 2002; Xin et al. 2002; Hill and Donald 2003; de

Beurs and Henebry 2004). These phenological indicators emphasize different characteristics of terrestrial ecosystems to gain a better understanding of structure and function of land cover and associated changes (Schwartz 2003; Ganguly et al. 2010; Kariyeva and Van Leeuwen 2011). Phenology, i.e. the timing of recurring life cycle events, may for example shift in response to natural or anthropogenic disturbances in agricultural ecosystems (Bradley and Mustard 2008; Yu et al. 2010). Environmental scientists have an increasing interest in spatially explicit phenological data to better understand agricultural change processes associated with land use and climate change. In this context, remote sensing-based time series of NDVI are increasingly used to obtain phenological data at regional to global scales (Zhang et al. 2003; Martinez-Beltran et al. 2009; Gu et al. 2010; Alcantara et al. 2012).

Daily NDVI series of global coverage derived from AVHRR data have been extensively used for land change research, including agricultural ecosystems (Tucker et al. 1985; de Beurs and Henebry 2004; Geerken and Ilaiwi 2004; Wessels et al. 2007; Li et al. 2010a; Bégué et al. 2011). Because AVHRR was originally designed for deriving information about the Earth's atmosphere, its radiometric and spatial resolution is not optimized for vegetation monitoring (Steven et al. 2003; Lillesand et al. 2008). Nevertheless, the AVHRR systems are the only available instruments that have provided repeated, long-term observations of global vegetation properties in an operational mode since June 1979, the launch of NOAA-6.

Since the late 1990s, satellite missions have tremendously improved monitoring capabilities and data quality, specifically with regard to data calibration and standardized pre-processing schemes. Among others, bandwidths and spectral response in the red and near-infrared bands needed for NDVI calculation have been improved compared to AVHRR (Huete et al. 2002; Tarnavsky et al. 2008). While newer remote sensing instruments such as SPOT-VEGETATION and MODIS supply higher quality data, their relatively short service record compared to AVHRR has been a limiting factor for analyzing long-term surface conditions. Therefore, AVHRR remains an invaluable and irreplaceable archive of historical land surface information when targeting long-term change processes in ecosystem analysis, such as agricultural expansion and intensification (Jiang 2005; Tucker et al. 2005; Li et al. 2007).

Despite the need for integrating NDVI time series from different sensors, it is not well understood how phenological parameters and change trends derived from NDVI time

series compare across sensors in different regions. Little information exists on which factors might lead to systematic biases, specifically in areas with low and strongly varying NDVI (Alcaraz-Segura et al. 2010). With the advent of new generations of sensors, van Leeuwen (1999), for example, pointed out that differences between AVHRR and MODIS time series in the spectral, radiometric, and spatial domain need to be better understood to meet the needs of long-term agricultural change research. In general, it is crucial to better understand differences in time series products from different NDVI archives acquired from, among others, NOAA AVHRR, SPOT VGT and MODIS (Gitelson and Kaufman 1998; Brown et al. 2006; Fontana et al. 2008).

There have been several studies showing a generally acceptable agreement between NDVI time series from AVHRR sensors and MODIS, MERIS (MEdium Resolution Imaging Spectrometer), or SPOT VGT. Gallo (2005) examined NDVI time series between 2002 and 2003 derived from AVHRR (NOAA-16 and NOAA-17) and MODIS (MOD13A2; Collection 4), and found good linear relationships for 89% of the NDVI values for the conterminous United States. Swinnen and Veroustraete (2008) found a good linear agreement between the SPOT-VGT 10-day synthesis product (S10) and the AVHRR Local Area Coverage (LAC) Level 1b datasets after conducting sensor calibrations to improve consistency for Southern Africa.

However, these studies were based on correlation analyses, which mainly proof the coherence of the seasonal, sinusoidal-like NDVI patterns. As phenological changes are often much greater than long-term vegetation trends, these analyses are not sensitive enough to allow inferences on long-term vegetation trends. Less research has focused on directly comparing trends derived from different NDVI datasets. For regional and global agriculture monitoring, however, it is crucial to know whether trends derived from different NDVI archives are comparable or not. Using four NDVI time series derived from AVHRR spanning 1982 to 1999, Alcaraz-Segura et al (2010) evaluated the differences in spatial patterns of trends in Pathfinder (PAL), Fourier-Adjustment, Solar zenith angle corrected, Interpolated Reconstructed (FASIR), GIMMS, and Land Long Term Data Record (LTDR) datasets. They found that GIMMS-derived trends differed the most and concluded that it is necessary to compare trends from different AVHRR-based NDVI products with those derived from other sensors. One study focusing on the comparability of NDVI-based trend derivatives from AVHRR, MODIS and SPOT VGT data was performed by Fensholt et al (2009) for the Sahel region. They concluded that GIMMS, MODIS 16-day NDVI and SPOT VGT 10-day composites produced largely similar trends,

with variations increasing towards more humid climate regimes, i.e. higher biomass. Song et al (2010) examined correlation and compared trend maps from AVHRR GIMMS and SPOT VGT visually across China from 1999 to 2006, they concluded that these two products correlated well and trends are largely coherent, apart from desert areas. A global comparison between the newly-processed GIMMS3g archive and MODIS data showed that global class-wise trends across biomes exhibit similar tendencies, but spatial patterns at the local to regional scale do often correlate less well (Fensholt and Proud 2012).

Findings on the comparability of vegetation trends derived from different satellite data archives are inconclusive and not available across the full range of biomes. While the AVHRR GIMMS dataset has been cross-calibrated with data from other sensors (Tucker et al. 2005), a deeper knowledge on the compatibility of vegetation trends derived from these cross-calibrated data is needed across a range of different agricultural systems.

We chose Inner Mongolia as a test region, which allowed us to compare NDVI-based trends from different sensors across a climatic gradient from sub-humid to arid environments. While agricultural intensification in Inner Mongolia started in the late 1970ies, policies to protect the environment were mostly implemented since the late 1990ies, i.e. related effects will only be detectable in recent data. Such long time periods of agricultural change require a coupling of different NDVI archives in a consistent framework to capture the full range of change processes. The aim of this paper is a comprehensive comparison of vegetation trends in various agricultural systems derived from AVHRR GIMMS and SPOT VGT NDVI archives, using MODIS as a benchmark for SPOT VGT. We strive to better understand how consistent indicators of vegetation change are between these archives. We therefore ultimately pose the question which restrictions apply when analyzing long-term trends from joint NDVI archives for agricultural areas.

2 Materials

2.1 Study area

Our study area is located in central and western Inner Mongolia (Figure II-1). The region is characterized by an arid to sub-humid climate with a strong zonal distribution of rainfall and vegetation from East to West (Lee et al. 2002; Yu et al. 2003). Along with the zonal precipitation patterns, land uses follow a distinct gradient. The northeastern part of the study area is dominated by deciduous forest and in the lowlands by agriculture. Between

the forested East and the desert in the West, land cover is dominated by various grassland ecosystems.

We selected the Hinggan region in densely-vegetated northeast Inner Mongolia and the sparsely vegetated Ordos region as two prototypic landscapes for testing our analysis scheme and for an in-depth evaluation of results. Hinggan is known as an ecological transition zone, with landscapes ranging from cultivated cropland in the eastern plain to forests in the mountainous West. Ordos is dominated by dry grasslands, desert and irrigated cropland along the Yellow River (Nemani et al. 2003; Tao et al. 2005).

Considering agricultural change during the last decades, Inner Mongolia has undergone several land use transitions. Those changes are on the one hand triggered by a tremendously increasing demand for agricultural products in China (Liu et al. 2003; Liu et al. 2010b), and on the other hand by the need to stop ongoing land degradation (Jiang 2005; Wang et al. 2007b). In Inner Mongolia, four different change processes can be distinguished on agricultural land: First, the semi-arid to sub-humid grasslands of the steppe regions have been and still are intensively grazed. Extended areas heavily degraded over time, which enforced restrictive grassland exclosure policies (Tong et al. 2004; Jiang 2006; Li et al. 2007). Second, in the more humid regions of Inner Mongolia intensive cropping systems developed. These also prevail along the river valleys of the semi-arid areas of Inner Mongolia, where irrigation systems allow for higher yields and more water-demanding crop species. This trend is still ongoing (Chen et al. 2003; Qiao et al. 2009). Third, agricultural land on slopes has been affected by China's Sloping Land Conversion Program, also referred to as the national "Grain for Green" Program (Deng et al. 2006; Bennett 2008). In mountainous terrain we consequently expect a greening up of previously cropped areas. Fourth, natural forest protection and afforestation in croplands as wind shelter is extensively practiced in Inner Mongolia to combat land degradation and prevent sand storms, known as the "Green Great Wall" and "The Combating Desertification Program in Wind-Sand Source Areas Affecting Beijing and Tianjin" initiatives (Chen et al. 2003; Qiao et al. 2009). Almost all the croplands in the study region are covered by these programs, while the exact time of implementation depends on local policies and may accordingly vary.

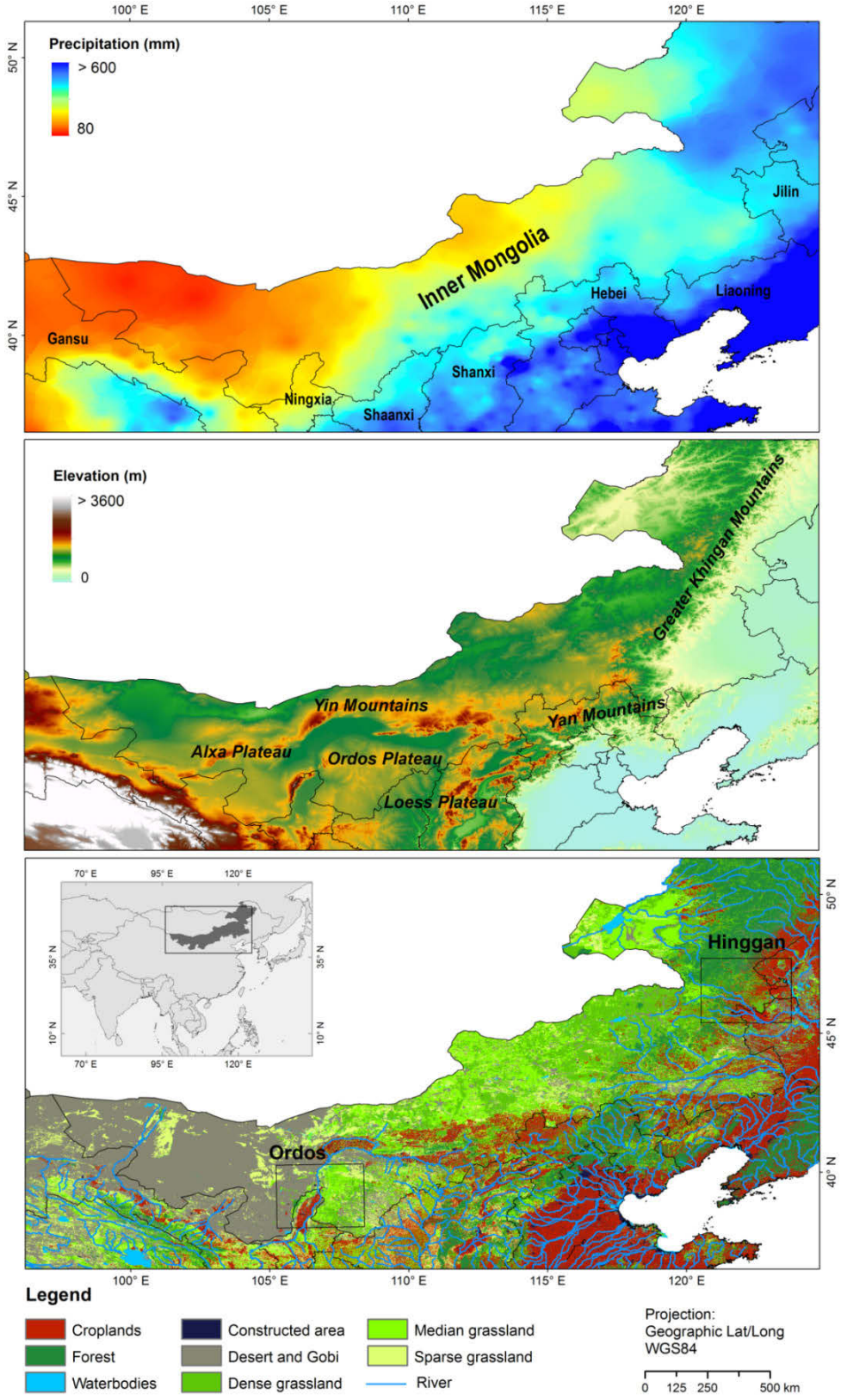

Figure II-1: Mean annual rainfall (1999–2006) in Inner Mongolia interpolated from China Meteorological Administration (CMA; http://cdc.cma.gov.cn/) data (top). Elevation data from Shuttle Radar Topography Mission (SRTM) digital elevation model (center). Reclassified land cover map of Inner Mongolia as provided by the Chinese Academy of Science (CAS, Liu et al. 2002) for the year 2000. Black frames showing focus regions. Inset showing Inner Mongolia in Asia (bottom).

2.2 Data

2.2.1 AVHRR NDVI composites

The AVHRR NDVI archive employed in this study was obtained from the NASA GIMMS group (Pinzon et al. 2007) and covered the years 1999 to 2006. We selected AVHRR GIMMS because it is the only updated archive and also the most widely used global AVHRR dataset (Tucker et al. 2005). GIMMS data are 15-day maximum value composites (MVC) at 8-km spatial resolution produced from Global Area Coverage (GAC) 1B data (Tucker et al. 2005). Data from six AVHRR instruments on different satellite platforms were used to produce this dataset. To ensure the continuity of NDVI time series derived from different instruments, GIMMS data have undergone rigorous data post-processing, including corrections of residual differences between sensors, viewing geometry caused by orbit drift, volcanic aerosols effects, and low signal-to-noise ratios due to sub-pixel cloud contamination (Tucker et al. 2005). Furthermore, Empirical Mode Decomposition (EMD) has been employed to identify and remove components of the NDVI signal that are largely related to the satellite drift on the Solar Zenith Angle (SZA) (Pinzon 2002; Pinzon et al. 2004). Finally, temporally overlapping SPOT Vegetation NDVI time series were used to intercalibrate the NOAA-14 and NOAA-16 NDVI time series (Pinzon et al. 2004). To this end, non-linear regression was performed to establish coefficients that transform historical data into the same value range as that of MODIS and SPOT (Tucker et al. 2005; Mangiarotti et al. 2010).

2.2.2 SPOT-VGT NDVI composites

The SPOT-VGT S10 products obtained from the Vlaamse Instelling voor Technologisch Onderzock (VITO) Image Processing center (http://free.vgt.vito.be/) are derived from SPOT-VGT P (P=physical) products. Launched on 24 March 1998, the VGT 1 on board SPOT-4 began capturing data until February 2003, when VGT 2 on board SPOT-5 became the nominal instrument. The VEGETATION instrument has several advantages compared to AVHRR, including better navigation, improved radiometric sensitivity, reduced geometric distortions, and 4 spectral bands instead of 2 in the visible to near infrared (VISNIR) spectral domain (Gobron et al. 2000). The SPOT-VGT S10 products are compiled by merging segments (data strips) acquired in a 10-day MVC at 1-km spatial resolution based on VGT-P products, which have been atmospherically corrected for molecular and aerosol scattering, water vapor, ozone and other gas absorptions (SPOT Vegetation user's guide 2012). A slight increase in NDVI after 2003 has been reported due to differences in radiometric calibration methods and band widths between VGT 1 and

VGT 2. The observed 3.5% increase in NDVI (for values > 0.3 only) is related to a bias in the near-infrared and red band of 6.3% and 2.1%, respectively (Henry and Meygret 2001; Fensholt et al. 2009; SPOT Vegetation user's guide 2012).

2.2.3 MODIS Terra NDVI composites

We obtained MODIS-based NDVI data between 2001 and 2010 from the MODIS-Terra Vegetation Index (VI) products (MOD13Q1, Collection 5). We acquired the data from the United States Geological Survey (USGS) Land Processes (LP) Distributed Active Archive Center (DAAC) at the Earth Resources Observation and Science (EROS) Data Center. The MODIS VI archive is available at a nominal 250-m spatial resolution and composited with a time interval of 16-days. Unlike AVHRR GIMMS and SPOT-VGT products, which use the simpler MVC method for compositing, MODIS VI products use a more sophisticated compositing algorithm that consists of two components: 1) a bidirectional reflectance distribution function composite (BRDF-C), and 2) a constrained view angle - maximum value composite (CV-MVC). These algorithms were designed to constrain the strong angular variations encountered in the MVC method and to reduce spatial and temporal discontinuities in the composited product (Huete et al. 2002). The MODIS VI archives have shown a better ability to provide useful radiometric and biophysical information for land surface characterization than previously available NOAA-AVHRR datasets (Huete et al. 2002; Vermote et al. 2002).

2.2.4 Other data

The Chinese Academy of Sciences' (CAS) Land-Use/Land-Cover Change (LUCC) database (Liu et al. 2002) was used as the main source of high resolution land use and land cover information. This vector dataset was derived from 505 Landsat TM scenes acquired in 2000 that were classified with an overall accuracy of 81% for all of China. Compared to other coarser land cover products such as the IGBP DISCover or GLC2000, the CAS LUCC database has a finer spatial resolution and is more accurate (Ran et al. 2009). The original 25 land cover types of the CAS LUCC database were merged into 8 relevant classes for our study region (Table II-1, Figure II-1).

Table II-1: Reclassified CAS land cover scheme.

Land cover types	Description
Sparse grassland (SG)	Herbaceous land with 5-20% canopy cover
Medium dense grassland (MG)	Herbaceous land with 20-60% canopy cover
Dense grassland (DG)	Herbaceous land with over 60% canopy cover
Croplands (CL)	Agricultural land with crops
Forestland (FL)	Coniferous, broadleaf and mixed tree cover
Waterbodies (WB)	Ocean, lakes, reservoirs, and rivers
Constructed area (CA)	Artificial surfaces
Non-vegetated land (NL)	All other land cover with less than 5% vegetation cover

3 Methods

We used the relatively short time series of MODIS-Terra NDVI between 2001 and 2010 to better understand how well this time series correlates with the SPOT VGT derived NDVI over time. The idea behind this benchmarking was to test how well spatio-temporal patterns can be reproduced between state-of-the-art NDVI archives. If patterns are similar, we can conclude that those are not arbitrary and we can rely on the underlying time series. In a second step we evaluated how AVHRR-GIMMS differs against this benchmark. Comparing AVHRR GIMMS to SPOT VGT data allowed us to take advantage of the maximum temporal overlap between both archives from 1999 to 2006. We first smoothed all the NDVI products by time series fitting and then extracted phenological parameters, NDVI amplitude and integral, from each NDVI time series. We then performed a correlation analysis to investigate the relationship between different NDVI archives. Lastly, we compared NDVI trends based on NDVI values and also based on phenological parameters using non-parametric statistics.

3.1 Time series fitting and phenological metrics

Several approaches have been developed to eliminate noise in NDVI time series caused by clouds, ozone, dust, as well as off-nadir viewing and low sun zenith angles (Holben 1986; Gutman and Ignatov 1997; Jonsson and Eklundh 2004; Udelhoven 2011). Most widely used techniques include Best Index Slope Extraction (BISE), Fourier based filtering, Savitzky-Golay and asymmetric Gaussian filters. These techniques are based on a temporal approach, which provides an estimate of NDVI noise through temporal interpolation (Julien and Sobrino 2010). Here, the double logistic function fitting provided in the TIMESAT software was chosen to smooth NDVI time series because of its proven general

applicability and superiority to many other filters (Jonsson and Eklundh ; Hird and McDermid). Pixels flagged as no data (value=-1), snow/ice covered (value=2) or cloud contaminated (value=3) in the MOD13Q1 pixel reliability layer were excluded prior to the temporal interpolation. Outliers were identified by a Seasonal-Trend decomposition based on Loess (STL) (Holben 1986), which is global in character and not dependent on ancillary data (Cleverland et al. 1990; Jonsson and Eklundh 2004).

Based on the fitted time series, we computed land surface phenological parameters for the AVHRR GIMMS, SPOT-VGT and MODIS Terra NDVI archives. Two frequently used phenological metrics based on NDVI time series, NDVI seasonal amplitude and integral, were derived to analyze both functional and structural dynamics of vegetation. Seasonal amplitude is defined as the difference between the base and maximum NDVI values in each growing cycling. NDVI amplitude indicates the intra-annual dynamics in vegetation phenology and thus has often been used in terrestrial ecosystem classification (Bradley and Mustard 2008). The NDVI integral, estimated as the cumulative value of NDVI time series in vegetation growth during the season (Jonsson and Eklundh 2002; White et al. 2009), is closely related to net primary productivity. Using TIMESAT, the start of season is defined as 20% of the fitted curve amplitude. We used the so-called “large NDVI integral” defined in TIMESAT (Jonsson and Eklundh 2002; Heumann et al. 2007; White et al. 2009).

3.2 Correlation analysis

Following Song et al (2010), we conducted a correlation analysis to test the linear relationship between different NDVI products. In a first step, fitted MODIS Terra NDVI time series data were spatially resampled to meet the coarser resolution of SPOT VGT NDVI time series. Both time series were aggregated to monthly data. MVC and a bilinear interpolation algorithm were used to generate a monthly 1-km MODIS Terra NDVI time series. We then calculated the pixel-wise linear Pearson correlation coefficient (r) between monthly 1-km SPOT VGT and MODIS Terra NDVI values between 2001 and 2010. We compared SPOT VGT and AVHRR GIMMS NDVI time series in a similar fashion. SPOT VGT was aggregated into monthly and 8-km resolution time series for calculating r between SPOT VGT and AVHRR GIMMS NDVI time series.

3.3 Trend analysis

We calculated linear trends in NDVI time series to analyze patterns of changes and also to test whether a good correlation between NDVI from different global archives can be used to infer a good correlation between trends. We used non-parametric statistical tests, the

Modified Seasonal Mann-Kendall (MSK) and Mann-Kendall (M-K) test to evaluate the statistical significance of trends based on a) all data from monthly fitted NDVI time series and b) annual values of the NDVI phenological metrics, respectively (Mann 1945; Kendall 1975; Hirsch and Slack 1984). Unlike ordinary least squares regression, the MSK trend test is less affected by missing values and uneven data distribution, and are robust towards extreme values and serial dependence (Udelhoven 2011). To identify the magnitude of a trend, we calculated Sen's slope (Sen 1968; Hirsch et al. 1982) which is a form of robust linear regression and less affected by gross data errors or outliers compared to linear regression analysis (Gilbert 1987; Bouza-Deano et al. 2008).

The quantitative comparison of trends was conducted based on sampling plots of 8km x 8km. To assure homogeneity and minimize the effects of mixed pixels and misregistration, we overlaid the reclassified Landsat-based CAS LUCC database with the sample plots and selected only plots with at least 80% of a single land cover type. Based on that strategy, 2770 samples were selected for trend analysis, among which 278 plots were labeled as cropland, 199 plots as forestland, 955 plots as dense grassland, 742 plots as medium dense grassland, and 596 as sparse grassland. We then calculated for each sample plot average values of Sen's slope for SPOT VGT, MODIS Terra and AVHRR GIMMS.

4 Results

4.1 Correlation analysis and comparing trends from SPOT VGT and MODIS Terra NDVI archives

The correlation between NDVI time series from SPOT VGT and MODIS in vegetated areas of Inner Mongolia was larger than 0.9 (Figure II-2, top). In comparison, NDVI time series showed a correlation less than 0.2 for non-vegetated areas such as the desert in the Alxa Plateau and for water bodies.

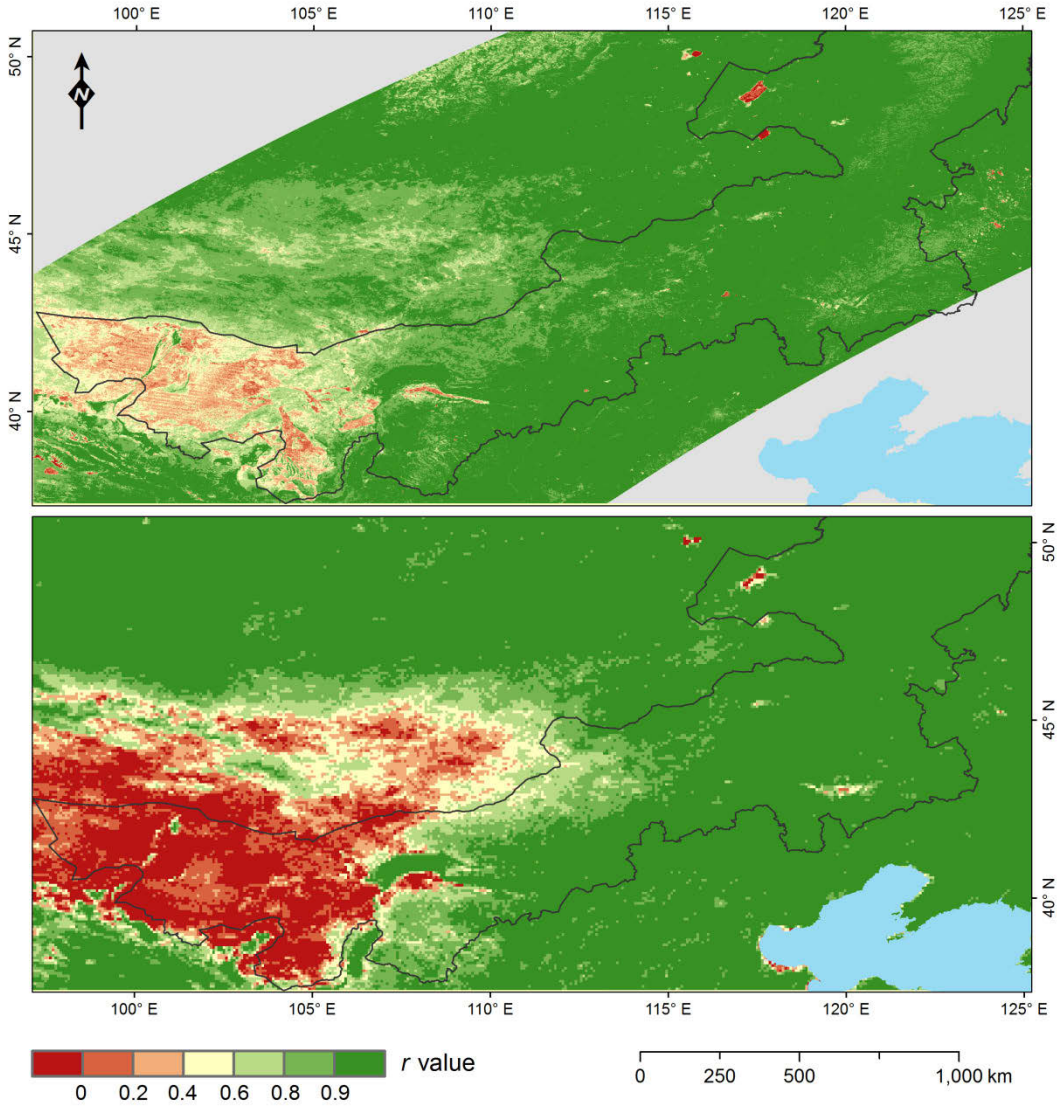

Figure II-2: Pearson's correlation coefficient (*r* value) between monthly 1-km SPOT VGT and MODIS (top), monthly 8-km SPOT VGT and AVHRR GIMMS (bottom).

Temporal trends derived from SPOT VGT and MODIS time series showed similar spatial patterns (Figure II-3). Most areas in Inner Mongolia did not show a significant trend during the past 10 years in neither SPOT VGT nor MODIS data ($p<0.05$, MSK test). Some regions, however, exhibited significant trends which were also captured in both datasets, e.g. a greening pattern extending from southern Inner Mongolia to the northern Shannxi and Shanxi provinces (Figure II-1, Figure II-3). Overall, 0.1% of Inner Mongolia exhibited significant negative and 3.3% significant positive NDVI trends based on SPOT VGT data. MODIS Terra based analyses resulted in 3.4% of the area having a statistically significant vegetation decrease, and 6.0% with a significant increase. Few regions showed trend disagreements ($p<0.05$, MSK test). Major discrepancies were found in the central Inner Mongolia, where SPOT VGT based trends showed little change and MODIS Terra NDVI decreased. In Hinggan, MODIS Terra NDVI increased less than that from SPOT VGT.

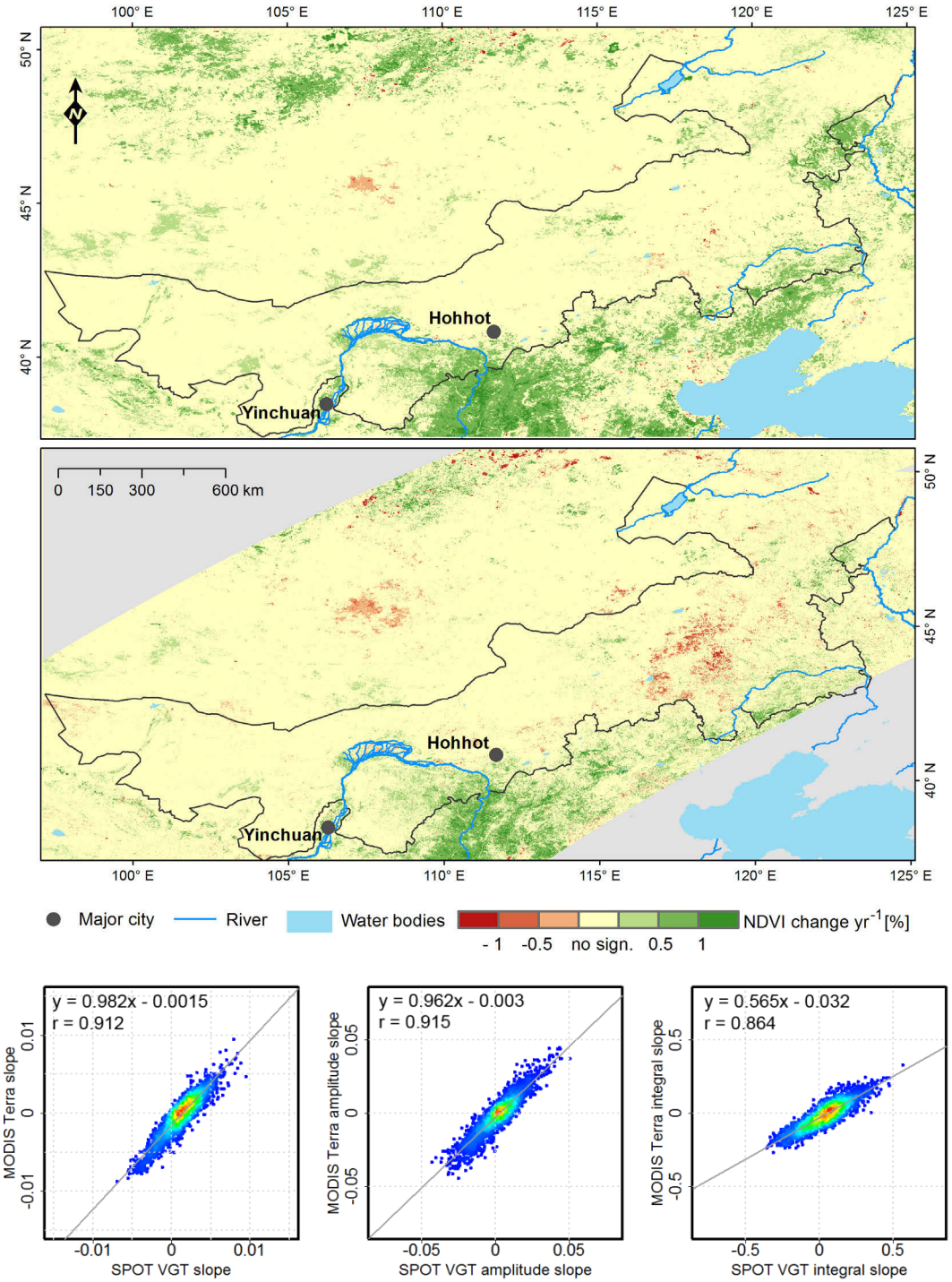

Figure II-3: Maps of NDVI change between 2001 and 2010 based on statistically significant Sen's slope of 1-km SPOT VGT (top) and 250-m MODIS (centre) time series (p<0.05, MSK test). Comparison of Sen's slope values for different phenological parameters based on 2770 sampling plots (bottom).

Compared to grassland, croplands showed more widespread increase in NDVI in both NDVI archives (Table II-2). About 18.0% and 24.3% of the pixels classified as croplands exhibited a positive trend based on SPOT VGT and MODIS Terra, respectively. Only 0.1% and 1.0% of the cropland pixels were characterized by a decreasing trend in SPOT

VGT and MODIS Terra data, respectively. Both NDVI archives showed the smaller NDVI changes for grassland areas. Only 9.8% of the grassland areas showed a significant increase and 0.4% a significant decrease in SPOT VGT data, while based on MODIS Terra 15.4% and 3.9% area of the NDVI in grasslands increased and decreased, respectively.

Table II-2: Statistics for SPOT VGT and MODIS Terra NDVI linear trend analysis from 2001 to 2010 (p<0.05, MSK test).

Observation	Cropland area (%)	Grassland area (%)
SPOT VGT NDVI positive slope	18.0	9.8
SPOT VGT NDVI negative slope	0.1	0.4
MODIS Terra NDVI positive slope	24.3	15.4
MODIS Terra NDVI negative slope	1.0	3.9

Similarly, we found that the spatial patterns of the trends derived from the NDVI amplitude and integral exhibited high similarities between SPOT VGT and MODIS Terra (not shown here for brevity). The regression analysis between SPOT VGT-derived and MODIS-derived trend parameters further confirmed a good agreement between the two NDVI time series (Figure II-3, bottom). For example, there was a strong correlation between NDVI trends derived from SPOT VGT and MODIS Terra (r = 0.91) time series, and also between trends in NDVI amplitudes (r = 0.92). The slope of the fitted regression functions showed a close to a 1:1-relationship. The correlation between Sen's slope of the integral of SPOT VGT against MODIS Terra was lower, but still indicated good correlation (r = 0.86). We therefore used the longer SPOT VGT time series for further analyses.

4.2 Correlation analysis and comparing trends from SPOT VGT and AVHRR GIMMS NDVI archives

The direct comparison between the NDVI time series from SPOT VGT and AVHRR GIMMS showed a similar strong linear correlation between the cyclic vegetation dynamics that dominate both archives. Comparable to the results from our comparison of SPOT VGT and MODIS Terra, NDVI time series from SPOT VGT and AVHRR GIMMS were positively correlated with generally high r values (r > 0.9) in vegetated areas of Inner Mongolia (Figure II-2, bottom).

However, when comparing inter-annual trends between SPOT VGT and AVHRR GIMMS NDVI, major disagreements became apparent (Figure II-4 top and center). Trends from AVHRR GIMMS showed, for example, a significant NDVI decrease in the vegetation-free

western part of Inner Mongolia. Almost the whole desert area exhibited this decreasing trend. In comparison, SPOT VGT did not show any significant trends in these areas. Considerable trend disagreement was also evident in northeast Inner Mongolia, where only AVHRR GIMMS-derived trends showed a strong greening pattern. Although the trend patterns from AVHRR GIMMS exhibit similarities with those derived from SPOT VGT in some regions, e.g. greening patterns in southern Inner Mongolia, trend discrepancies clearly prevail at a regional scale. Generally, the substantial trend disagreement in the maps was supported by a low *r* of 0.28, 0.42 and 0.37 (for trends derived from NDVI, amplitude and integral, respectively; Figure II-4, bottom).

As we were interested in better understanding the causes for the discrepancies, we analyzed if trend differences were associated with specific land cover categories and also if low NDVI values were differently affected than high NDVI values. To answer these questions we first grouped all pixels based on five land cover classes derived from the reclassified CAS map (excluding waterbodies, constructed area, and non-vegetated land), and then we grouped pixels based on 0.1 NDVI intervals from multiannual averages of SPOT VGT NDVI (Figure II-5). The slope differences derived from the two archives increased with higher NDVI levels (Figure II-5 left). This was also in agreement with forested areas exhibiting the largest trend disagreement between archives, while sparse grassland correlated better (Figure II-5 right). As grassland fractional cover increased, higher variance in differences and stronger average differences were observed between trends from both archives.

Trends derived from amplitude and integral also support these findings (not shown). Similarly, correlations of AVHRR GIMMS and SPOT VGT-derived Sen's slope values for all phenological parameters were low (Figure II-4 bottom).

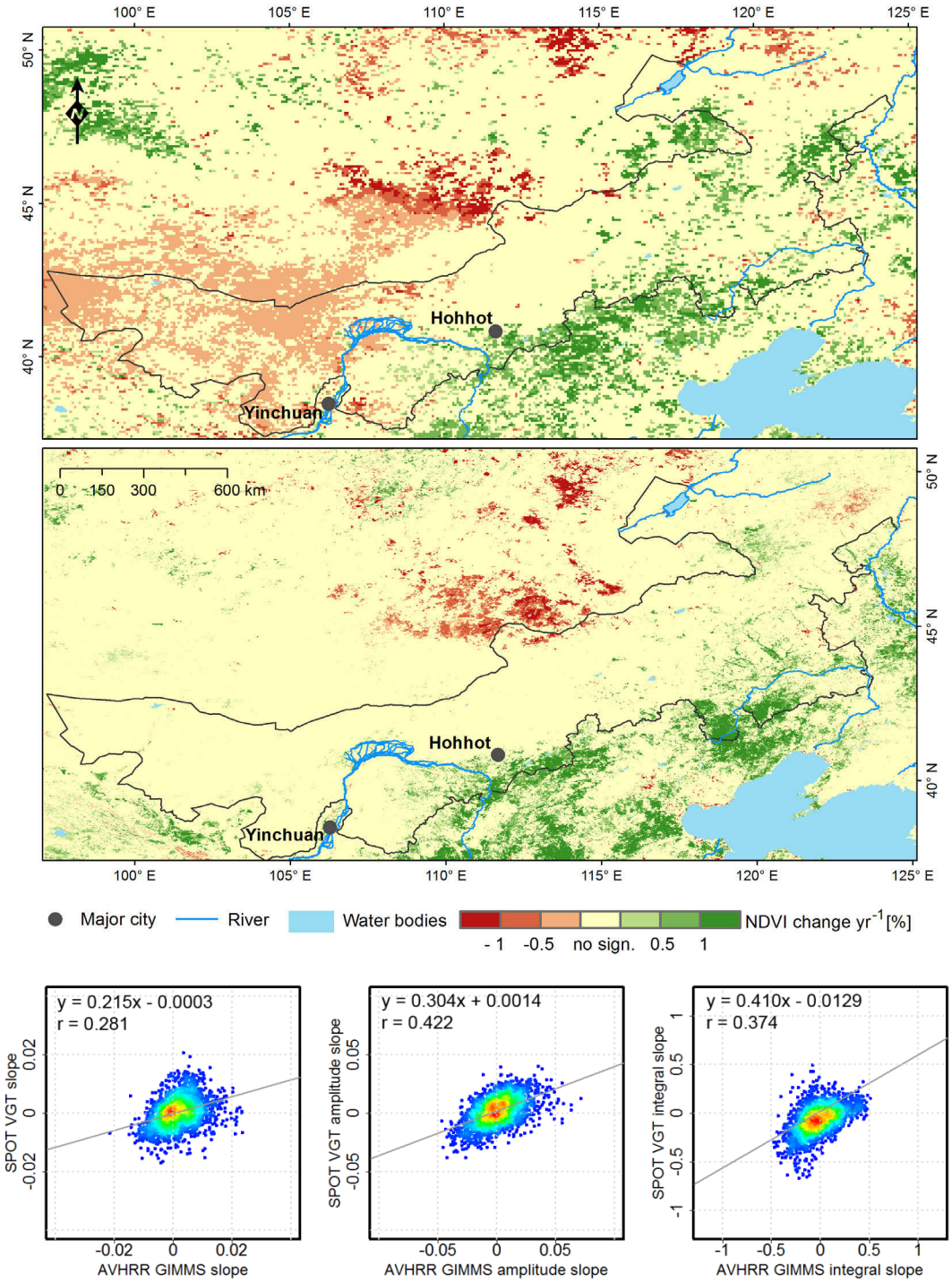

Figure II-4: Maps of NDVI change between 1999 and 2006 based on statistically significant Sen's slope of 8-km AVHRR GIMMS (top) and 1-km SPOT VGT (centre) time series (p<0.05, MSK test). Comparison of Sen's slope values for different phenological parameters based on 2770 sampling plots (bottom).

Large trend discrepancies between SPOT VGT and AVHRR GIMMS can be found in our test regions Ordos and Hinggan (Figure II-6). Grazing land did generally not exhibit strong trends for the Ordos region (Figure II-6, A), which is reflected in the SPOT VGT derived map. Significant changes between 1999 and 2006 relate to the growing city of Yinchuan

and intensified irrigation in its surroundings and along the Yellow River. Quite the opposite, trends from AVHRR GIMMS data clearly suggest strong vegetation cover decreases in the dryland areas, while there is no detection of increased productivity in irrigated west Yinchuan plain. Interestingly, AVHRR GIMMS data estimate changes in the opposite direction for the Hinggan region (Figure II-6, B).

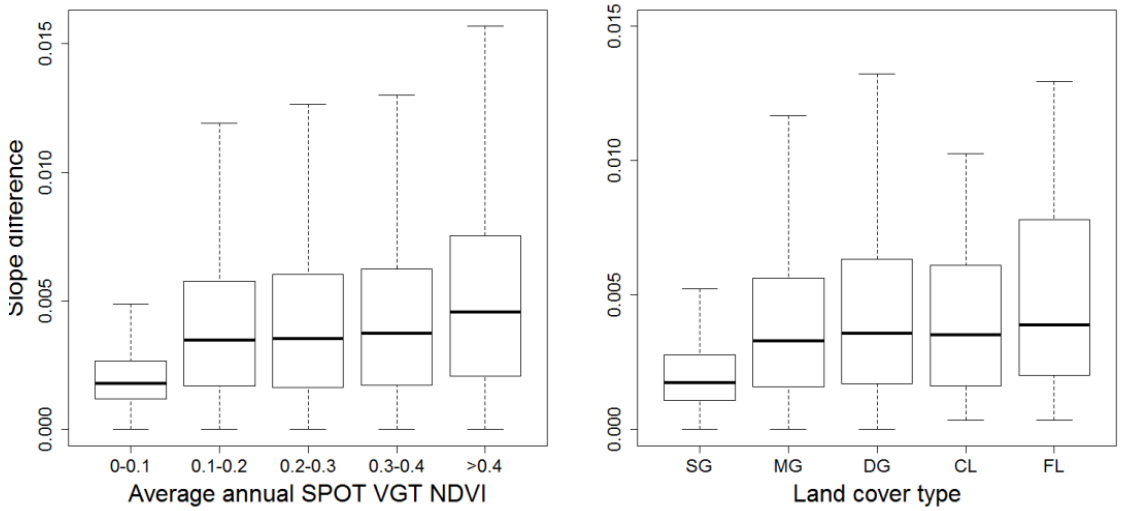

Figure II-5: Boxplots of absolute differences between regression (Sen's) slopes derived from SPOT VGT and AVHRR GIMMS time series grouped by land cover types (right) and SPOT VGT-based NDVI intervals (left). See Table 1 for a description of land cover types. The boxes represent first (25%) and third (75%) quartiles; the whiskers are defined as 1.5 times interquartile. The bold horizontal line in the box represent median.

To illustrate the disagreement in NDVI trends from the two archives, we plotted NDVI time series for selected pixels from both focus regions (Figure II-6). The samples show that SPOT VGT was able to depict the vegetation seasonality in a semi-arid to arid environment in the Ordos region, while AVHRR GIMMS did not resolve such information in years with low average NDVI (e.g. 2003 and 2005; Figure II-6). Major discrepancies also existed in 1999 and 2000 when NDVI values from AVHRR GIMMS were much higher compared to SPOT VGT, leading to a significantly decrease in NDVI for the Ordos region. In the Hinggan region, AVHRR GIMMS deviated from SPOT VGT mostly at the start of the time series (1999 and 2000), while the similarity much improved between these two products for later years. However, the considerably lower values from AVHRR GIMMS NDVI in these two years overall lead to a more positive trend compared to SPOT VGT.

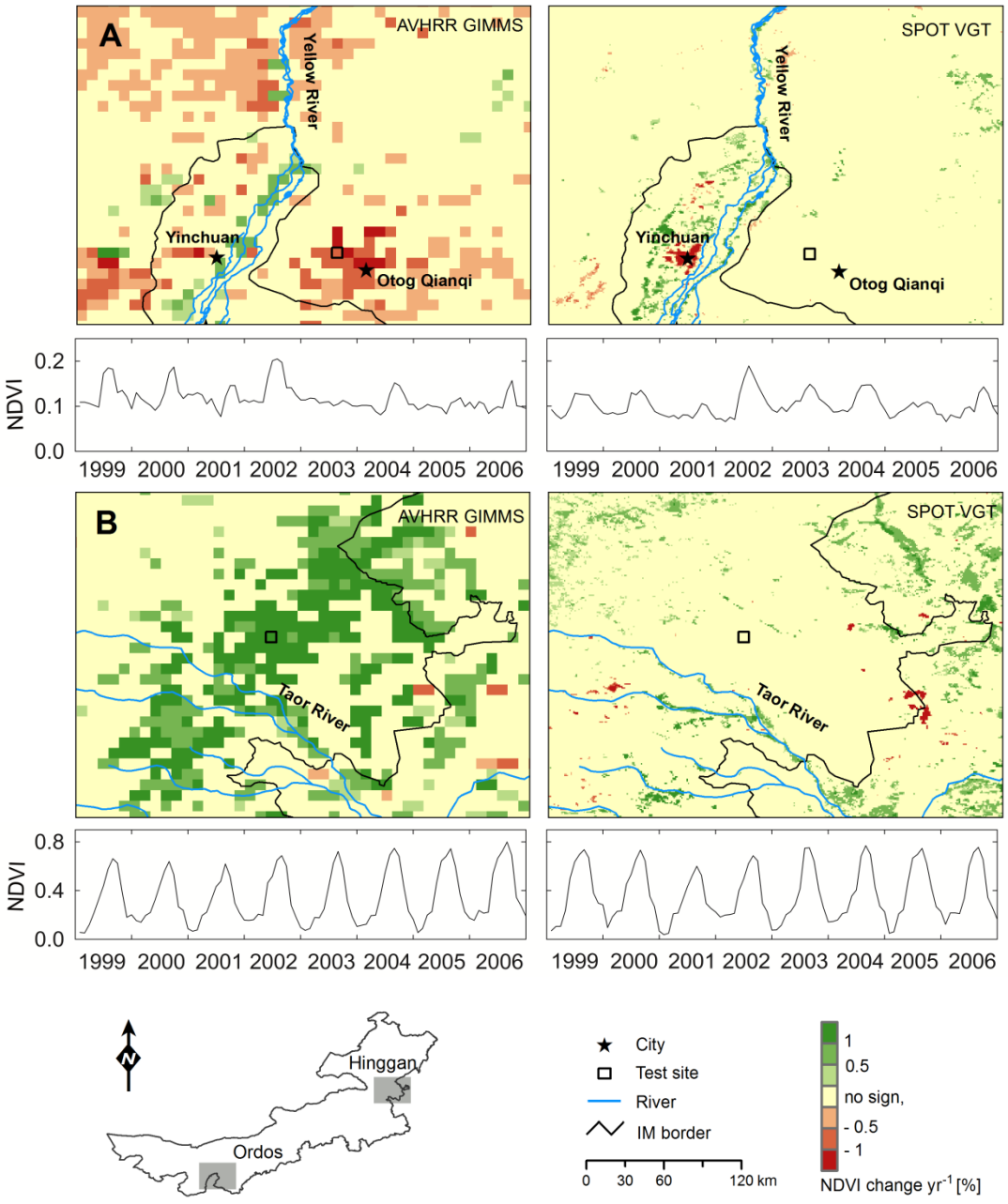

Figure II-6: Maps of Sen's slope for AVHRR GIMMS and SPOT VGT from 1999 to 2006 in Ordos (A) and Hinggan (B). NDVI time series for a sample location in Ordos and Hinggan (below respective maps)

5 Discussion

The high temporal resolution of global data sets such as AVHRR, MODIS and SPOT VGT allows us to derive indicators of agricultural dynamics across the globe. However, spectral mixtures and a broad range of problems largely related to the pre-processing of global remote sensing data sets complicate the interpretation of trends from such coarse resolution data (250m- 8 km). Thus, it is important to gain a deeper knowledge on the reliability of

temporal patterns derived from coarse resolution datasets before we interpret trends and link change trajectories to specific agricultural processes.

AVHRR-based NDVI datasets such as the AVHRR GIMMS data constitute the longest hyper-temporal remote sensing records for agricultural monitoring at global scales. Much research related to the impact of global climate change on agricultural productivity and to land degradation monitoring in arid and semi-arid agriculture is based on AVHRR GIMMS (Symeonakis and Drake 2004; Heumann et al. 2007; Dent et al. 2008; Helldén and Tottrup 2008; Fensholt and Proud 2012).

We established a benchmark for analyzing the consistency of AVHRR GIMMS-derived vegetation trends in Inner Mongolia, an important area of agricultural production in China, based on a comparison of MODIS and SPOT-derived trend parameters. Integrating large areas implies that average changes in NDVI are subtle. Still, similar patterns are found when comparing these effects in MODIS and SPOT VGT derived time series. The high consistency between MODIS Terra and SPOT-derived results proves the general reliability of analyses based on these archives. Our comparison shows that different satellite platforms and sensors, differing pre-processing schemes and moderately different spatial resolutions do not hamper the analytical potential of time series analysis when using MODIS Terra and SPOT-derived vegetation products. In Inner Mongolia, analysis based on both MODIS Terra and SPOT VGT allow for successfully analyzing multiple agricultural processes related to a set of agricultural and environmental policies in China addressing increasing agricultural production and decreasing environmental degradation.

Our results from the trend analysis of SPOT VGT and MODIS Terra time series indicate that land degradation processes only marginally affected the agricultural sub-systems of Inner Mongolia during the last decade. Most of Inner Mongolia's grasslands did not exhibit a significant change after the restrictive fencing policies were introduced for all the grassland in Inner Mongolia around the turn of the century. The significantly increasing trend of NDVI in mountainous environment (e.g. Loess Plateau, Yan Mountains) reflects the process of afforestation based on massive subsidization. The "greening" pattern also confirms the effectiveness of China's "Grain for Green" program in Inner Mongolia in the last decade (Figure II-3). However, comparing trends derived from SPOT-VGT and AVHRR GIMMS reveals that major discrepancies can occur when comparing trends from NDVI archives that are more profoundly different. This is also the case when compared the trends from all three NDVI archives during their overlap period (2001-2006) and using

increasing kernel size (3 x 3 GIMMS pixels) of sampling plots (not shown for brevity). Differences between NDVI trends seem to increase with increasing NDVI levels (Figure II-5 left). Fensholt et al (2012) assume on a global level that these deviations relate to land cover classes. Comparing different agricultural land cover categories with trend discrepancies (Figure II-5 right), our findings generally agree with this assumption. From our quantitative analysis across arid to semi-arid biomes, we conclude differently from Song et al (2010) that the differences in NDVI trends not only affected desert regions but also semi-arid landscapes. However, further tests across a broader range of biomes with in-depth regional information on land use and land cover changes will be needed to quantitatively confirm this finding. Different regional land surface biophysical properties and the limitations of NDVI in relation to the respective sensor characteristics and preprocessing schemes hence contribute to these trend differences (Kobayashi and Dye 2005; Nagol et al. 2009). Moreover, the sensitivity of trend analysis needs to be tested further to gain a more confident assessment for long-term land degradation (Wessels et al. 2012).

The two focus regions of Ordos and Hinggan served for a more detailed analysis of GIMMS- and SPOT VGT based trends. The Ordos region exhibited a clear decreasing trend in NDVI based on the GIMMS data for the Otog Qianqi grasslands that was not evident from SPOT VGT (Figure II-6). Likewise, the GIMMS-based trend analysis did not reflect the immense growth of Yinchuan city (negative trends), which was correctly identified in SPOT VGT-derived trends (Figure II-6). Our results for Ordos are in line with findings derived from Landsat data by Zhu et al (2008), which indicate a slight vegetation increase across different ecosystems during our observation period. Also, field-based measurements of vegetation cover, height and biomass indicate no broad-scale degradation in the vast grasslands of Otog Qianqi (Hasbagen 2009). The patterns related to agricultural intensification along the Yellow River in Ningxia (Figure II-1, Figure II-6) was captured both by SPOT VGT and AVHRR GIMMS. However, cropland intensification and expansion in the western Yinchuan Plain was not well detected based on AVHRR GIMMS data (Figure II-6).

In Hinggan, positive trends were extracted from SPOT VGT data along the Taor River valley. Rice is the main crop along the Taor River, and these positive trends correspond well with the intensified cropping system that was established in the early-1990s (Xia and Hu 2004; Liu et al. 2007a). AVHRR GIMMS derived trends did clearly not preserve the patterns retrieved from SPOT VGT (Figure II-6). While the overall trend is also positive,

the greening up for a major area north of the Taor River is largely overestimated, as the intensified irrigation does not prevail across these several 1,000 km^2. Moreover, land use and land cover change assessments based on Landsat data do not support the positive trends identified in AVHRR GIMMS data (Liu et al. 2010b).

We also observed an overall decreasing trend in AVHRR GIMMS-derived NDVI values across non-vegetated areas of Inner Mongolia. This trend was likely caused by satellite drift effects in the signal (Deng and Di 2001). NOAA AVHRR platforms do not allow for orbital drift adjustments, resulting in illumination differences affecting NDVI values (Sobrino et al. 2008). According to Pinzon et al (2007), EMD largely minimizes effects related to orbital drift. However, as AVHRR GIMMS data are not accompanied by metadata on applied pixel-wise EMD correction, it is not possible to conclude on the local effects of EMD.

Further, differences in atmospheric correction algorithms likely contributed to trend discrepancies. Natural variability in column water vapor, ozone and aerosol optical thickness (AOT) in the atmosphere can greatly affect land surface reflectance estimates (Kaufman 1988). Unlike MODIS on the Terra and Aqua platforms, AVHRR does not provide additional spectral channels that allow us to derive information on atmospheric composition to be used for correction (King et al. 1992; Nagol et al. 2009). To minimize impacts from the atmosphere, a bimonthly MVC is applied for the top-of-atmosphere GAC data to produce AVHRR GIMMS. However, it has been reported that MVC does not significantly improve data quality in regions with persistently high AOT (Kobayashi and Dye 2005; Nagol et al. 2009). This is most likely the case for Inner Mongolia, where high aerosol loads prevail due to frequent dust storms (Wang et al. 2004a).

Different spatial aggregation algorithms applied for producing NDVI archives certainly contribute to trend discrepancies as well. The input data used for producing the AVHRR GIMMS archive is the GAC 1B product, which is sampled spatially through a combination of line skipping and averaging (Goward et al. 1993; POES (U.S.) and NCDC (U.S.) 1997). Each GAC pixel (roughly 3km by 5km) is binned into one of the 8 km pixels of the output product based on a forward, nearest neighbor mapping, where the GAC pixel with the highest NDVI value is selected (James and Kalluri 1994). As a consequence, at least four GAC 1B pixels are mapped to one bin. At nadir, the binning can include up to 6 pixels (James and Kalluri 1994). The much coarser spatial resolution per AVHRR GIMMS pixel certainly hampers the comparability of AVHRR GIMMS to finer spatial resolution NDVI

archives. Specifically, knowledge on the detectability of fine scale processes in 64 km^2 pixels is limited, and statistically valid experiments for increasing our understanding based on field data are complex (Gupta et al. 2000; Hufkens et al. 2008). The small average patch size of Inner Mongolian croplands limits the ability of AVHRR GIMMS for consistent change detection. This is specifically the case for agricultural intensification along the river valley. Taking the smaller absolute vegetation variation in arid and semi-arid environments into account, NDVI derived from AVHRR data are generally less sensitive and hence less correspondent to finer spatial resolution NDVI archives.

Summarizing, our findings indicate a good agreement between trends from SPOT VGT and MODIS Terra for different agricultural land uses across Inner Mongolia, although the spatial and temporal resolution, the spectral bandwidths and preprocessing algorithms are different. This consistency is supported by trends based on phenological indicators derived from original NDVI time series. Overall, trend analyses from AVHRR-related products did in most cases not reproduce similar patterns of change across different agricultural systems across Inner Mongolia.

6 Conclusions

AVHRR GIMMS has regularly been employed for detecting hot-spots of land surface changes via NDVI trend analyses or NDVI-based phenological parameters derived from time series. While comparisons based on the raw time series indicate congruence between AVHRR GIMMS and other NDVI archives, more recent studies based on trend parameters derived from these archives indicate that inconsistencies exist between trends (Baldi et al. 2008; Alcaraz-Segura et al. 2010; Beck et al. 2011). We here demonstrated that considerable discrepancies in trend magnitude and direction exist between AVHRR GIMMS and SPOT VGT-based NDVI products (r = 0.28). These discrepancies are exemplified for a range of agricultural land use systems across Inner Mongolia. Analyses based on phenological parameters derived from such NDVI time series lead to comparable dissimilarities (supported by a low r of 0.42 and 0.37 from amplitude and integral, respectively). While quantifying the magnitude of different factors contributing to these inconsistencies is beyond the scope of this paper (and probably not possible due to the lack of empirical evidence), it is obvious that hyper-temporal NDVI products and related trend analyses from AVHRR GIMMS can strongly differ from those retrieved from instruments such as MODIS Terra and SPOT VGT.

We have shown that such deviations can occur regardless of the chosen trend indicator and across a range of agricultural systems. Comparing significant positive and negative trend hotspots in Ordos and Hinggan derived from SPOT VGT and AVHRR GIMMS revealed that even broad scale changes in vegetation cover can be missed in 8 km AVHRR GIMMS data.

There is an urgent need to better understand the opportunities and limitations of AVHRR GIMMS data in different regions of the world to advise a broad user community on where and how different NDVI archives can be reliably linked to derive longer and more reliable time series. Based on our findings along climate and land-use gradients from the Gobi desert to the northeast of China across the 3,000 km of Inner Mongolia, we caution that monitoring of agricultural lands based on hyper-temporal imagery from AVHRR GIMMS needs to be underpinned with viable consistency checks on the comparability of trends derived from time series in the respective regional setting. We conclude that AVHRR GIMMS and NDVI products from other sensors cannot be combined into homogeneous, long-term time series across the globe without regional sensitivity analyses.

Acknowledgements

This work was supported by the China Scholarship Council (CSC), Grant 2009601084. We want to thank Sebastian van der Linden for helpful comments on the manuscript. We are grateful to Zhengguo Li from the Chinese Academy of Agricultural Sciences (CAAS). We also thank Xueyong Zhao, Hao Qu, and Jie Lian of the Chinese Academy of Sciences (CAS) for their support on field data.

Chapter III:
Mapping annual land use and land cover changes using MODIS time series [1]

IEEE Journal of Selected Topics in Applied Earth Observations and Remote Sensing(in revision)

He Yin, Dirk Pflugmacher, Robert E. Kennedy, Damien Sulla-Menashe and Patrick Hostert

[1] A modified version of this chapter was published in *IEEE Journal of Selected Topics in Applied Earth Observations and Remote Sensing*, 2014, 7, 3421-3427

Abstract

Mapping land use and land cover change (LULCC) over large areas at regular time intervals is a key requisite to improve our understanding of dynamic land systems. In this study, we developed and tested an automated approach for mapping LULCC at annual time intervals using data from the Moderate Resolution Imaging Spectroradiometer (MODIS). Our approach characterizes changes between land cover/use types based on annual time series of per-pixel land cover probabilities. We used the temporal segmentation algorithm MODTrendr to identify trends and changes in the probability time series that were associated with land cover/use conversions. Accuracy assessment revealed good performance of our approach (overall accuracy of 92.0%). The method detected conversions from forest to grassland with a user's accuracy of 94.0±2.0% and a producer's accuracy of 95.6±1.6%. Conversions between cropland and grassland were detected with a user's and a producer's accuracy of 65.8±4.8% and 72.2±9.2%, respectively. We here present for the first time an approach that combines probabilities derived from machine learning (random forest classification) with time series based analysis (MODTrendr) for land cover/use change analysis at MODIS scale.

1 Introduction

Land use and land cover change (LULCC) is one of the critical drivers of global environmental change. Monitoring land use and land cover change is vital for a number of environmental monitoring applications, including carbon emission estimation, biodiversity conservation and land degradation mitigation (De Sherbinin et al. 2002). In this context, mapping LULCC at frequent (e.g. annual) time intervals is needed to improve our understanding of complex anthropogenic and natural drivers of change. Equally important, quantifying the consequences of land transitions is only possible based on frequent and reproducible LULCC monitoring procedures (Kuemmerle et al. 2013).

Coarse resolution satellite sensors like Advanced Very High Resolution Radiometer (AVHRR), SPOT-Vegetation (SPOT-VGT), Medium Resolution Imaging Spectrometer (MERIS), and Moderate Resolution Imaging Spectroradiometer (MODIS) have great potential for consistent large-area land surface monitoring because of their frequent revisit times and wide swaths. The near daily observations have enabled spatial analyses of land surface phenology (Ganguly et al. 2010) but to-date only few studies have used MODIS time series to map land cover changes at annual intervals. For example, Lunetta *et al*. (2006) used multi-temporal MODIS NDVI composites and a standard normal distribution statistical approach to detect land cover changes on a yearly basis. They successfully detected changes in non-agricultural areas using a 4-year MODIS time series from 2002 - 2005. Recently, Sulla-Menashe *et al*. (2014) created annual maps of forest disturbance from MODIS Normalized Burn Ratio (NBR) time series using a temporal segmentation algorithm. The continuous and increasing record of MODIS makes it suitable for long-term land cover change monitoring.

Given the importance of regional and global environmental monitoring, developing cost-effective, accurate, and consistent methods for mapping LULCC over large areas is a growing area of research (Clark et al. 2012). While methods for regional and global land cover monitoring have greatly evolved and annually updated land cover maps have been produced for many regions (Friedl et al. 2002; Clark et al. 2010), automated methods and standards for mapping LULCC at annual intervals are not readily available. This disparity has consequences for land change analyses. It is commonly accepted that land cover change cannot be accurately mapped via simple post-classification analyses of existing land cover products due to the large year-to-year variability of spectrally similar classes

(Friedl et al. 2010; Fritz et al. 2011). A variety of studies have developed approaches to overcome this problem. For example, Liu and Cai (2012) developed a classification approach to classify Landsat images from multiple time periods simultaneously instead of individually. Incorporating contextual information of spatially and temporally neighboring pixels into a probabilistic classification model helped to reduce the impact of classification errors on change detection. However, the approach requires specifying a transition probability model, and including spatial context information may be less suitable for coarse-resolution imagery, at least in heterogeneous environments. Other studies have employed temporal filters with transition rules (Clark et al. 2012) and change-based updating to develop temporally consistent land cover time series (Pouliot et al. 2014). For example, Pouliot et al. (2014) generated a base map from MODIS time series and recursively updated it using land cover change maps and land cover change transition matrices. Change-based updating methods have improved the inter-annual consistency of land cover time series, but their performance in estimating land cover changes has not been rigorously assessed.

Recently, novel approaches have emerged for land cover change mapping from satellite images time series. These trajectory-based methods make full use of dense image time series to identify trends and breakpoints that represent land cover change on the ground. Several packages and algorithms such as LandTrendr (Landsat based detection of trends in disturbance and recovery) (Kennedy et al. 2010), BFAST (Breaks For Additive Season and Trend) (Verbesselt et al. 2010a), and TimeStats (Udelhoven 2011) have been developed and applied to monitor regional to global land surface change. Trajectory-based change mapping has greatly increased the capacity of depicting a variety of land cover changes that are difficult to detect with traditional two-date or multi-date methods, e.g. long-term, gradual change processes like degradation and afforestation and short-term changes in highly resilient systems.

In past studies, trajectory methods have been applied to single spectral bands, vegetation indices such as NBR (Meigs et al. 2011), tasseled cap (TC) components (Pflugmacher et al. 2012), normalized difference vegetation index (NDVI) (Stellmes et al. 2013), and to biophysical metrics such as aboveground biomass (Powell et al. 2010; Main-Knorn et al. 2013). In either case, a priori knowledge of the per-pixel land cover type or condition is needed to translate spectral quantities into physical land surface properties. This process is straightforward if only changes between two end-member conditions are sought, e.g. forest and non-forest or high biomass and low biomass. To our knowledge, all past studies have

therefore focused on changes between two conditions within the scope of forest monitoring. However, if changes between multiple land surface conditions are of interest, the change attribution becomes challenging.

One possible means to facilitate time series analyses of multiple land cover conditions is by using land cover class probabilities. Land cover probabilities describe the chance that a pixel belongs to a certain land cover class. Therefore, probabilities should be more directly related to land cover changes than the underlying spectral values or vegetation indices (Broich et al. 2011). By representing land cover as a continuous measure rather than a discrete class, quantitative time series methods can be applied to separate inter-annual changes in class membership resulting from classification uncertainties from true changes. Compared to discrete classifications, land cover probabilities can also capture sub-pixel heterogeneity and mixtures of different land cover types in coarse-resolution data (Colditz et al. 2011). The utility of probabilities or probability-like metrics for tracking changes in satellite time series have previously been demonstrated in the context of forest change detection (Huang et al. 2010; Broich et al. 2011). Huang *et al*. (2010) used a z-score (also standard score) to detect changes in forest-ness and to reconstruct historic forest disturbance events. Broich *et al*. (2011) quantified forest loss using time series of forest probability metrics derived from a decision tree classifier.

In summary, methods for mapping annual LULCC across different biomes and at regular time intervals are much needed. Despite the recent advances in trajectory-based change detection, there is a specific need to test such approaches not only to detect forest changes, but also to map changes in other land cover types. Considering that probability metrics are useful quantitative descriptors of land cover class membership, it seems logical that integrating probability-metrics with trajectory-based change models can provide a potential solution. In this work, we aim to test the utility of a trajectory-based change detection approach applied to MODIS data to map annual LULCC using time series of land cover class probabilities for multiple land cover class trajectories.

2 Study area

To test our approach we selected a study region in Inner Mongolia (China), more specifically an area of 656,819 km^2 covered by MODIS tile h26v04 (Figure III-1). The region is an interesting test area because Inner Mongolia has experienced substantial changes in land use in the last decade. On one hand, strict vegetation protection and

regeneration policies have been implemented in this region for mitigating severe land degradation since 2000s (Wang et al. 2013). Most of the natural forests have been protected and massive investments were poured into forest recovery programs (Liu et al. 2008). On the other hand, the increasing price of agricultural products led to cropland cultivation on grassland, whereas governmental programs have encouraged the conversion of existing croplands to grassland (Wang et al. 2012b). The combination of multiple land cover/use changes, the rapid change regimes and our knowledge on change trajectories in the region render this area a good test case for evaluating our proposed method of annual LULCC detection.

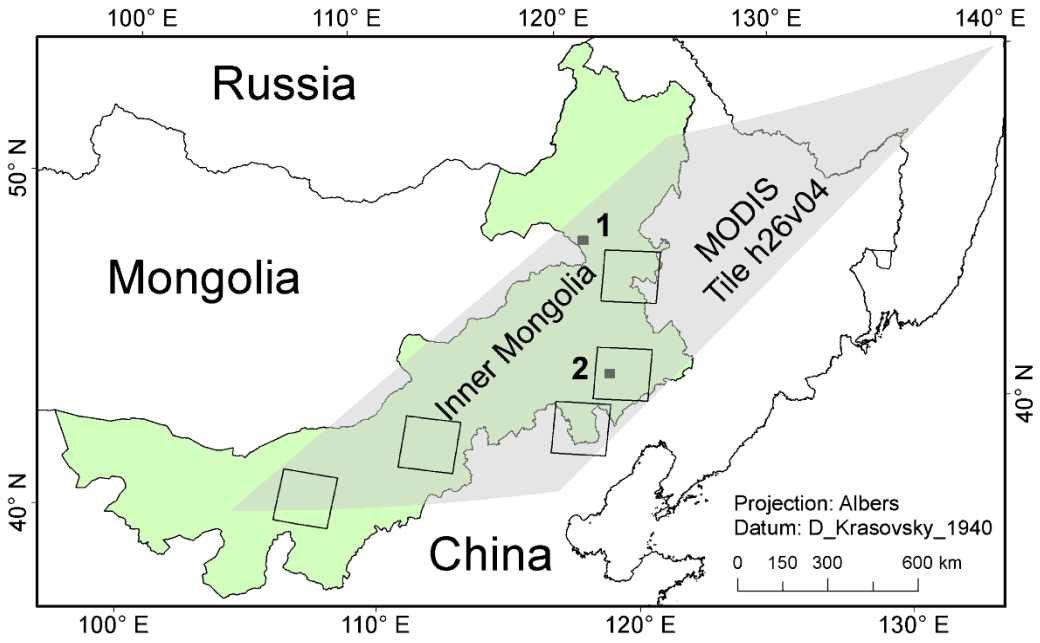

Figure III-1: Location of study area (MODIS tile h26v04) within Inner Mongolia, China, the grey dots with numbers marked the regional subsets in Figure III-2 (1) and Figure III-3 (2). Five Landsat scenes used for labeling validation samples are shown as black frames.

3 Methodology

3.1 Data and data preparation

We used the MODIS-Terra Vegetation Index (VI) product (MOD13Q1, Collection 5) for mapping annual land cover probabilities. The MODIS VI product is a 16-day composite with a nominal 250-m spatial resolution. MODIS VI includes Normalized Difference Vegetation Index (NDVI), Enhanced Vegetation Index (EVI), surface reflectance in the blue, red, near-infrared (NIR), mid-infrared (MIR) wavelengths, and pixel quality data. We

obtained all available imagery for MODIS tile h26v04 between mid-February 2000 and December 2011 from the United States Geological Survey (USGS) Land Processes Distributed Active Archive Center (https://mrtweb.cr.usgs.gov/).

To reduce residual noise in the time series caused by clouds, ozone, dust, off-nadir viewing and low sun zenith angles, we smoothed the data using a Savitzky-Golay filter from the TIMESAT software (Jonsson and Eklundh 2004). Pixels flagged as no data, snow/ice or cloud in the MOD13Q1 pixel reliability layer were excluded prior to the filtering. Outliers that were not identified as such in the MODIS reliability layer were removed by a Seasonal-Trend decomposition based on Loess (STL) (Cleveland et al. 1990), which is global in character and not dependent on ancillary data.

The Chinese Academy of Sciences' (CAS) Land-Use/Land-Cover (CAS-LUCC) database (Liu et al. 2002), Landsat imagery and Google Earth™ (GE) imagery covering Inner Mongolia were used as reference data for labeling training samples. The CAS-LUCC dataset was derived from Landsat TM and CBERS-1 (China-Brazil Earth Resources Satellite-1) imagery acquired during 1999-2000. The map has six land use and land cover classes in level I, including cropland, forest, grassland, constructed area, water and bare lands. CAS-LUCC has a reported overall accuracy of 81.0% for all of China.

3.2 Predicting annual land cover probability

We used random forest (RF) classification (Breiman 2001) implemented in the EnMAP-BOX software (Rabe et al. 2014) to predict land cover class probabilities for each year between 2000 and 2011. The number of variables randomly sampled as candidates at each split (mtry) was set to the square root of the number of input variables, the minimum size of the terminal nodes and the number of the trees was set to we used 10 and 500 respectively. Per-pixel probability for each land cover class was estimated as the proportion of tree votes for a given class. Focal classes were: cropland, forest, grassland, water and non-vegetated areas (constructed areas and bare lands). The CAS-LUCC dataset served as an initial source for training data generation. Because training data were not available for every year, we employed a signature generalization approach that trains individual classification models for each year based on reference locations with stable land cover (e.g. (Gray and Song 2013)). We identified and labeled stable training samples as follows: First, we randomly distributed samples with the center of each sample snapped to the center of the nearest MODIS pixel. We enforced a minimum distance of 1500 m between samples to avoid spatial autocorrelation and along-scan triangular point spread function (PSF) effects

(Tan et al. 2006). Each sample unit was set to a square with 1.5 times the side length of a MODIS pixel. Second, we calculated the land cover proportions in each sample using the CAS-LUCC dataset and labeled each sample according to the dominant land cover class while retaining only samples with a single dominating class of more than 80%. To generate a temporally stable dataset, we then calculated, for each sample, the linear regression slope of the average growing season NDVI across the 12-year time series and eliminated samples with a statistically significant slope ($p<0.05$). Finally, we visually cross-checked the remaining samples against the Landsat archive and GE™ imagery to eliminate and correct miss-classified samples. In all, 49,852 samples were available for model training.

We calculated several seasonal statistics from the MODIS time series to serve as predictor variables in the RF models. For each smoothed MODIS time series (NDVI, EVI, and four reflectance bands) and each year, we computed the mean, minimum, maximum, range and standard deviation for the first half (March – June), and the second half of the growing season (July – October), as well as the entire growing season, respectively.

3.3 Temporal segmentation of probability time series and LULCC labeling

Even class probabilities based on smoothed time series may contain residual inter-annual noise (e.g. due to model prediction errors). Thus, we used the time series segmentation algorithm MODTrendr (Kennedy et al. 2010; Sulla-Menashe et al. 2014) to detect and describe changes in each pixel's class probabilities over time. MODTrendr fits a series of linear segments to each pixel's time series, where each segment describes a distinct period of change or no change between two points in time (Kennedy et al. 2010). The fitting reduces inter-annual noise and a variety of change statistics can be extracted from individual segments or groups of segments. Key metrics include the class probability and the year of the segment start and segment end, segment duration (years) and change magnitude (difference between probability of segment end and segment start). MODTrendr is an adaptation of the Landsat-based LandTrendr algorithm (Kennedy et al. 2010) for MODIS data. The algorithm has recently been applied for detecting forest disturbances in the Pacific Northwest, USA. After a few tests, we decided to use the same fitting parameters as in Sulla-Menashe et al (2014), except that we used a more restrictive significance threshold for model fitting (p-value=0.05) and a higher number of trajectory segments (6) as in Kennedy et al (2010).

We applied MODtrendr to all five land cover class probability time series. We identified pixels with permanent land cover (no change) where the highest MODTrendr-fitted

probability always belonged to the same land cover class across the entire time period. For example, a pixel was labeled as permanent forest if the forest class probability was always higher than the other class probabilities during the 12 years. To detect and describe pixels that underwent land cover change, we used the change magnitudes of the MODtrendr segments. For each land cover probability time series, we derived two metric sets - greatest decrease and greatest increase to represent land cover loss and gain, respectively. First, we labeled segments representing land cover loss when the change magnitude was -0.4 or less and the pre-change probability was greater than 0.5, as these thresholds resulted in balanced omission and commission errors. For each pixel we recorded the converted land cover class and the timing of the conversion based on the year when the change segment ended. To identify the land cover class following the conversion, we selected class probability segments with a positive change magnitude of 0.4 or greater occurring within 1 year of the detected conversion. Thus, a pixel was flagged as a land cover conversion when a pronounced land cover loss in one land cover probability trajectory occurred simultaneously with a gain in another land cover type.

3.4 Accuracy assessment

Validating LULCC classes was challenging because the number of change classes substantially increases with the number of land cover classes for which change is observed (Olofsson et al. 2013). In our case, annual changes between five land cover types resulted in 220 change classes over 12 years. Collecting reference samples for all change classes and years is not feasible. Thus, we temporally aggregated change classes for the accuracy assessment and focused on four conversions that represent major land use and land cover change processes in Inner Mongolia during the first decade of 21th century, i.e. on conversions between forest and grassland, and conversions between cropland and grassland (Liu et al. 2009).

Each conversion class was aggregated into two time windows: 2000-2005 and 2006-2011, as those two periods relate to the early and late impact periods of policy-induced changes in Inner Mongolia. Grassland-forest conversions were assessed across the entire time period (2000-2011) because the gradual process of tree growth requires longer records for assessment.

We used a disproportionate stratified estimator at pixel level for our accuracy assessment. We randomly selected five Landsat footprints (p121r28, p121r30, p122r31, p126r31, p129r32) across our study area and randomly selected 100 MODIS pixels as reference

samples within each change class and 200 pixels for non-change classes across footprints (except water: 100 only, due to class size). Each reference sample was manually labeled by an expert interpreter without knowledge of the mapped class label using Landsat images acquired around 2000, 2005 and 2011 during the late growing season (July-October). In addition to the Landsat images, the interpreter also used temporal profiles of MODIS NDVI time series (MOD13Q1) to aid labeling samples with data gaps in the Landsat images and gradual change classes (e.g. conversion from grassland to forest). For each time period, the interpreter recorded the dominant land cover based on the area proportion in the sampling unit. If no change occurred, the sample was labeled as permanent class, e.g. permanent forest and permanent grassland. If the dominant land cover changed between two time periods, the sample was labeled as change classes, e.g. cropland to grassland.

Finally, we constructed an error matrix adjusted for the disproportional sampling (Card 1982; Olofsson et al. 2013), from which we calculated overall accuracy, commission and omission errors.

4 Results

In all, MODTrendr mapped land use and land cover changes with a high overall accuracy (OA) 92.0% (Table III-1). Permanent forest had the lowest commission error (CE) rate of 2.0%, followed by permanent cropland (4.0%) and permanent non-vegetated areas (5.0%). Forests also showed a low omission error (OE) rate of 3.3%, whereas croplands and grasslands had higher OE but less than 10%. Among change classes, MODTrendr detected conversions from forest to grassland most accurately. Here, omission and commission errors of forest changes were lower than 10%. The conversions between croplands and grassland were mapped with less accuracy (e.g. CE between 30-40%). However, conversions from grassland to cropland were consistently better detected than conversions from cropland to grassland. With respect to timing of the detected changes, we found little confusion between different time periods (e.g. CG1 and CG2, Table III-1). This suggests that, for the periodic assessment, the timing of the change was accurately detected.

Figure III-2 and III-3 shows two examples of probability time series and the corresponding MODTrendr results. The first example shows the detection of forest loss in the transitional zone between grassland and forest. A fire disturbance in 2003 spread from the western plains to the mountainous areas in the East causing forest conversion to open grassland. In

the land cover probability time series, the change is marked by a sudden decrease of forest probability and a rapid increase of grassland probability (Figure III-2, E).

Table III-1: Error matrix showing estimated area proportions (%) of land cover/use conversion after adjusting for disproportional sampling.

	PC	PF	PG	PW	PN	FG1	FG2	GF	GC1	GC2	CG1	CG2	O	CE
PC	20.83	0	0.87	0	0	0	0	0	0	0	0	0	0	0.04
PF	0	8.96	0.14	0	0	0	0	0	0	0	0	0	0	0.02
PG	1.66	0.28	50.18	0	3.33	0	0	0	0	0	0	0	0	0.10
PW	0	0	0.00	0.18	0	0	0	0	0	0	0	0	0.02	0.11
PN	0	0	0.49	0	9.36	0	0	0	0	0	0	0	0	0.05
FG1	0	0.01	0	0	0	0.18	0.01	0	0	0	0	0	0	0.08
FG2	0	0	0	0	0	0.01	0.12	0	0	0	0	0	0	0.04
GF	0	0.02	0	0	0	0	0	0.12	0	0	0	0	0	0.14
GC1	0.05	0	0.02	0	0	0	0	0	0.20	0.02	0	0	0	0.32
GC2	0.05	0	0.04	0	0	0	0	0	0.02	0.26	0	0	0	0.30
CG1	0.02	0	0.02	0	0	0	0	0	0	0	0.09	0	0.01	0.39
CG2	0.01	0	0.03	0	0	0	0	0	0	0	0.01	0.10	0.01	0.36
O	0	0	0.14	0.05	0.05	0	0	0.02	0.05	0.02	0.05	0.05	1.88	0.18
OE	0.08	0.03	0.03	0.21	0.26	0.03	0.06	0.16	0.26	0.15	0.37	0.33	0.02	

Class codes: PC: permanent cropland, PF: permanent forest, PG: permanent grassland, PW: permanent water, PN: permanent non-vegetated areas, FG1: conversion from forest to grassland (2001-2005), FG2: conversion from forest to grassland (2006-2011), GF: conversion from grassland to forest (2001-2011), GC1: conversion from grassland to cropland (2001-2005). GC2: conversion from grassland to cropland (2001-2005), CG1: conversion from cropland to grassland (2001-2005), CG2: conversion from cropland to grassland (2006-2011), O: other change types, CE: commission error, OE: omission error

The second example illustrates the expansion of cropland into grassland previously used for grazing (Figure III-3). The replacement of grassland with cropland is visible by an abrupt decrease of grassland probability and a simultaneous rapid increase of cropland probability (Figure III-3, E). The final change map shows that cultivation in this region started in areas close to permanent croplands and then quickly expanded into the grassland area.

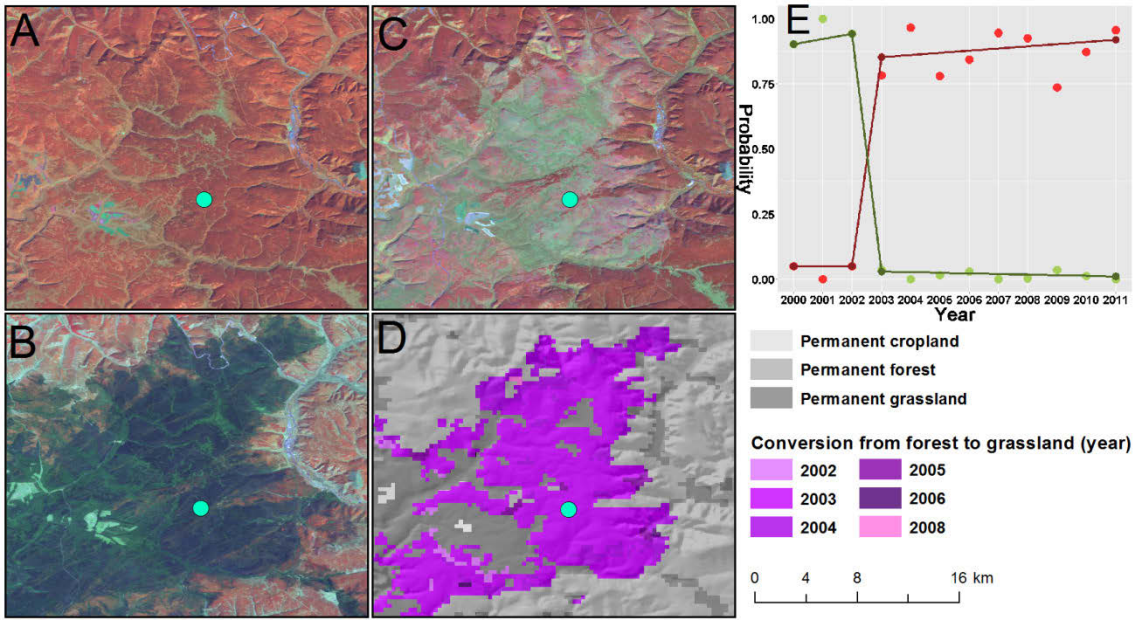

Figure III-2: Conversion from forest to grassland. Landsat composites (p122r27, RGB=4, 5, 3) for 2002 (A), 2003 (B) and 2011 (C). D: LULCC map. E: Source values and fitted probability trajectories in red (grassland) and green (forest); source location marked in cyan in A-D.

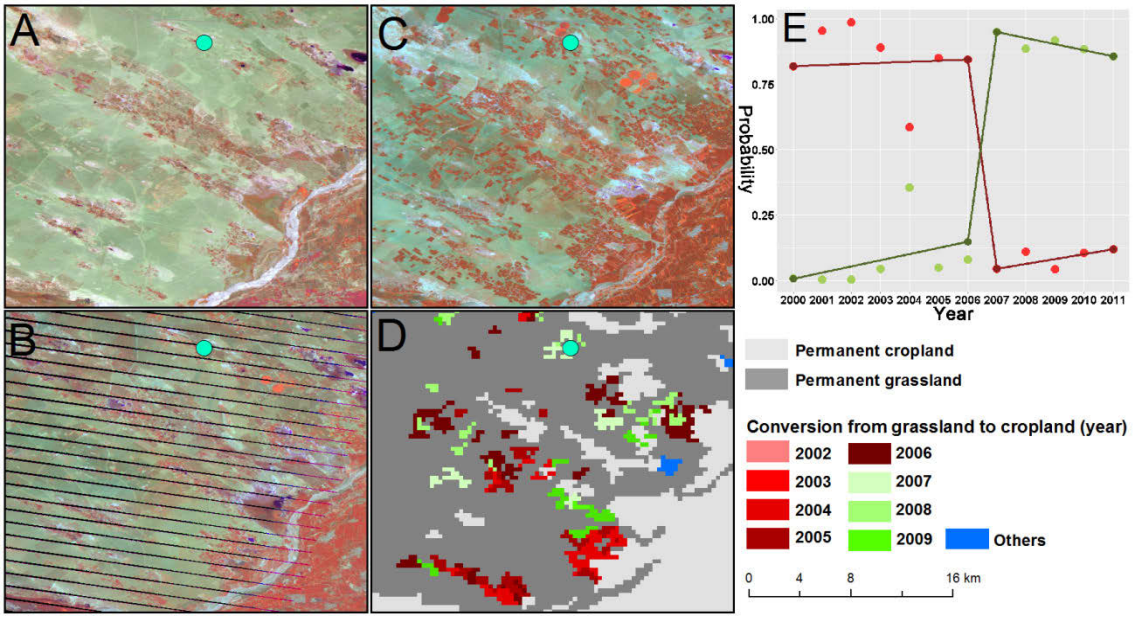

Figure III-3: Conversion from grassland to cropland. Landsat composites (p121r30, RGB=4, 5, 3) for 2000 (A), 2005 (B) and 2010 (C). D: LULCC map. E: Source values and fitted probability trajectories in red (grassland) and green (cropland); source location marked in cyan in A-D.

5 Discussion

We demonstrated that time series of land cover probabilities derived from MODIS data can be used to map land-cover and land-use changes at annual intervals. To detect and map

changes, we used a trajectory-based change detection algorithm MODTrendr, which has previously been applied to detect forest disturbances. Here we applied the algorithm to map multiple LULCC, and achieved an overall mapping accuracy of 92.0%.

Despite the high overall accuracy, uncertainties still exist: Errors in LULCC maps may relate either to poor land cover probability estimates or from MODTrendr model fitting. For permanent classes, we found most of the errors stemming from the confusion between permanent grassland and permanent non-vegetated areas. This is due to the confusion between very low vegetation coverage in sparse grasslands and barren land in semi-arid environments (Huttich et al. 2011). Moreover, rainfall is the main driver for vegetation growth in drylands and exhibits large temporal variance, which makes it even more challenging to distinguish permanent grassland and barren lands. Similarly challenging was mapping conversions between croplands and grasslands. As grassland and cropland, especially non-irrigated cropland, can exhibit similar spectral and temporal responses, it can be difficult to separate these two classes and map the conversions reliably on remote sensing data alone, regardless of the underlying methodology. Generally, grassland to cropland conversion was more reliably detected than the other way around. Based on our knowledge of the study area, the confusion between permanent cropland and the conversion of grassland to cropland was most likely caused by agricultural intensification on previously non-irrigated croplands.

Uncertainties also remained in model fitting. To provide a conservative estimate for each land cover conversion, a relatively high threshold of change magnitude was set to balance commission and omission errors. However, reducing false positives may lead to underestimating subtle change classes, e.g. the gradual desertification of grasslands to barren land. However, to test the sensitivity of our approach in these sparsely vegetated areas will require more accurate reference data than what we could obtain from Landsat and Google Earth. Moreover, our observation period is relatively short with regard to long-term change processes in comparison to the data-inherent signal-to-noise ratio over time. Nevertheless, the forest-cropland and cropland-grassland changes in our study regions were distinct enough to enable their detection with a 12-year MODIS time series.

The high mapping accuracy was derived using both homogenous and heterogeneous validation samples, suggesting the capacity of combining land cover probability and MODTrendr for sub-pixel change detection. As illustrated in Boschetti et al (2004), depicting sub-pixel classes from coarse resolution satellite data could be biased either due

to omission or commission errors. Though sub-pixel fractional error matrices can assess the accuracy of static land cover mapping in mixed pixels (Latifovic and Olthof 2004), validating sub-pixel changes between multiple land cover classes remains challenging because of the inherent data limitation and the complexity of land cover conversions. Further efforts are therefore needed to address the mapping accuracy of land cover conversions at sub-pixel scales using coarse resolution imagery.

6 Conclusion

In this study, we illustrated the potential of using land cover probabilities derived from MODIS data for annual LULCC mapping. While the idea of using land cover probabilities for mapping land cover is not new, the utility of probability time series for subsequent land cover change monitoring has not yet been exploited. Using probability estimates instead of spectral indices in trajectory-based change detection has the advantage that observed changes and trends are more directly linked to specific changes in land cover and land use. This facilitates monitoring of multiple land conversion trajectories. At the same time, the approach requires that probabilities be estimated for each image in the time series, which can be initially more time consuming. Here, we used RF models and a signature generalization approach to estimate per-pixel land cover probabilities for each year. However, probability maps can be produced with a variety of different methods. In fact, probabilities are often "by-products" of discrete classifications. Thus, land cover probabilities might be a useful way to combine information from different map sources and sensors. This should encourage map producers to release probability maps in addition to the original products. The presented study highlights the capacity of trajectory-based methods for LULCC mapping at annual intervals. To our knowledge, this is the first study that has applied a trajectory-based approach for mapping land cover conversion. We demonstrated the capacity of our approach for monitoring different change types (e.g. abrupt and gradual change) and categories (e.g. conversions between cropland and grassland) using dense MODIS time series. In all, this study provides a thorough insight for detecting *how* and *when* land surface was altered thus benefit deeper understanding about the change drivers in the context of global environmental change.

Acknowledgements

This work was supported by the China Scholarship Council (CSC), Grant 2009601084. MODIS data provided by USGS and the LUCC dataset from CAS are highly appreciated.

Chapter IV:
Land use and land cover change in Inner Mongolia – understanding the effects of China's re-vegetation programs

in preparation

He Yin, Dirk Pflugmacher, Ang Li, Zhengguo Li and Patrick Hostert

Abstract

During the past decades, overuse of land resources has increasingly contributed to environmental crises in China. To mitigate wide-spread land degradation, actions have been taken to maintain and restore ecologically valuable landscapes such as natural forests. However, the effects of the various vegetation protection policies that have been implemented in China since the late 1990's still remain largely unknown. In this paper, we therefore focus on mapping land use and land cover change (LULCC) in Inner Mongolia, one of the key regions targeted by Chinese ecological restoration programs. We used 250-m MODIS time series and a random forest classification approach to generate annual probabilities for each land cover class between 2000 and 2012. We then applied a trajectory-based change detection algorithm, a modified version of LandTrendr (Landsat-based detection of trends in disturbance and recovery), to the probability time series to map land cover changes. We found that our trajectory-based approach achieved high accuracies (overall accuracy 0.92). It provides spatio-temporal land change maps that allow land-use related interpretation of change patterns. Our change maps show, that i) deforestation decreased rapidly after 2000 and forest regeneration occurred in the ecological program zones, leading to a net forest increase in Inner Mongolia, and ii) cropland retirement mostly occurred at the early stage of ecological programs and mainly concentrated in drier environments and steep terrain. Our results suggest that ecological programs implemented in China during the past decade played a positive role for maintaining forests, promoting forest regrowth, and reducing human pressure on land in Inner Mongolia. Overall, land cover mapping and trajectory-based remote sensing data analysis allowed a consistent characterization of LULCC over large areas, which is crucial for gaining a better understanding of environmental changes in the light of rapidly changing environmental policies and governance regimes.

1 Introduction

Land use and land cover change (LULCC) is one of the most important processes related to global environmental change (Foley et al. 2005). Political decisions or institutional change, however, often cause non-linear trends in land systems (Lambin and Geist 2006). Land laws or regulations largely determine whether or not land is developed or utilized. Rapid land system changes are often directly related to changing governance regimes, e.g. reduced deforestation rates after a logging ban (Wang et al. 2004b; de Blas and Perez 2008; Barsimantov and Antezana 2012), cropland expansion on grassland (Ojima et al. 2004; Wang et al. 2012b; Miao et al. 2013), or land abandonment in post-communism after the breakdown of the Soviet Union (Kuemmerle et al. 2008; Alcantara et al. 2012; Renwick et al. 2013).

In the face of the environmental consequences of land over-use, some developing countries have taken political decisions to preserve and restore ecosystems (Nesheim et al. 2014). Among them, China has the largest land restoration initiatives worldwide in terms of spatial scale, payment, and duration (Zhang et al. 2000; Xu et al. 2006a; Liu et al. 2008). China suffers widespread environmental consequences caused by overexploitation of land resources, particularly in ecologically vulnerable arid and semi-arid regions (Ding 2003; John et al. 2009; Wang et al. 2013). Since the year 2000, ecological programs have come into act in form of reducing deforestation, promoting forest regeneration, and relieving human pressure on land through converting cropland to grassland (cropland retirement) (Zhang et al. 2000; Uchida et al. 2005; Wang et al. 2007a; Wang et al. 2012b).

Considered as one of the most severely degraded areas, almost all of the national land restoration projects for environmental protection were implemented in Inner Mongolia, making it the most invested in province in China (SFA 2000-2013). By adopting the nation-wide Natural Forest Conservation Program (NFCP) in 2000, Inner Mongolia intended to maintain natural forests by decreasing deforestation and increasing the productivity of forest plantations (Li 2012; Guo et al. 2013). Also launched in 2000, the Returning Farmlands to Forest and Grassland Project (also known as “Grain to Green Program”, GGP) plans to convert farmland on steep slopes or with low yield and grassland into forest (Uchida et al. 2005; Wang et al. 2007b). Including the functionalities of GGP, phase I of the Beijing and Tianjin Sandstorm Source Treatment Project (BTSST, 2001–2012) tries to reduce the sources of sandstorms that affect Beijing and its neighboring

Tianjin Municipality through cropland retirement and vegetation regeneration (Li and Zhang 2004; Zhang et al. 2012).

Previously, the land use pattern changed substantially in Inner Mongolia after the establishment of the People's Republic of China in 1949. Vast grassland in the cropping-grazing transitional zones was cultivated and the area of cropland was doubled by the end of the 20th century (Lin and Ho 2003; Sorgog et al. 2013). The spatial pattern and the change rate of cropland retirement in the 2000's, however, are largely unknown. The forest ecosystem, too, changed substantially in Inner Mongolia after 1949 (Liu et al. 2008). Since the goal of China's forest management in the early years was to maximize timber production to support the economy, forest was heavily harvested and the forested area shrunk significantly (Zhang and Song 2006; Song et al. 2014). Apart from human factors, natural disturbances, especially fire, also played an important role in the forest loss in Inner Mongolia (Tao et al. 2013). With more afforestation and reforestation efforts in the 2000's, the forest cover has been reported to increase in general (IMARBS 2000-2013).

Despite the relevant important ecological and socioeconomic regional to global implications, however, to date, spatially and temporally coherent documentation of land use and land cover change is still missing in Inner Mongolia (Wang et al. 2012b). Most assessments were limited to localized areas (Du 2006; Peng 2010) and divergences emerged when the observations were conducted from different perspectives at different levels and regions (Cao et al. 2010a, b; Yang et al. 2010). Zhou et al. (2012) found GGP induced forest increase in the dry Loess Plateau using multi-temporal Landsat imagery. A field survey conducted by Song (2014) concluded low deforestation risk for forests created by GGP, although risk varied greatly across sites. However, Cao et al. (2008) and Wang (2010b) argued large-scale afforestation failed in arid and semi-arid China, based on the local observations and meta-analysis. Previous LULCC monitoring in Inner Mongolia usually took the land cover information observed from two single- or multi-date images to deduce the changes (John et al. 2009). The comparison approach, however, is not well-suited for determining rapid land surface changes (Dearing et al. 2010; Kenneny et al. 2014). Therefore, high-frequency observations are needed for investigating the drastic changes in land systems triggered by political factors.

Remote sensing has a long tradition; mapping land use and land cover changes across local to global scales (Meyer and Turner 1994; Lambin et al. 2003; DeFries et al. 2004a; Clark et al. 2012). Previously, we demonstrated for a sub-region in Inner Mongolia that land cover

probabilities derived from a Random Forest classifier are useful to characterize changes between multiple land cover classes at annual intervals, e.g. forest to grassland and grassland to cropland (Yin et al. under review). By describing the chance that a pixel from satellite imagery belongs to a specific land cover class (Colditz et al. 2011), land cover probabilities are more sensitive to land cover change compared to the underlying spectral values or vegetation indices (Broich et al. 2011). More important, land cover probabilities provide a quantitative land surface measurement and therefore can be used as input variables for time series models. Rather than detecting the simplistic from-to change from two- or multiple-date land cover maps, our approach took advantage of the hyper-temporal resolution of the MODIS archive to explore detailed changes using a trajectory-based approach which captures the rapid transformation in the land system.

Accordingly, we extended our approach to map annual land cover change for Inner Mongolia, China, to understand how the land system is altered against the background of national land restoration programs. Methodologically, we aimed to answer the question how probability-based land change trajectories from machine learning can support such insights. We focused on three specific land cover change processes that should closely correlate with China's ecological programs, meeting the interests of most: deforestation, forest regeneration and cropland retirement.

2 Methodology

2.1 Study area

Inner Mongolia is an autonomous region located in Northern China with twelve prefecture-level divisions which are subdivided into 101 counties (Figure 1). It covers about 1.18 million km² area with a population of 27 million people in 2010 (IMARBS 2000-2013). Lying in a climatic transitional zone from sub-humid to dry environments, land covers in Inner Mongolia follow a distinct gradient. With higher precipitation, the northeastern part of the study area is dominated by mostly deciduous forest and by agriculture in the lowlands. Croplands in the East then give way to grassland in the West. Between the forested East and the vast desert in the West, land cover is dominated by various grassland ecosystems.

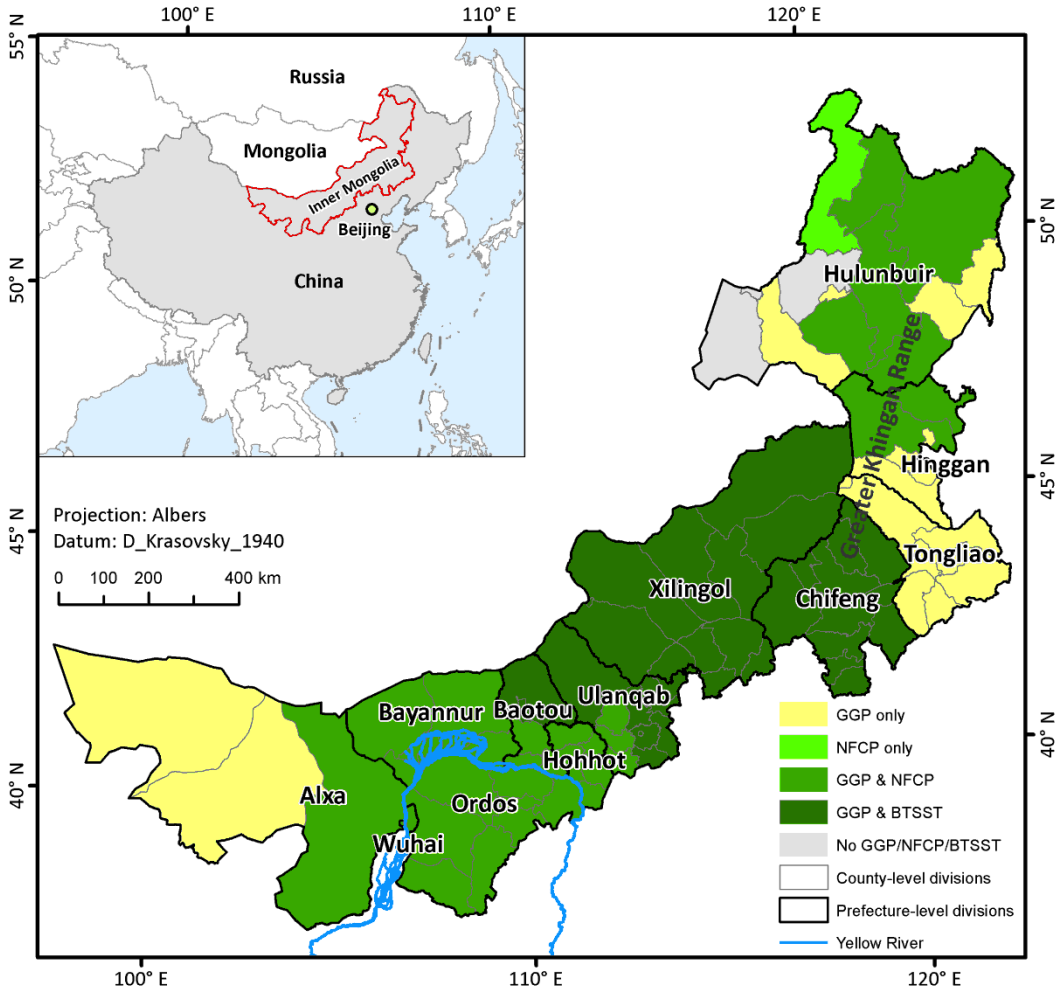

Figure IV-1: Inner Mongolia and ecological programs conducted in administrative divisions at prefecture- and county-level. GGP refers to Grain for Green Program, NFCP refers to Natural Forest Conservation Program, and BTSST is Beijing and Tianjin Sandstorm Source Treatment Project.

2.2 Image data and reference data generation

The MODIS-Terra Vegetation Index (VI) product (MOD13Q1, Collection 5) (Huete et al. 2002) was used as the main data source to predict land cover probability between 2000 and 2012. The MOD13Q1 comprised the Normalized Difference Vegetation Index (NDVI), the Enhanced Vegetation Index (EVI), surface reflectance in the blue, red, near-infrared (NIR), shortwave-infrared (SWIR) waveband, and pixel quality data with nominal 250-m spatial resolution and a composite time interval of 16 days. We used the Savitzky-Golay filter from the TIMESAT software (Jonsson and Eklundh 2004) to generate smooth time series of NDVI, EVI and other four reflectance bands so as to reduce the noises caused by atmosphere, off-nadir viewing and low sun zenith angle. For each calendar year during the growing season (March–October), we computed the mean, minimum, maximum, range and standard deviation for the first half (March–June), second half (July–October), as well as the entire growing season. This reduced the number of input variables for the classifier

while keeping phenological information helpful for distinguishing different land cover classes (Huttich et al. 2011; Clark et al. 2012).

We adopted the level 1 legend from the Chinese Academy of Science (CAS) national cover mapping initiative as a tradeoff between the need of meeting regional settings and the ability of MODIS for land cover mapping (Liu et al. 2002; Liu et al. 2005). The reference data for Random Forest model training was generated following Yin et al. (under review), with modifications of the signature generation approach. Here we used a more cost-effective and robust automatic signature generalization approach that adapts the class spectral signature to individual images (Gray and Song 2013). Change vector analysis (CAV) was used to screen the areas where land covers are stable, and only the samples located in the stable areas were kept for model training between 2000 and 2012. We selected red band and NDVI for CAV analysis as they are sensitive to ground change and similarly affected by atmospheric effects across different land cover types (Gray and Song 2013). We stacked the mean value of the smoothed red band and NDVI during the growing season for 2000 and 2012, respectively. A linear regression function was used for radiometric normalization to reduce the effects of atmospheric difference or other factors (Hall et al. 1991). The CAV analysis was hereafter conducted on the differenced red band and NDVI value. As we aimed to minimize omission errors, a relative relaxed threshold of change magnitude was set and nearly 15% of the study area was detected as changed areas.

Collecting a sufficient number of references for precisely validating a land cover change map is challenging, because the number of change classes increases substantially compared to a single-date land cover map (Olofsson et al. 2013; Wickham et al. 2013). Hence we used a disproportionate stratified estimator and six randomly selected Landsat footprints (p121r27, p121r30, p122r24, p124r29, p126r32, p129r32) to validate the map. We collected 98 Landsat L1T images acquired mostly in late summer or early autumn for nearly every year between 2000 and 2012 as reference data. The spectral and spatial patterns of the Landsat imagery, as well as the phenological discrepancies of different land cover types helped to distinguish land cover classes visually. A size of one MODIS pixel was used as the sample unit. We randomly selected 300 pixels for each stable class, except permanent water bodies which have a relative smaller reference size of 150 pixels, 50 pixels for each strata within each land cover change class, and 150 pixels for other change classes. Where no Landsat image was available (i.e. data gap due to ETM SLC-off or cloud cover), or the samples were undecidable in visual interpretation, a temporal profile from the MOD13Q1 NDVI time series was employed as ancillary information. In all, a number

of 3062 reference samples were labeled. The accuracy was reported in form of a confusion matrix, including the omission error, commission error and overall accuracy.

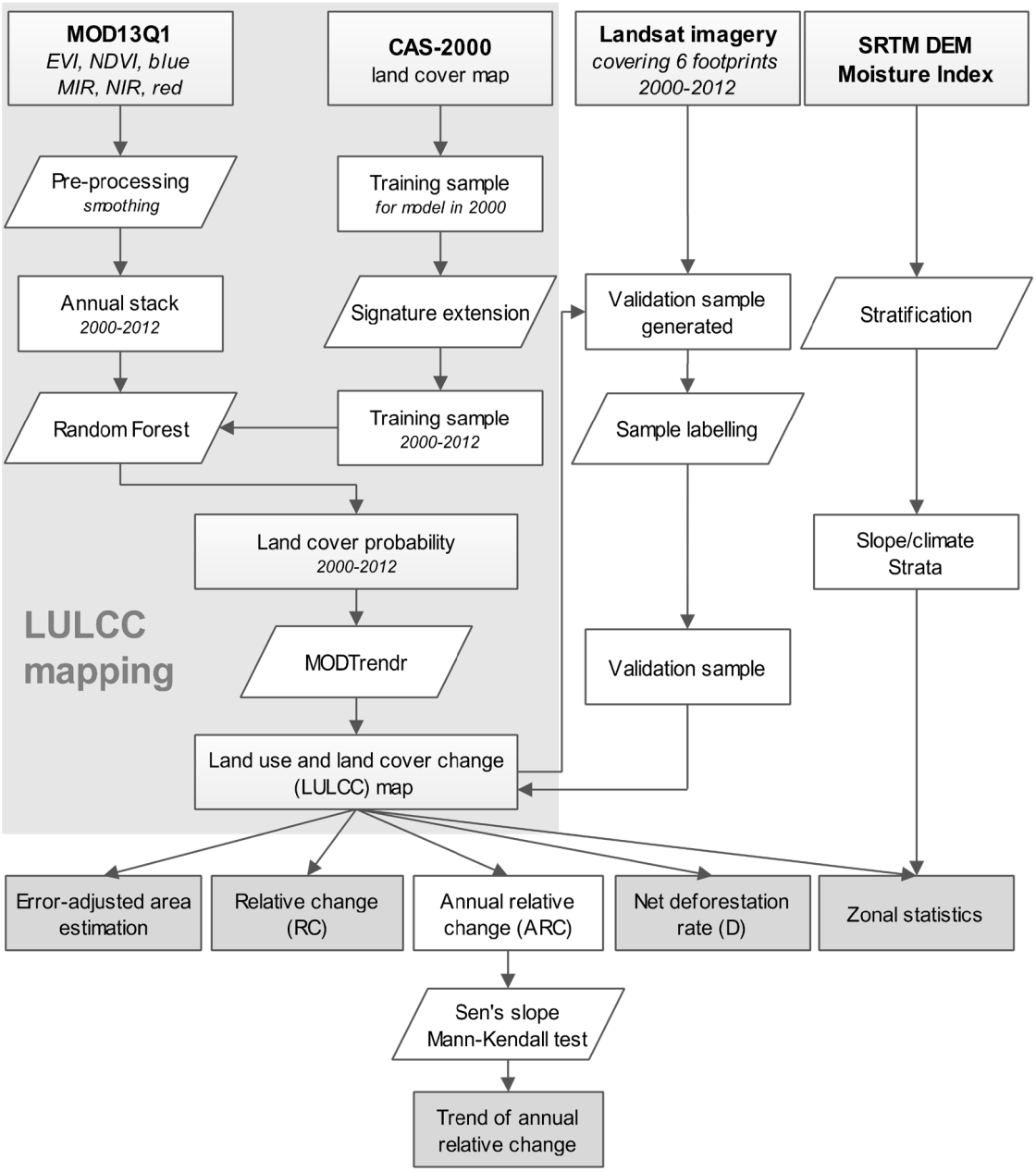

Figure IV-2: Methodology overview showing the dataset and algorithms used.

2.3 Land use and land cover change mapping

Pixel-wise probabilities for forested land, cropland, grassland, waterbodies and non-vegetated land were estimated using the Random Forest model for each year during 2000 and 2012. Land probability time series and a temporal segmentation approach, MODTrendr (Sulla-Menashe et al. 2014), were employed to investigate the change within each land cover. The conversions between different land cover classes were mapped hereafter based on the summary of structural changes class (Yin et al. under review).

Adapted from the LandTrendr algorithm, MODTrendr was used to generate temporal segmentation in class-wise land cover probability time series where the directional change of a temporal segment is interpreted as a proxy for change on the ground (Sulla-Menashe et al. 2014). Several metrics provide the characteristic summary of the segments, including the start and the end timing of the segment, segment duration (years) and change magnitude (probability difference between segment end and segment start). These metrics help interpreting the segment for translating the segments to the ground change. We ran MODTrendr on all the land cover probability time series separately and derived the metrics of the segments. As we had no ground reference to calibrate MODTrendr, we decided to use the same fitting parameters as in (Sulla-Menashe et al. 2014), except that we used a more restrictive significance threshold for model fitting (p-value=0.05) and a higher number of trajectory segments (5). This was considered to eliminate noise due to the misestimation and large inter-annual variation of land cover probability in drylands, while capturing more abrupt and quick recovery land change processes.

For each land cover probability time series, we derived two metric sets – the largest decrease and the largest increase of land cover probabilities, respectively. For retrieving largest decrease/increase metrics, we first labeled segments representing land cover loss when the change magnitude was -0.4 or less and the pre-change probability was greater than 0.5, as these thresholds resulted in balanced omission and commission errors. For each pixel we recorded the converted land cover class and the timing of the conversion based on the year when the change segment ended. To identify the land cover class following the conversion, we selected class probability segments with a positive change magnitude of 0.4 or greater. Thus, a pixel was flagged showing a land cover conversion when a pronounced land cover loss in one land cover probability trajectory occurred simultaneously with a gain in another land cover type. A ±2 year difference in timing label was allowed and the conversion time was decided by the detected loss time of the land cover trajectory. Detailed descriptions of the metrics can be found in Kennedy (2010) and Sulla-Menashe (2014).

A thematic land map was created for the year 2000 from the fitted probability time series and each pixel was assigned a land cover label, based on the majority land cover probability. We combined the land cover change map with the baseline map in 2000, to create a single map representing stable land cover classes and the change categories. We labeled five non-change land classes including permanent cropland (PC), permanent forested land (PF), permanent grassland (PG), permanent waterbodies (PW), and

permanent non-vegetated land (PN). Conversions from forested land to grassland and cropland were integrated as deforestation (DF), the conversions from grassland and cropland to forested land were combined as forest regeneration (FR), and the conversion from cropland to grassland represents cropland retirement (CR). Other class changes, such as changes of waterbodies or non-vegetated land, were integrated into a single class as other changes (OC).

2.4 Spatial and temporal patterns of LULCC

For each class, we estimated the error-adjusted area and associated 95% confidence intervals using formulas provided by Olofsson (2013). Because we were interested in the human influence on the forest change, we separated fire-induced forest loss from the total deforestation using the Collection 5.1 MODIS Burn Area Product (MCD45A1) download from the University of Maryland (ftp://ba1.geog.umd.edu).

To assess the regional response to the ecological programs implemented for a given land cover conversion class, we estimated the total relative change (RC) and annual relative change (ACR). Sen's slope and the Mann-Kendall test of the annual relative change at county level were calculated to assess possible trends in the change rates, except for forest regeneration. As forest growth requires a longer period of time, the detected area of forest regeneration is hypothesized to be decreasing during the late-stage of the investigation period. Net deforestation rates (D) were calculated for the forested land. RC, ACR and PNC were calculated using the following formulas:

$$RC = 100 * (\sum_{i=2001}^{2012} AC_i / A_{2000}) \quad (1)$$

where AC_i is the converted area at year i, and A_{2000} denotes the area of land cover in 2000. For example, when calculating the relative change for forest regeneration, A_{2000} denotes the area of herbaceous land in 2000. In the case of deforestation, A_{2000} stands for the area of forested land in 2000.

$$ACR_j = 100 * (AC_j / A_{j-1}) \quad (2)$$

where ACR_j is the relative change ratio in year j, AC_j denotes the area of the conversions in year j and A_{j-1} equals the area of the land cover class in year $j-1$. Overall, the net deforestation rate (D) was estimated as follows:

$$D(\%) = 100 * \sum_{i=2001}^{2012} (R_i - D_i) / F_{2000} \quad (3)$$

where R_i and D_i stand for the area of forest regeneration and deforestation in year *i*, respectively, and F_{2000} denotes the forested area in 2000.

We investigated how land cover changes vary among different topographic and climatic conditions, because ecological programs are largely set up according to the environmental settings. The Shuttle Radar Topography Mission (SRTM) digital elevation model (DEM) database v4.1 was used to represent topography. The original 90-m SRTM dataset was resampled and reprojected to the same resolution as the LULCC map, before calculating the RC for each land cover change type among each stratum of slope at 5-degree breaks. The climate moisture index (I_m) dataset covering Inner Mongolia, downloaded from the Data Sharing Infrastructure of Earth System Science of China (http://www.geodata.cn), was used to assess climatic conditions of the land on which LULCC occurred. The 500-m resolution climate moisture index dataset was produced by the Institute of Agricultural Resources and Regional Planning of the Chinese Academy of Agricultural Sciences, using long-term ground gauges of precipitation and temperature based on the method of Thornthwaite and Mather (1955). We stratified the climate moisture index into 12 strata where each stratum corresponded to a certain climate type: semi-arid (SA, $I_m \leq -35$), dry sub-humid (DS, $-35 < I_m \leq 0$) and moist sub-humid (MS, $I_m > 0$). Each climate type was divided into sub-classes at an interval of five. We then estimated the total relative change of each LULCC class within each stratum.

3 Results

3.1 Mapping accuracy

The accuracy assessment revealed reliable land cover change mapping in Inner Mongolia with an overall accuracy of 91.8%, though errors varied among land categories and change classes (Table IV-1). For the permanent land classes, the user's accuracies were higher than 90% for permanent cropland, forest, and water. Apart from permanent cropland and non-vegetated land, other permanent land cover classes achieved producer's accuracies greater than 90%.

Compared to the permanent land cover classes, change classes were in general less accurately mapped and variations of the errors in each individual class are larger (Table IV-1, Table IV-2). Deforestation, however, showed the most promising mapping accuracy. The user's accuracy varied little (standard deviation = 0.06) and was higher than 85% across all the individual classes of deforestation. The highest commission error was found in 2001

due to confusion with the classes in the following years (e.g. 2003) (Table IV-2). The producer's accuracies also confirmed the good capacity of deforestation mapping with an average omission error of less than 5% and a standard deviation of 0.06. Forest regeneration from 2001 to 2012 was also well captured, with an average user's and producer's accuracy of 83.7% and 84.7%, respectively. Similar to that of deforestation, the individual forest regeneration class in 2001 showed larger inter-annual timing label confusion (user's accuracy = 62.0%). In contrast to the high accuracies in deforestation and forest regeneration mapping, cropland retirement was less well detected due to a mapping error with an average user's accuracy (62.0%) and producer's accuracy (81.8%). The confusions of cropland retirement were mainly with permanent cropland and grassland, which account for 65% of the errors. Compared to deforestation and forest regeneration, the change of timing was less accurately labeled in cropland retirement. We also found least accuracy in the individual cropland retirement class of 2001.

Table IV-1: Accuracy assessment report showing omission errors (OE, %) and commission errors (CE, %) for deforestation (DF), forest regeneration (FR), and cropland retirement (CR) and permanent classes: permanent cropland (PC), permanent forested land (PF), permanent grassland (PG), permanent waterbodies (PW), and permanent non-vegetated land (PN).

Year	DF OE	DF CE	FR OE	FR CE	CR OE	CR CE
2001	0	16.0	0	38.0	0	54.0
2002	2.3	4.0	21.8	20.0	4.7	36.0
2003	3.9	0	33.5	16.0	8.0	34.0
2004	0	14.0	25.3	10.0	29.6	32.0
2005	0	2.0	13.8	16.0	47.8	40.0
2006	0.4	6.0	0	16.0	16.7	44.0
2007	10.8	8.0	28.8	12.0	20.1	42.0
2008	8.4	10.7	18.7	10.0	7.3	36.0
2009	0	12.5	4.9	16.0	26.6	34.0
2010	0	10	5.8	8.6	17.6	38.0
2011	5.8	0	--	--	9.1	46.0
2012	--	--	--	--	30.8	44.0
Overall Accuracy = 91.8%						
OE for permanent classes: PC (11.8), PF (1.4), PG (6.6), PW (3.5), PN (11.8)						
CE for permanent classes: PC (5.6), PF (5.3), PG (10.6), PW (14.7), PN (6.3)						

Table IV-2: Error matrixes based on sample counts and the area-adjusted proportion for deforestation (DF), forest regeneration (FR), and cropland retirement (CR) and permanent classes: permanent cropland (PC), permanent forested land (PF), permanent grassland (PG), permanent waterbodies (PW), and permanent non-vegetated land (PN).

	PC	PF	PG	PW	PN	DF2001	DF2002	DF2003	DF2004	DF2005
PC	1.26E-01	-	7.56E-03	-	-	-	-	-	-	-
PF	-	1.22E-01	4.28E-04	-	6.42E-03	-	-	-	-	-
PG	1.58E-02	1.43E-03	3.84E-01	-	2.87E-02	-	-	-	-	-
PW	-	-	2.25E-05	2.89E-03	-	-	-	-	-	-
PN	-	-	1.79E-02	-	2.64E-01	-	-	-	-	-
DF2001	-	-	5.34E-06	-	-	1.12E-04	2.67E-06	1.33E-05	-	-
DF2002	-	-	-	-	-	-	1.11E-04	4.65E-06	-	-
DF2003	-	-	-	-	-	-	-	7.78E-04	-	-
DF2004	-	-	-	-	-	-	-	1.37E-05	8.41E-05	-
DF2005	-	-	1.01E-06	-	-	-	-	-	-	4.96E-05
DF2006	-	1.81E-05	-	-	-	-	-	-	-	-
DF2007	-	-	-	-	-	-	-	-	-	-
DF2008	-	6.43E-06	-	-	-	-	-	-	-	-
DF2009	-	1.33E-06	1.99E-06	-	-	-	-	-	-	-
DF2010	-	6.43E-07	6.43E-07	-	-	-	-	-	-	-
DF2011	-	-	-	-	-	-	-	-	-	-
FR2001	-	3.46E-05	-	-	-	-	-	-	-	-
FR2002	-	1.51E-05	-	-	-	-	-	-	-	-
FR2003	-	1.83E-05	-	-	-	-	-	-	-	-
FR2004	-	-	-	-	-	-	-	-	-	-
FR2005	-	7.48E-06	-	-	-	-	-	-	-	-
FR2006	-	2.15E-06	-	-	-	-	-	-	-	-
FR2007	-	1.84E-06	-	-	-	-	-	-	-	-
FR2008	-	1.49E-06	-	-	-	-	-	-	-	-
FR2009	-	-	-	-	-	-	-	-	-	-
FR2010	-	-	-	-	-	-	-	-	-	-
CR2001	5.77E-05	-	1.73E-04	-	-	-	-	-	-	-
CR2002	1.05E-04	-	1.20E-04	-	-	-	-	-	-	-
CR2003	7.01E-05	-	1.23E-04	-	-	-	-	-	-	-
CR2004	3.04E-05	-	1.22E-05	-	-	-	-	-	-	-
CR2005	1.32E-05	-	4.95E-06	-	-	-	-	-	-	-
CR2006	4.74E-05	-	2.84E-05	-	-	-	-	-	-	-
CR2007	2.68E-05	-	2.08E-05	-	-	-	-	-	-	-
CR2008	2.70E-05	-	3.37E-06	-	-	-	-	-	-	-
CR2009	1.37E-05	-	8.22E-06	-	-	-	-	-	-	-
CR2010	1.92E-05	-	2.41E-06	-	-	-	-	-	-	-
CR2011	3.94E-05	-	3.29E-05	-	-	-	-	-	-	-
CR2012	6.81E-05	-	1.57E-05	-	-	-	-	-	-	-
Other changes	5.28E-04	2.11E-04	6.34E-04	1.06E-04	3.17E-04	-	-	-	-	-
PA	8.82E-01	9.86E-01	9.34E-01	9.65E-01	8.82E-01	1.00E+00	9.77E-01	9.61E-01	1.00E+00	1.00E+00

Table IV-2: Error matrixes based on sample counts and the area-adjusted proportion (Continued)

	DF2006	DF2007	DF2008	DF2009	DF2010	DF2011	FR2001	FR2002	FR2003	FR2004
PC	-	-	-	-	-	-	-	-	-	-
PF	-	-	-	-	-	-	-	-	-	-
PG	-	-	-	-	-	-	-	-	-	-
PW	-	-	-	-	-	-	-	-	-	-
PN	-	-	-	-	-	-	-	-	-	-
DF2001	-	-	-	-	-	-	-	-	-	-
DF2002	-	-	-	-	-	-	-	-	-	-
DF2003	-	-	-	-	-	-	-	-	-	-
DF2004	-	-	-	-	-	-	-	-	-	-
DF2005	-	-	-	-	-	-	-	-	-	-
DF2006	4.25E-04	9.03E-06	-	-	-	-	-	-	-	-
DF2007	1.63E-06	7.48E-05	4.88E-06	-	-	-	-	-	-	-
DF2008	-	-	5.35E-05	-	-	-	-	-	-	-
DF2009	-	-	-	2.32E-05	-	-	-	-	-	-
DF2010	-	-	-	-	2.89E-05	6.43E-07	-	-	-	-
DF2011	-	-	-	-	-	1.04E-05	-	-	-	-
FR2001	-	-	-	-	-	-	8.93E-05	1.44E-05	5.76E-06	-
FR2002	-	-	-	-	-	-	-	1.01E-04	1.01E-05	-
FR2003	-	-	-	-	-	-	-	4.58E-06	1.92E-04	-
FR2004	-	-	-	-	-	-	-	9.15E-06	3.05E-06	1.37E-04
FR2005	-	-	-	-	-	-	-	-	-	7.48E-06
FR2006	-	-	-	-	-	-	-	-	-	-
FR2007	-	-	-	-	-	-	-	-	-	-
FR2008	-	-	-	-	-	-	-	-	-	-
FR2009	-	-	-	-	-	-	-	-	-	-
FR2010	-	-	-	-	-	-	-	-	-	-
CR2001	-	-	-	-	-	-	-	-	-	-
CR2002	-	-	-	-	-	-	-	-	-	-
CR2003	-	-	-	-	-	-	-	-	-	-
CR2004	-	-	-	-	-	-	-	-	-	-
CR2005	-	-	-	-	-	-	-	-	-	-
CR2006	-	-	-	-	-	-	-	-	-	-
CR2007	-	-	-	-	-	-	-	-	-	-
CR2008	-	-	-	-	-	-	-	-	-	-
CR2009	-	-	-	-	-	-	-	-	-	-
CR2010	-	-	-	-	-	-	-	-	-	-
CR2011	-	-	-	-	-	-	-	-	-	-
CR2012	-	-	-	-	-	-	-	-	-	-
Other changes	-	-	-	-	-	-	-	-	2.11E-04	1.06E-04
PA	9.96E-01	8.92E-01	9.16E-01	1.00E+00	1.00E+00	9.42E-01	1.00E+00	7.82E-01	4.55E-01	5.48E-01

Table IV-2: Error matrixes based on sample counts and the area-adjusted proportion (Continued)

	FR2005	FR2006	FR2007	FR2008	FR2009	FR2010	CR2001	CR2002	CR2003	CR2004
PC	-	-	-	-	-	-	-	-	-	-
PF	-	-	-	-	-	-	-	-	-	-
PG	-	-	-	-	-	-	-	-	-	-
PW	-	-	-	-	-	-	-	-	-	-
PN	-	-	-	-	-	-	-	-	-	-
DF2001	-	-	-	-	-	-	-	-	-	-
DF2002	-	-	-	-	-	-	-	-	-	-
DF2003	-	-	-	-	-	-	-	-	-	-
DF2004	-	-	-	-	-	-	-	-	-	-
DF2005	-	-	-	-	-	-	-	-	-	-
DF2006	-	-	-	-	-	-	-	-	-	-
DF2007	-	-	-	-	-	-	-	-	-	-
DF2008	-	-	-	-	-	-	-	-	-	-
DF2009	-	-	-	-	-	-	-	-	-	-
DF2010	-	-	-	-	-	-	-	-	-	-
DF2011	-	-	-	-	-	-	-	-	-	-
FR2001	-	-	-	-	-	-	-	-	-	-
FR2002	-	-	-	-	-	-	-	-	-	-
FR2003	1.37E-05	-	-	-	-	-	-	-	-	-
FR2004	3.05E-06	-	-	-	-	-	-	-	-	-
FR2005	1.05E-04	-	4.98E-06	-	-	-	-	-	-	-
FR2006	-	9.02E-05	8.59E-06	-	-	-	-	-	-	-
FR2007	-	-	4.06E-05	2.77E-06	-	-	-	-	-	-
FR2008	-	-	4.95E-07	2.23E-05	4.95E-07	-	-	-	-	-
FR2009	-	-	-	2.35E-06	3.29E-05	2.35E-06	-	-	-	-
FR2010	-	-	2.37E-06	-	1.19E-06	3.80E-05	-	-	-	-
CR2001	-	-	-	-	-	-	2.65E-04	-	2.31E-05	3.46E-05
CR2002	-	-	-	-	-	-	-	4.80E-04	1.50E-05	3.00E-05
CR2003	-	-	-	-	-	-	-	1.75E-05	5.79E-04	1.75E-05
CR2004	-	-	-	-	-	-	-	6.08E-06	1.22E-05	2.07E-04
CR2005	-	-	-	-	-	-	-	-	-	4.95E-06
CR2006	-	-	-	-	-	-	-	-	-	-
CR2007	-	-	-	-	-	-	-	-	-	-
CR2008	-	-	-	-	-	-	-	-	-	-
CR2009	-	-	-	-	-	-	-	-	-	-
CR2010	-	-	-	-	-	-	-	-	-	-
CR2011	-	-	-	-	-	-	-	-	-	-
CR2012	-	-	-	-	-	-	-	-	-	-
Other changes	-	-	-	-	-	-	-	-	-	-
PA	8.62E-01	1.00E+00	7.12E-01	8.13E-01	9.51E-01	9.42E-01	1.00E+00	9.53E-01	9.20E-01	7.04E-01

Table IV-2: Error matrixes based on sample counts and the area-adjusted proportion (Continued)

	CR2005	CR2006	CR2007	CR2008	CR2009	CR2010	CR2011	CR2012	Other changes	UA
PC	-	-	-	-	-	-	-	-	-	9.43E-01
PF	-	-	-	-	-	-	-	-	-	9.47E-01
PG	-	-	-	-	-	-	-	-	-	8.93E-01
PW	-	-	-	-	-	-	-	-	4.73E-04	8.53E-01
PN	-	-	-	-	-	-	-	-	-	9.37E-01
DF2001	-	-	-	-	-	-	-	-	-	8.40E-01
DF2002	-	-	-	-	-	-	-	-	-	9.60E-01
DF2003	-	-	-	-	-	-	-	-	-	1.00E+00
DF2004	-	-	-	-	-	-	-	-	-	8.60E-01
DF2005	-	-	-	-	-	-	-	-	-	9.80E-01
DF2006	-	-	-	-	-	-	-	-	-	9.40E-01
DF2007	-	-	-	-	-	-	-	-	-	9.20E-01
DF2008	-	-	-	-	-	-	-	-	-	8.93E-01
DF2009	-	-	-	-	-	-	-	-	-	8.75E-01
DF2010	-	-	-	-	-	-	-	-	1.29E-06	9.00E-01
DF2011	-	-	-	-	-	-	-	-	-	1.00E+00
FR2001	-	-	-	-	-	-	-	-	-	6.20E-01
FR2002	-	-	-	-	-	-	-	-	-	8.00E-01
FR2003	-	-	-	-	-	-	-	-	-	8.40E-01
FR2004	-	-	-	-	-	-	-	-	-	9.00E-01
FR2005	-	-	-	-	-	-	-	-	-	8.40E-01
FR2006	-	-	-	-	-	-	-	-	6.44E-06	8.40E-01
FR2007	-	-	-	-	-	-	-	-	9.22E-07	8.80E-01
FR2008	-	-	-	-	-	-	-	-	-	9.00E-01
FR2009	-	-	-	-	-	-	-	-	1.57E-06	8.40E-01
FR2010	-	-	-	-	-	-	-	-	-	9.14E-01
CR2001	-	-	-	-	-	-	-	-	2.31E-05	4.60E-01
CR2002	-	-	-	-	-	-	-	-	-	6.40E-01
CR2003	1.75E-05	1.75E-05	-	-	-	-	-	-	3.51E-05	6.60E-01
CR2004	1.82E-05	-	-	-	-	-	-	-	1.82E-05	6.80E-01
CR2005	4.95E-05	3.30E-06	1.65E-06	-	-	-	-	-	4.95E-06	6.00E-01
CR2006	9.48E-06	1.33E-04	1.42E-05	-	-	-	-	-	4.74E-06	5.60E-01
CR2007	-	2.97E-06	8.62E-05	2.97E-06	5.95E-06	-	-	-	2.97E-06	5.80E-01
CR2008	-	-	3.37E-06	1.08E-04	2.02E-05	-	-	-	6.74E-06	6.40E-01
CR2009	-	2.74E-06	-	5.48E-06	9.04E-05	2.74E-06	-	-	1.37E-05	6.60E-01
CR2010	-	-	2.41E-06	-	-	7.46E-05	7.22E-06	-	1.44E-05	6.20E-01
CR2011	-	-	-	-	6.57E-06	1.31E-05	1.77E-04	2.63E-05	3.29E-05	5.40E-01
CR2012	-	-	-	-	-	-	1.05E-05	1.47E-04	2.10E-05	5.60E-01
Other changes	-	-	-	-	-	-	-	1.06E-04	1.36E-02	8.60E-01
PA	5.22E-01	8.33E-01	7.99E-01	9.27E-01	7.34E-01	8.24E-01	9.09E-01	5.27E-01	9.54E-01	OA

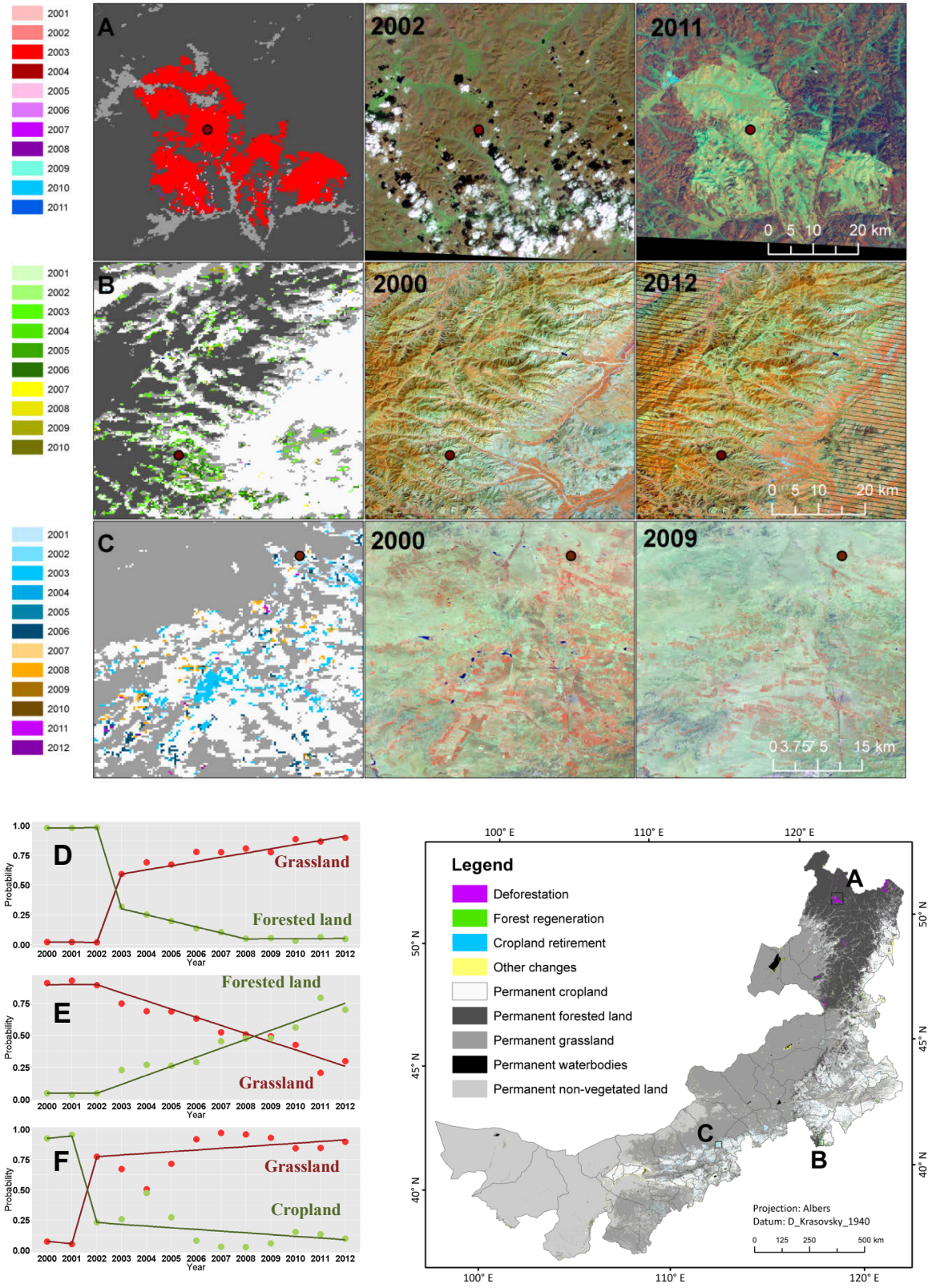

Figure IV-3: Land use and land cover change map (downright). Three subsets, indicated in the black frame, show the detailed map and the comparison of that from Landsat imagery (RGB=453): (A) deforestation, (B) forest regeneration and (C) cropland retirement. The trajectory in figure (D), (E) and (F) indicate the source and the fitted values of land cover probability located in (A), (B) and (C) respectively. The location is indicated in dot in three subsets.

3.2 Deforestation and forest regeneration

The forest area in Inner Mongolia increased between 2001 and 2012, though the change differed in different periods across the regions (Figure IV-4, Figure IV-5). For the deforestation, the estimated forest loss area was 205,534±14,556 hectare (0.42% of all the forest in 2000) between 2001 and 2012 (Figure IV-4A). Two notable years were 2003 and 2006, with above-average change caused by natural fire disturbances. The MODIS burnt product revealed fire introduced forest disturbances. This was the largest factor of forest loss which constitutes nearly 71.5% of the whole lost area. The fire-excluded forest loss showed a decreasing trend in the time series of the deforestation area (Figure IV-4B). The annual net deforestation area gradually decreased from 10,770 ha (0.07% of the whole forest) in 2001 to 930 ha (0.01% of the forest) in 2011, while no forest loss was detected in 2012.

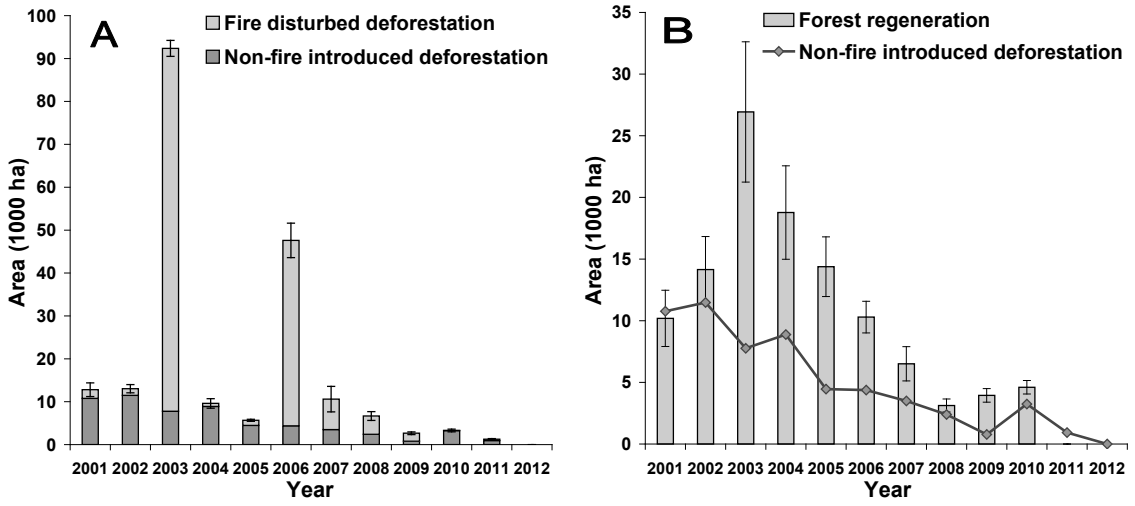

Figure IV-4: (A) Error-adjusted area estimates of deforestation and the fire introduced forest loss and (B) Fire-excluded deforestation and error-adjusted area estimates of forest generation. The associated 95% confidence intervals were shown as error bars.

The deforestation rate and its temporal trend were found to be heterogeneous at county level (Figure IV-5). Counties with higher rate of forest loss were mainly located in the southern Greater Khingan Range where the NFCP program was not implemented (Figure IV-5A, Figure IV-1). Taking Hinggan and Tongliao, for example, the counties enrolled in the NFCP program showed less forest decline, compared to the non-NFCP implemented counties. All counties in Inner Mongolia exhibited a decreasing trend of deforestation while the magnitude of change varied regionally (Figure IV-5B). The NFCP installed counties had a statistically significant (α=0.01) negative trend of deforestation ratio, indicating faster deforestation reduction.

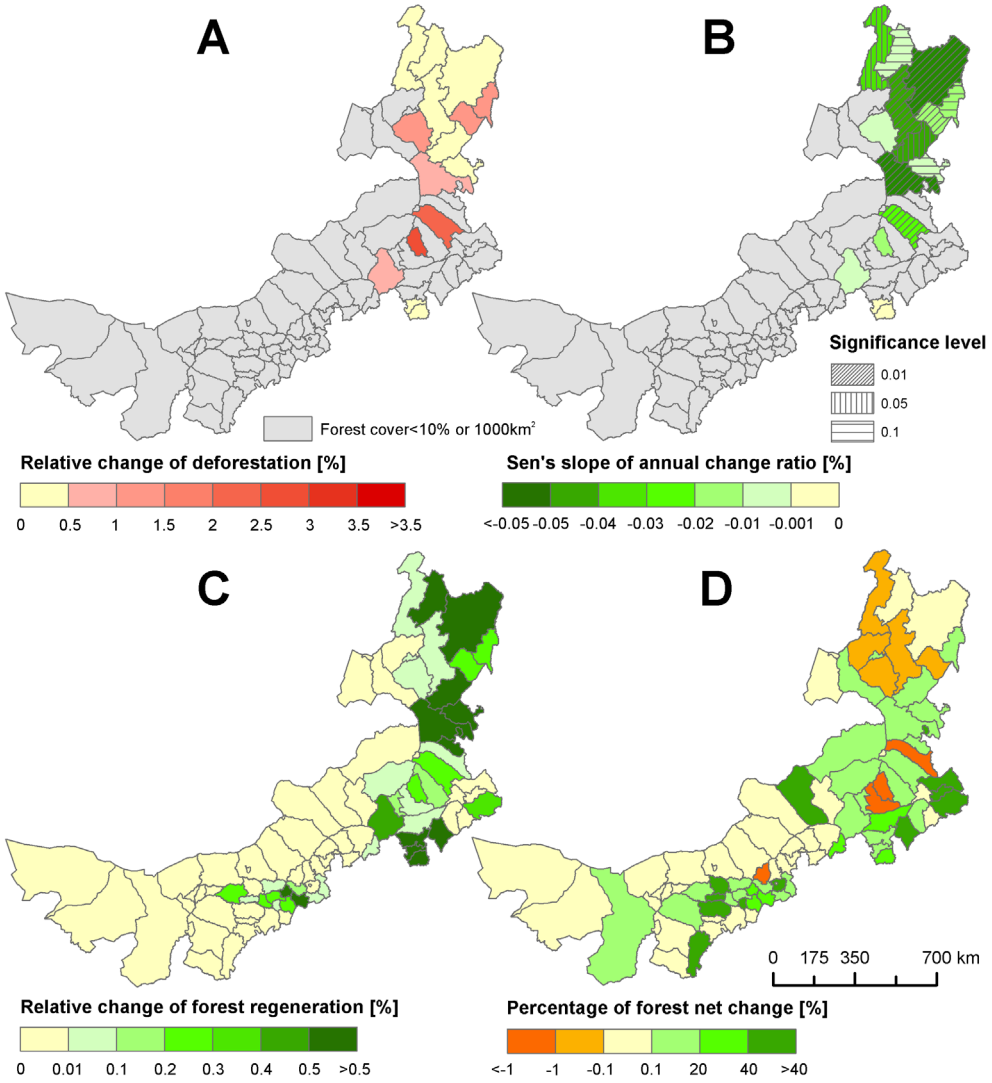

Figure IV-5: Forest changes at county-level between 2000 and 2012. (A) Relative change ratio calculated and (B) Sen's slope and Mann-Kendall test of annual relative change ratio of deforestation. (C) Relative change ratio of forest regeneration and (D) Percentage of forest net change.

We estimated an area of 112,898±21,154 hectare forest regeneration accounting for 0.18% of the herbaceous land in Inner Mongolia during the investigation period (Figure IV-4B). Unlike the gradual decrease of deforestation, forest increase showed a more dramatic path. A rapid increase of forest gain occurred between 2001 and 2003, when the area of forest increase reached a peak. Gradual decreases followed afterwards, leading to the lowest forest gain in 2008. The forest gain subsequently increased slightly until 2010, with a much lower absolute change magnitude than that between 2001 and 2003. No forest gain was found in 2011 and 2012.

The spatial pattern of the forest gain showed regional heterogeneity, with most of the forest gain detected in the NFCP and BTSST installed regions (Figure IV-1, Figure IV-5C). For example, we found considerable forest increase in both NFCP sub-zones, the Yellow River and the Greater Khingan Range. Southern counties in Chifeng, where close to Beijing, also

increased forest cover. In all, forested area in Inner Mongolia increased by 54,321±35,710 ha after balancing forest gain and fire-excluded forest loss. Areas of the northern and southern-most Greater Kinghan Range, Hulunbuir, Hinggan and Chinfeng, exhibited net forest cover loss, while Tongliao, southern Chifeng and the counties close to the Yellow River showed pronounced net forest gain (Figure IV-1, Figure IV-5D).

The relative change across mountain slopes and climatic strata showed a distinguished difference between deforestation and forest regeneration (Figure IV-6). A greater proportion of forest was converted to herbaceous lands in the flatter environments (slope<5°), where nearly 0.5% of the forest was lost (Figure IV-6A). With increasing mountain slope, the percentage of forest loss dropped with a gradually decreasing trend. The discrepancy between proportional forest loss in areas flatter than 5 degrees and steeper than 25 degrees was 0.24%. In contrast to deforestation, the conversion of herbaceous land to forest tended to occur at steeper slopes. Only 0.05% of the herbaceous lands in areas flatter than 5 degrees was converted to forest, while more than 1.5% of the herbaceous lands were detected with a forest gain in the steeper areas (slope>15°). The increased forest cover in the herbaceous areas was most notable in the regions where slopes are between 20 and 25 degrees. We found forest change differed with climatic conditions as well (Figure IV-6B). Deforestation was most prominent in the drier sub-humid areas. In general, the ratio of forest loss decreased in the more humid regions. In the semi-arid area, however, little forest loss was detected. Conversely, forest gain tended to occur in places with better moisture conditions. The ratio of forest regeneration on herbaceous land gradually rose up from 0.01% in semi-arid areas to 0.6% in moist sub-humid regions.

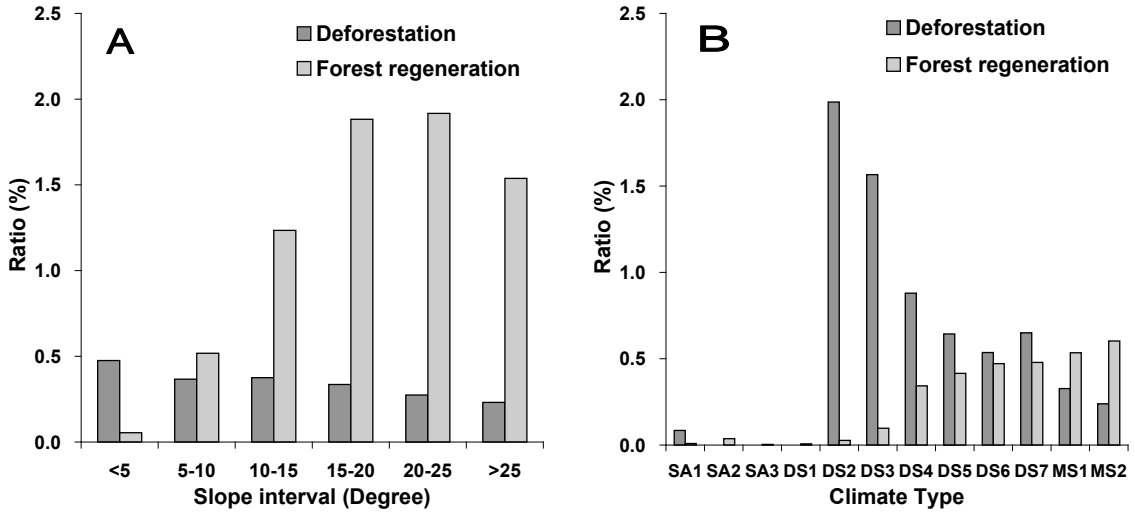

Figure IV-6: Rates of deforestation and forest generation by (A) topographic slope and (B) climatic types. SA1 stands for the strata (Im≤-45), SA2 for -45<Im≤-40 and SA3 for -40<Im≤-35. DS1 to DS7 correspond to the Im values ranging from -35 to 0 at an interval of 5. MS1 and MS2 are 0<Im≤ 5 and Im>5 respectively.

3.3 Cropland retirement

We observed temporal and spatial variances in cropland retirement between 2000 and 2012 in Inner Mongolia (Figure IV-7, Figure IV-8). The error-adjusted area estimate suggested 1.9% of cropland (313,956±79,151 ha) was converted to grassland during the investigation period. The cropland return increased rapidly before 2003, when the change area reached the all-time peak (Figure IV-7). The change was decelerated drastically in 2004 after which the cropland return continued, though at a much smaller change rate. Spatially, we found cropland retirement was more pronounced in the GGP and BTSST counties where a greater fraction (>0.5%) of cropland was converted to grassland (Figure IV-1, Figure IV-8A). The rate of cropland retirement was slowing down in most of the cropland returned counties (Mann-Kendall test p-value< 0.05) (Figure IV-8B).

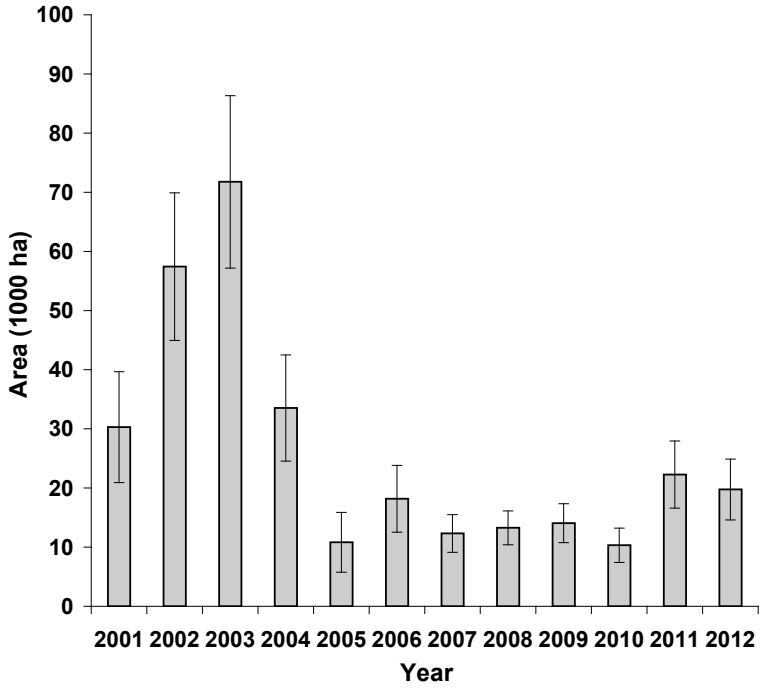

Figure IV-7: Error-adjusted area estimates of cropland retirement. The associated 95% confidence intervals were shown as error bars.

Cropland retirement was also found to be topographically and climatically correlated (Figure IV-9). Cropland in steeper environments (slope>10°) had a higher likelihood to be converted to grassland (Figure IV-9A). We found that 2.5% of the cropland in flat areas with a slope lower than five degrees was returned, in contrast to 6.7% (10° ≤slope<15°) and 6.3% (slope≤15°) of cropland converted in the steeper areas. Crop retirement tended to occur in the dry areas (e.g. SA3, DS1) (Figure IV-9B). Nearly 2.7% of the cropland in the sub-humid zone was returned to grassland, while cropland was relatively stable in the semi-arid (1.6%) and moist sub-humid (0.8%) regions.

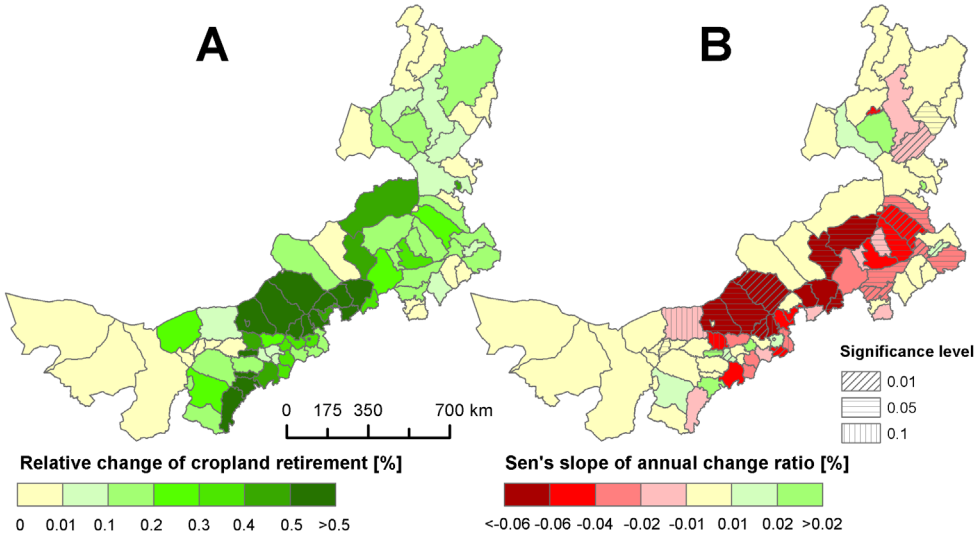

Figure IV-8: Summary of the cropland retirement at country-level of Inner Mongolia during 2000 and 2012: (A) Relative change ratio calculated and (B) Sen's slope and Mann-Kendall test of annual relative change ratio.

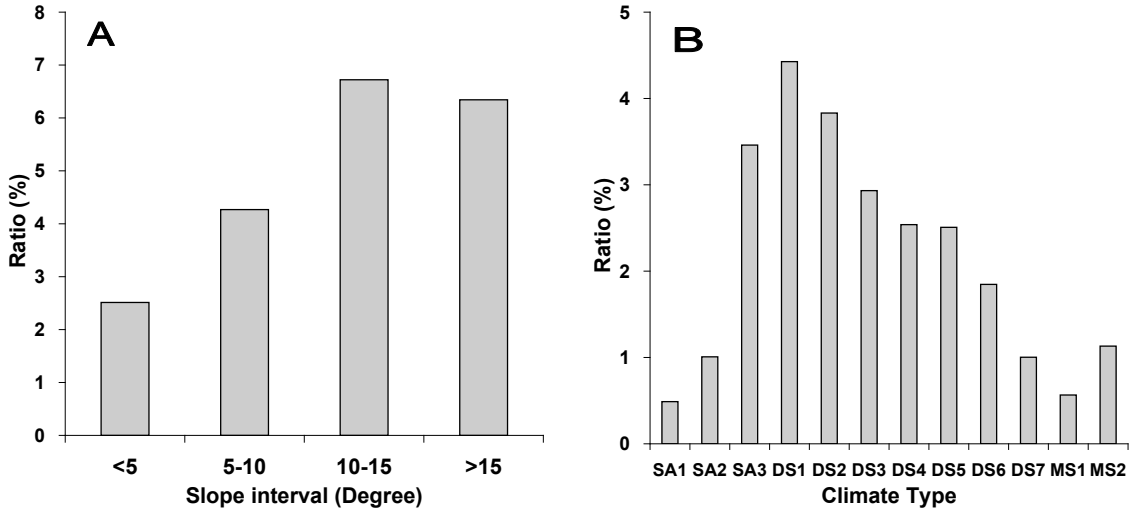

Figure IV-9: Ratio of cropland retirement by (A) topographic slope and (B) climatic types.

4 Discussion

Monitoring land use and land cover change helps understanding better how land surfaces interact with human decisions. Observations at high-frequency time intervals benefit the investigation of abrupt and gradual change processes, avoiding ambiguous cognitions of the non-linear land system. On the other hand, wall-to-wall land cover change mapping supports a complete view of land changes in different regions, which is crucial for evaluating land policies widely implemented. In this work, we mapped annual land cover changes across broad scales to investigate how the land system in Inner Mongolia was

altered against the background of China's ecological programs after 2000. We found decreasing deforestation trends, which reflected the direct influences of the NFCP grogram. Net forest increase, after excluding fire-disturbance, implied the forest regeneration efforts encouraged by the governments. Our results show, that the peak time of forest regeneration appeared in 2003, concurring with the all-time high investment of the government in afforestation and reforestation (Figure IV-10) (SFA 2013). We also found cropland retirement mostly concentrated in the years before 2004, suggesting that the local farmers were willing to join at early stages of the GGP and BTSST programs (Liu et al. 1999; Guan 2008). The much lower rate of cropland return afterwards, however, was largely due to the diminishing cropland retirement plan for the purpose of food security (Barthold et al. 2013).

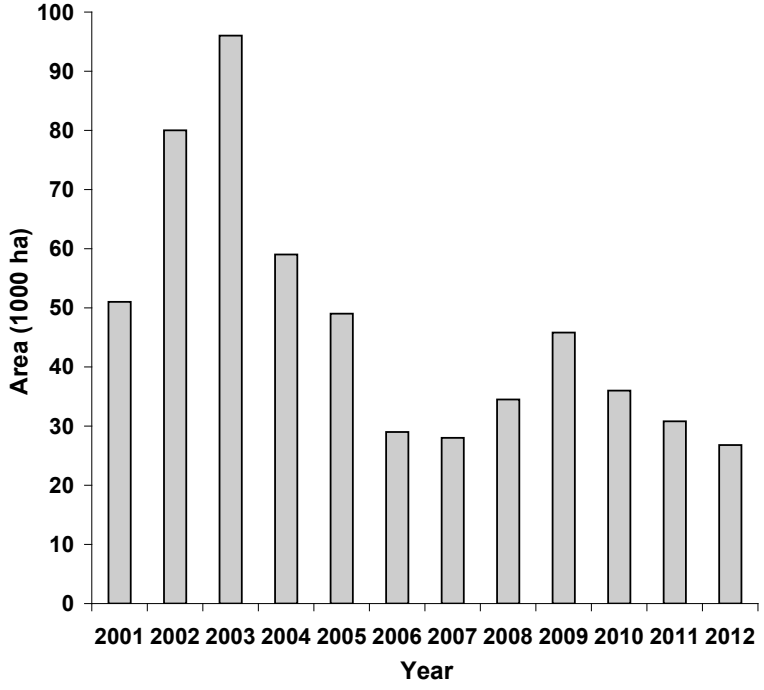

Figure IV-10: Annual statistics of national forest regeneration from the major national forestry programs in China (SFA, 2013)

Forest was reported to be shrinking in Inner Mongolia prior to the end of the 1990s (Zhan et al. 2004; Zhang et al. 2006). Our results indicate that human-introduced forest loss is rapidly decreasing after the year 2000 (Figure IV-4B), likely caused by the forest protection regulations. The NFCP installed counties, such as those located in the northern Greater Khingan Range, showed a smaller deforestation ratio and a more pronounced decreasing trend of forest loss (Figure IV-5A). A similar trend was found in other provinces implementing NFCP (Shi et al. 2011; Liu et al. 2014; Van Den Hoek et al. 2014). One

prerequisite ensuring implementation of China's forestry policy is the state-controlled ownership of the majority of forested land. Covering the largest forested area of China, the Inner Mongolia Forest Industry Group (IMFIG) functions both as the enterprise and the forestry administrative body (Wang 2006; Wang and Shen 2008; Gong 2011). The mixed function of IMFIG warranted the effectiveness of adopting the central government's decisions. For instance, IMFIG transferred 96,698 forestry works to the tertiary and other economic sectors during 2000 and 2011, so that the goal of logging reduction required by the NFCP program could be achieved (SFA 2000-2013).

We found most counties with forest increase concentrated in the NFCP and BTSST program zones (Figure IV-5C), in accordance with the forest gain detected in the individual regions of Inner Mongolia (Ouyang et al. 2008; Guo and Zhang 2009; Zhang 2011a; Hou et al. 2013). We also found that the steeper areas tended to have more forest regeneration than the flatter regions, reflecting the intention of reducing soil erosion in the mountainous environment (Figure IV-6A). Temporally, the remote sensing detected forest increases in Inner Mongolia agree, in general, with the overall trend of nation-wide census data (Figure IV-4B, Figure IV-10). The rapid increase in forest regeneration before 2004 is in line with investments at the early stages of the ecological programs (Liu et al. 2008). However, following diminishing grain production at the expense of forest expansion, the goal of forest regeneration was reduced after 2003 and led to the decreasing trend of forest gain (Tao et al. 2004; Xu et al. 2006b). We did not observe forest gain in 2011 and 2012, probably due to the time-lag between the recent forest regeneration efforts and the long growing process of the trees.

Different factors suggest that the increase in forest was largely forest expansion on the non-forest lands rather than regrowth on the post-disturbed forested land. First, we found little forest that was fully recovered on the post-fire forested land during 2000 and 2012. Most of the disturbances occurred in Inner Mongolia's cold-temperate forest ecosystems and the slow growth of the tree species on the post-fire ground determined a long recovery process which often requires more than 20 years or much longer (Luo 2002; Yu et al. 2009; Cai et al. 2013; Tao et al. 2013). Second, if the forest disturbed before 2000 had fully recovered during our investigation period, the detected timing label for forest increase would be 2000 from our trajectory approach. Instead, we found a forest regeneration peak in 2003, suggesting forest increase was merely the recovery from the disturbance in early years. Third, the detected forest increase was mainly located in the marginal grassland and

cropland areas rather than the center of the forested land, implying that the ecological programs promoted forest expansion on the non-forested land (Figure IV-3B).

Despite the general forest increase in Inner Mongolia, the long-term sustainability of the new generated forest needs to be further investigated. The planting of native and ecologically functional tree species was encouraged for forest regeneration in the ecological programs (SFA 2013). However, the planting of fast-growing and water consuming tree species (e.g. *Populus Tremula* L.) could also be found in the arid and semi-arid areas (Wang et al. 2007b; Cao 2008). Water consuming trees planted in drylands may produce unfavorable ecological consequences (Jiang 2005; Wang et al. 2010b). Correspondingly, we discovered that most of the successfully generated forest could be found in the areas with better humid conditions (Figure IV-6B), suggesting tree planting needs to consider the regional climatic conditions. On the other hand, land use decisions of the farmers enrolled in the programs after their contracts expired may have influenced land use and land cover changes. Though field surveys confirmed the farmers' positive attitude towards participating in GGP and BTSST programs (Liu and Zhang 2006; Ma et al. 2008; Hu et al. 2010), land productivity, local market conditions and other regional contexts influenced the decisions on whether the newly planted forest would be maintained or converted back after the contract expired (Liu et al. 2010a; Li et al. 2011; Song et al. 2014).

Conversions from cropland to grassland changed drastically before and after 2004 was coincident with that of forest regeneration (Figure IV-7), implying that the GGP and BTSST projects played an important role in land use decision making. As mentioned previously, the rapid decrease in cropland retirement after 2003 was a result of political decisions. The GGP program, launched in 2000 in Inner Mongolia, caused a drastic decrease in sown areas of grain which eventually dropped by nearly 1 million ha, or more than 20% in 2003, from its peak in 1998 (IMARBS 2000-2013). The rapid shrinkage of cropland prompted the government to reduce cropland retirement in 2004 and 2005 (Hao 2011; Song et al. 2014). This is evidenced by the significantly decreasing trend of cropland retirement in the counties enrolled in the GGP and BTSST programs (Figure IV-1, Figure IV-8B).

While rainfall is limited and its large inter-annual variability does not favor cultivation in arid and semi-arid Inner Mongolia (Ellis et al. 2002), the GGP and BTSST programs seemed to help local farmers to shift from vulnerable cereal cropping to the more adaptive grazing. This is supported by the higher conversion rate in the dry sub-humid areas where

lands were vulnerable to more frequent droughts (Figure IV-9B). The willingness of farmers to participate in the government's land retirement plans was also confirmed by numerous household surveys in Inner Mongolia (Yan 2010; Su et al. 2011; Song et al. 2014). In the much drier areas (Figure IV-9B), we found that little land was converted. This suggests that the mostly irrigated and well managed cropland in the very dry environments (e.g. Yellow River irrigated lands in south Bayannur, Figure IV-1) still serves as a grain producing base and does not get involved in the ecological programs.

Other factors, such as urbanization and land degradation, may also stimulate conversion from cropland to grassland (Kawada et al. 2011; Yan et al. 2012). Driven by mining industry and economic boom in Inner Mongolia during the last decade, rural farmers were attracted to giving up cultivation and immigrating to cities for better lives (Yang and Min 2006). It has been estimated that the proportion of people engaged in agricultural activities has fallen from 57.8% in 2000 to 42.3% in 2012, with little change of the overall population in Inner Mongolia (IMARBS 2000-2013). Land degradation, on the other hand, further influenced land use decisions against the background of sociopolitical change. Vulnerable to climate change, soil erosion, and salinization, cultivated cropland in dry environments is prone to degradation, and land abandondment was observable in Inner Mongolia (Li 1999; Zhan et al. 2004; An et al. 2008).

The major goals of China's ecological programs were to mitigate frequent disasters and improve human well-being. The consequences of the political decisions need to be investigated comprehensively. In general, increasing forest and grassland benefits regional vegetation cover recovery (Yin et al. 2011; Li et al. 2012a; Yin et al. 2012), soil erosion alleviation (Li et al. 2010b; Deng et al. 2012; Zhou et al. 2012), carbon sequestration enhancement (Chang et al. 2011; Deng et al. 2013; Feng et al. 2013), and soil properties amelioration (Liu et al. 2007b; Qiu et al. 2011). However, it should be noted that changes of China's land policy may trigger land displacement in the form of maintaining and expanding domestic forests and grassland while increasing land degradation risks in the other regions (Liu and Diamond 2005; Lambin and Meyfroidt 2011). Such indirect land use changes need to be considered for understanding the ecological benefits and shifting environmental deterioration in the context of globalization and sustainable development (Meyfroidt et al. 2013).

Despite the relatively high mapping accuracy (Table IV-3), uncertainties still exist, either due to land cover class similarity, time series segmentation, or the capacity of the remote sensing data for complex land use change detection. First of all, using existing land cover

products and the CAV approach for reference data regeneration created reliable land cover probability estimation by the Random Forest model. However, spectral similarity of cropland and grassland caused a relatively higher mapping error between these two herbaceous classes. The confusions between cropland and grassland further influenced the conversions mapped, using the temporal segmentation algorithm. We also found considerable confusions with the permanent grassland and permanent non-vegetated land which was caused by the inter-annual variability in the dry, sparse vegetated land. Second, a relatively strict threshold was set in the temporal segmentation and change mapping in a trade-off to avoid time series over-fitting and capture more changes. The higher errors in the change classes of the early years are likely caused by the higher susceptibility of the segmentation approach to outliers (Griffiths et al. 2012). Nevertheless, our segmentation algorithm generated highly accurate estimations of the change timing labels. Third, the complex LULCC processes on the ground may not be coherently reflected from the perspective of remote sensing. Mapping and monitoring land use by remote sensing data can be problematic, since satellite imagery portrays land cover rather than use (Loveland and DeFries 2004a). For instance, we found that cropland retirement had considerable confusions with other changes. The confused cropland retirement was due to urban sprawl occurring on the cropland surrounding the cities in Inner Mongolia. A large area of land was taken out of cropping and kept unused for years. Therefore, we could only map the conversion from cropland to grassland before the impervious space gradually covered all land. Finally, fine-scale land change processes could be missed by the relatively coarse resolution MODIS. Although we observed a temporal pattern of forest regeneration similar to national census data, the detected absolute change area was much lower – taking into account that Inner Mongolia covers nearly 15% of all national program zones (Figure IV-4B, Figure IV-10). Compositing higher resolution archives, such as Landsat imagery, may improve detecting LULCC at fine scale across broad scales (Potapov et al. 2011; Griffiths et al. 2013). However, high-frequency observations are still needed to capture rapid changes in a non-linear land system.

5 Conclusion

Detecting LULCC is perhaps one of the most important tasks for the remote sensing community. The development of abundant and vigorous algorithms has greatly enhanced the capacity of land systems monitoring, especially at regional to global scales. The service of wide-swath satellite sensors and long-term data depositories further make global

LULCC mapping at regular interval feasible. In combining a temporal segmentation approach and a land cover probability time series derived machine-learning approach, this study provides an effective means of accurately mapping land cover changes across broad scales. Our mapping approach takes advantage of the hyper-temporal resolution of the MODIS archive, and exploits the different characteristic signatures of land use/cover properties in-depth to produce a pan-view of LULCC at an annual interval. To our knowledge, this study is the first to provide a spatially and temporally detailed documentation of how land use was altered in Inner Mongolia against the background of China's political decisions. We highlighted the capacity of our approach to detect rapid land cover conversion and gradual land change in non-linear land systems.

In this study, we found that China's ecological programs helped to reduce human pressure on the land system in Inner Mongolia. This is evidenced by the detected decreasing deforestation and net forest gain, as well as the significant cropland retirement in the policy implementation zones. The change of political decisions, however, caused drastic changes in land systems. Here we found a rapid decrease in the extent of forest regeneration and cropland retirement after 2003. Our findings contribute to the acknowledgement of the effectiveness of China's ecological programs and the broader discussion on whether China's experience is exemplary for the developing countries pursuing rapid economic development while mitigating land degradation. One should be aware, however, that the long-term and cross-border effects of China's ecological programs should be examined regardless of the current success stories. The sustainability of large-scale land restoration relying on massive subsidization needs to be observed in the future. On the other hand, we need comprehensive assessments to understand what LULCC processes triggered by political decisions mean for China and the world.

Acknowledgements

This work was supported by the China Scholarship Council (CSC), Grant 2009601084 and Humboldt Innovation.

Chapter V:
Synthesis

1 Summary

The overall aim of this thesis is to gain a better understanding about land changes in Inner Mongolia after the year 2000 by using a remote sensing approach and considering China's land restoration programs. Monitoring LULCC change helps one to evaluate the effectiveness of current land use policies and therefore provides important information for developing more sustainable policies. Such monitoring becomes more and more important for assessing policy effects in our era of globalization. As the world's largest and one of the most rapidly developing countries, China's land use policy on restoring natural ecosystems not only profoundly affects regional environments, but further triggers interconnected cross-border consequences due to indirect effects. Studying how the land system responded to China's land restoration programs is the premise for understanding the complex interactions and feedbacks between distant social-ecological systems (Lambin and Meyfroidt 2011; Meyfroidt et al. 2013). Inner Mongolia is a hot-spot of environmental change and policy implementation, and thus provides an interesting example in this context. To advance our understanding of land use and land cover change in Inner Mongolia, a deeper knowledge of long-term remote sensing time series and improved methodology for change detection is required.

This thesis investigated three core research questions to address the issues mentioned above, and here they are answered individually:

Research question I: How do time series from global satellite archives compare across Inner Mongolia, and how do trends derived from time series relate to land change?

In Chapter II, the trends of annual NDVI and the phenological indicators derived from AVHRR GIMMS, SPOT VGT and MODIS Terra time series were compared to reveal the strength and limits of using long-term hyper-temporal archives for change detection. To avoid spurious trends due to short-term (e.g., phenological) variations in the data or overall low signal-to-noise-ratios, a comparison was conducted between MODIS Terra and SPOT VGT, and between SPOT VGT and AVHRR GIMMS during their overlap periods so that longer time series could be used for analysis.

The results illustrated that temporal inconsistences exist in different archives and sensitivity analyses are needed before combing these different data for regional time series analysis. The spatial pattern of vegetation trends derived from SPOT VGT and MODIS Terra exhibited great similarities, and the regression analysis between these two NDVI

product-derived trend parameters further confirmed a strong agreement. However, major disagreements became apparent when inter-annual trends between SPOT VGT and AVHRR GIMMS NDVI were compared. Higher variance in differences and stronger average differences between trends from the two archives were found as vegetation cover increases. In the test regions of Ordos and Hinggan, AVHRR GIMMS was found to both neglect and overestimate land cover change processes in different cases. Various factors such as illumination differences due to platform change or sensor orbital drift, lack of atmospheric correction, or different spatial aggregation algorithms may hamper the capacity of AVHRR GIMMS to reliably detect land changes. Therefore, it is important to check the comparability of trends derived from hyper-temporal time series before drawing conclusions about the respective regional setting.

The vegetation trend derived from MODIS Terra and SPOT VGT suggests that cropland areas expanded while grassland remained relatively stable in Inner Mongolia during the past decade. From the MODIS Terra dataset, 24% of the cropland area showed an increasing NDVI trend, suggesting that agricultural intensification occurred in the past decade in Inner Mongolia. This finding is in line with the ground census data, which indicates that the land use intensification process in Inner Mongolia occurs largely due to increasing inputs such as fertilizer, machinery and irrigation (Song and Pijanowski 2014). About 15.4% of the grassland shows increasing vegetation cover, while only 3.9% of the area showed a decreasing trend from the MODIS Terra archive. This finding suggests the degrading trend of grassland was reversed after 2000.

Research question II: How can land use and land cover change be reliably mapped at an annual interval using hyper-temporal satellite imagery?

In Chapter III, an automated approach for mapping land cover changes at annual time intervals was developed using data from MODIS Terra. The underlying idea is to characterize changes between land use and land cover types across large areas using a trajectory-based approach. Rather than using the underlying spectral values or vegetation indices, machine learning estimated per-pixel land cover probabilities were employed to map changes among different land cover types. The temporal segmentation algorithm MODTrendr, on the other hand, enhances the capacity of depicting the process of various land cover changes that are difficult to detect with traditional multi-date comparison methods, e.g., long-term, gradual change processes such as afforestation and short-term changes in highly resilient systems.

The approach developed in this chapter achieved reliable accuracy for annual land cover change mapping. Both the abrupt and gradual land change processes were well depicted, though the levels of accuracy vary from one type to another. Forest change, for example, was found to be most reliably detected, while changes between herbaceous land cover types were less well detected due to their spectral similarity. This approach highlights that land cover probability can be used for tackling land cover change detection instead of only being treated as a by-product of discrete classification. The study suggested that land cover probability could even be used to channel land cover information derived from multi-sensor-based imagery, as long as they share the same land cover legend. This chapter also highlights the capacity of a trajectory-based method to explore the in-depth signature of land surface dynamics from time series. Regardless the spatial resolution, this approach could also be applied to the imagery from medium resolution sensors such as Landsat if a near-annual time series of land probability can be obtained.

Research question III: How was the land changed in Inner Mongolia considering national land restoration programs?

In Chapter IV, the approach developed in Chapter III was employed to investigate the spatial and temporal pattern of three land cover change processes that are mostly targeted by China's land restoration programs: deforestation, forest regeneration and cropland retirement. Results indicated that forest areas have been recovering during the past decade, whereas cropland retirement varies over space and time. Specifically, most of the forest loss (71.5%) was caused by fire disturbances, which brought a deforestation area of 205,534±14,556 hectares during the years 2000 and 2012. The fire-excluded deforestation rate rapidly decreased after 2000, and the counties that were enrolled in the NFCP program showed more decline in deforestation. The forest regeneration findings may suggest that China's land restoration programs help forest ecosystems to recover. Most forest gain was detected in the NFCP and BTSST installed regions where forest regeneration was promoted. The higher forest regeneration rates in the steeper areas seem to directly fulfill the program target, which aims to reduce soil erosion in the mountainous environments. Political decisions triggered a drastic change in forest regeneration. A rapid decrease in the area of forest regeneration was detected in 2004 due to the reduced scale of land restoration programs in response to rising national food security concerns. The spatial and temporal distribution of the forest regeneration further suggests that the forest gain was merely forest expansion, rather than the recovery of fire-disturbed forest.

A similar development compared to forest regeneration was found in cropland retirement. Most of the conversions from cropland to grassland occurred at the early stage of the land restoration programs. In the steeper and drier areas, which do not favor agricultural activities, higher cropland retirement rates were found. This finding suggests the GGP program has been accepted by the farmers, at least by those who are willing to use their vulnerable land in a more adaptive way. Other factors such as urbanization might also influence land use decisions and further encourage the conversion from cropland to grassland in Inner Mongolia. For example, 26.8% of people engaged in agriculture transferred to other economic sectors during 2000 and 2012. As the urbanization process continues, less labor will be involved in agricultural production, and this affect will change regional land use in the near future.

2 Conclusion

Monitoring land use and land cover change helps us to better understand how land use and land cover are impacted by human decisions and other factors, and thereby supports the development and implementation of sustainable land use policies. Thus, remote sensing techniques provide unique insights for monitoring how and when land use and land cover was altered, and help determine and evaluate drivers of the changes. This thesis monitored LULCC in Inner Mongolia using state-of-the-art remote sensing approaches to better understand the role of China's land use policies.

Results from this thesis clearly demonstrate the limit and the opportunities of coarse resolution remote sensing archive for monitoring long-term land change across broad scales. Radiometric consistency is the perquisite for reliably detecting land changes using satellite imagery, yet uncertainties exist, either due to the inherent sensor issues (e.g. sensor design, sensor degradation) or data processing. This is especially the case for AVHRR, which used different versions of sensors on multiple platforms over three decades. For users, the AVHRR-based products are often considered to be of high quality because of the careful and elaborate preprocessing that was implemented by the product developers. However, this thesis emphasizes that a critical data exploration of AVHRR GIMMS is essential prior to regional applications. Further improvement is also mandatory for producing more reliable AVHRR products for the user's community.

Dense time series from the coarse resolution archive allows us to better understand complex land changes. The hyper-temporal observation of coarse resolution archive is well

suited to monitor such intra/inter-annual land changes. For example, with equidistant and frequent observations, it is possible to derive phenological parameters that can be used for addressing land changes. As illustrated in this thesis, hyper-temporal imagery time series yields improved interpretation of complex land change processes. Thus, combining a trajectory-based approach and machine learning derived probability allows one to monitor both abrupt and gradual changes between multiple land use and land cover categories at an annual interval. The results can support better understanding of the drivers of land change, especially how land use policies quickly trigger surface changes.

So, how has land use and land cover in Inner Mongolia been influenced by China's land use policies and other underlying social-economic factors after 2000?

The results in Chapter II and Chapter IV showed that both gradual land modification and drastic land conversions occurred in Inner Mongolia during the observation period. Forest was generally reported to have shrunk before the year 2000 in Inner Mongolia (Zhan et al. 2004; Zhang et al. 2006); this thesis found that the trend of forest loss was reversed after 2000 and very little deforestation could be detected in recent years. Decreasing deforestation is not exceptional in Inner Mongolia; similar trends were also observed in the neighboring regions where NFCP programs were implemented (Zhou et al. 2011; Wang et al. 2012a).

The results of forest regeneration confirm the effectiveness of diverse efforts to promote forest recovery in Inner Mongolia. As opposed to the top-down command of reducing deforestation, forest was regenerated in a more diverse way. In the state-controlled forests (e.g. Greater Khingan Range) or collective barren lands, forests were mostly planted by local governments according to an annual plan. Correspondingly, a high rate of forest regeneration was detected in the northeast counties that are mostly covered by state-owned forested land. For non-state-owned land, farmers were encouraged to plant trees by offering subsidies higher than the opportunity cost. In counties such as south Chifeng, which were mostly dominated by croplands, a strong gain in forests was detected. Together with other field surveys (Yan 2010; Su et al. 2011; Song et al. 2014), this thesis supports the assumption that the political instrument of subsidies was effective at encouraging local farmers to join the government's ecological programs.

Agricultural lands underwent different types of development in Inner Mongolia. Reduced land use pressure in low-quality land and land use intensification were both observed after 2000. On the one hand, cropland retirement programs stimulated the conversion of

croplands to grasslands in ecologically fragile regions. While geographical conditions in dry and steep areas are not suitable for tree plantations, converting cropland to grassland is a better choice. On the other hand, this thesis found land use intensification in many cropland areas of Inner Mongolia (Figure II-3, Table II-II). As the land suitable for cultivation becomes scarcer in Inner Mongolia, intensification of arable land becomes a solution for meeting the increasing demand for agricultural products (Jiang et al. 2013).

The drastic changes of forest regeneration and cropland retirement after the year 2003 reflect the variability and inconsistency of the policies; the rapid decrease of cropland due to cropland retirement programs has cast a shadow on grain production. Therefore, the government largely reduced the scale of cropland retirement in 2004. Later in 2009, the central government of China set a "red line" (or bottom line, Chinese: 耕地红线) of minimum cropland area to guarantee food security. In consequence, the question is, can land use intensification compensate the loss of grain production caused by the cropland retirement program? From the official statistics data, grain production increased, though the area of croplands shrank between 2000 and 2012 (IMARBS 2000-2013). Thus, the intensified croplands might fill the gap of grain loss due to the cropland retirement program (Deng et al. 2006; Song and Pijanowski 2014). Therefore, the government should comprehensively re-evaluate the influence of current political decisions and make more concrete land use policies in the future.

Another question arises: What are the ecological consequences of land use and land cover change in Inner Mongolia?

The main purpose of China's land restoration program is to mitigate the negative ecological impacts of land cover use. Though implemented only for a decade, substantial ecological impacts might be introduced by the land restoration programs in Inner Mongolia. The net forest gain observed in this thesis suggests that the capacity of carbon sequestration was enhanced in Inner Mongolia. Some regions have shifted from net carbon sources to carbon sinks due to increased levels of vegetation cover (Feng et al. 2013). Converting croplands to grasslands also benefits long-term carbon sequestration in the arid and semi-arid Inner Mongolia (Zhang et al. 2007b; Deng et al. 2013). Promoting forest recovery in subarctic China might help inhibiting temperature to rise, though the exact effect on climate warming still needs to be quantified (Gao and Liu 2012; Peng et al. 2014). Another potential contribution of the increased forest and grassland areas is the reduction of soil erosion. In arid and semi-arid environments, converting croplands to

native ecosystems was effective for alleviating wind or water erosion (Fu et al. 2011; Deng et al. 2012). The increasing forest area and the conversion from croplands to grasslands was also found to have positive effects on biodiversity, though this effect largely depends on species selected for forest and grassland restoration (Yang et al. 2006; Zhang 2011b).

Agriculture intensification, however, may pose environmental challenges in Inner Mongolia. The increased yield was largely achieved through more production inputs such as fertilizer and irrigation, which could influence ecosystems in many ways. It is well recognized that industrial fertilizers change soil composition, contribute to the emission of N_2O and NO to the atmosphere, as well as increase nitrates in water runoff and the sediments therein (Matson et al. 1997; Steffen 2005; Qu et al. 2014). The increasing use of ground and underground water for irrigation may exacerbate water shortages in the dry and semi-dry Inner Mongolia, thus disrupting regional hydrological cycling and altering aquatic environments. Case studies indicated human activities—especially agriculture intensification—consumed much of the limited water resources, thus leading to the expansion of desertification in arid and semi-arid Inner Mongolia (Zhang et al. 2009; Lian et al. 2012; Hu et al. 2013).

Moving beyond Inner Mongolia, land use policies in China may trigger unexpected and indirect ecological consequences in other regions or countries. Indeed, cross-border trade has caused land use displacement, and brought with it unintended effects (Mayer et al. 2005; Stahls et al. 2010). The successful reduction of deforestation in China cannot be achieved without importing timber products from other countries to fill the timber shortage. In China during 1998 and 2011, the import of coniferous timber increased 21-fold, from 1.5 million to 31.5 million m^3, respectively (SFA 2000-2013). Therefore, the forest protection policy in Inner Mongolia has likely increased the risk of deforestation in other boreal areas such as Russia. On the other hand, land displacement as a regional specialization increases the efficiency of land use (Lambin and Meyfroidt 2011). Thus, retiring the low-yield croplands in the unsuited areas of Inner Mongolia and importing agricultural products from more productive regions could improve the efficiency of land use and relieve the human pressure on ecological fragile areas.

This thesis reveals the importance of national land use policies in shaping regional land use and land cover patterns. Using coarse resolution imagery time series, it is feasible to explore the in-depth information of previous land use and land cover change across large areas. Yet, monitoring land change back to 1980s poses specific requirements on the data

quality, which is particularly the case for the coarse-resolution archive. As shown in this thesis, the AVHRR GIMMS archive suffers considerable temporal inconsistency compared to other state-of-the-art sensor-derived NDVI products. The approach developed for detecting annual changes between different land use and land cover categories, on the other hand, highlights the capacity of remote sensing time series to capture complex land change processes. By applying the approach in Inner Mongolia, this thesis emphasizes how land use policy triggers ground changes. For example, the NFCP program triggered rapidly decreasing deforestation since the implementation year of 2000. Regardless of the present effectiveness of China's land use policies, there is a need to revise the current land use policies so that the goal of mitigating environmental deterioration can be better accomplished. Converting croplands in unproductive areas to grassland or forest does not threaten grain production; rather, resuming land restoration programs in Inner Mongolia will be ecologically and sociologically beneficial (Liu and Wu 2010). In this context, policy makers should comprehensively evaluate the consequences of land use policies through implementation, and thus create more effective policies that promote sustainable land use.

3 Outlook

This thesis has explored the data utility and methodological capacity for land system monitoring on one hand, and land dynamics in Inner Mongolia influenced by multiple factors, on the other. During the course of the thesis, some interesting perspectives for future research have surfaced.

Long-term monitoring supports increased understanding about how various factors shape land use and land cover. As Chapter II shows, AVHRR GIMMS suffers from temporal inconsistency due to multiple factors. Other AVHRR NDVI products, for example Pathfinder, were also found to have either temporal gaps or other quality problems (Nagol et al. 2009; Beck et al. 2011). The under-developed AVHRR NDVI products such as GIMMS-3g (Pinzon and Tucker 2014) may overcome the shortcomings of previous versions of AVHRR GIMMS. Still, the coarse 8-km resolution would neglect a fine-scale land change process. The 30-m resolution Landsat archive provides over 30 years of observations, and the recent granting of access to the archive greatly strengthens its capacity for land surface monitoring. The processing techniques that emerged partly in response to the free data policy, especially pixel-based compositing approaches (Roy et al.

2010; Potapov et al. 2011; Griffiths et al. 2013), seem to be a promising way to broaden Landsat data for land use and land cover change monitoring across large scales.

As the largest and most ambitious ecological programs in the world, NFCP, GGP and other programs no doubt influence national and even global land use patterns. While these programs are conducted nationwide and the implementation standards are relatively homogenous, regional variance may greatly influence the effectiveness of the programs. Previous research indicated that the success of implementation strongly depends on the local context (Grosjean and Kontoleon 2009; Yao et al. 2010; Persha et al. 2011). The results in this thesis suggest that China's land use policies effectively preserve and restore the forest ecosystem in Inner Mongolia, partly owing to the state-owned forestland ownership. Future research is therefore needed to assess whether successful implementation is also possible in other Chinese provinces with different regional contexts. A wide-area study on land system dynamics would facilitate regional comparisons, and thus support investigating the determinants of land use. This will further support revising and regionalizing the current programs.

Understanding land displacement and its associated consequences is necessary for promoting sustainable land use while avoiding shifting geographically negative environmental impacts. Such understanding requires one to better integrate factors associated with the demand-supply chain for land resources, yet few studies have established causal links between land use policy and actual land changes at the global scale (Meyfroidt et al. 2013). Analyzing the displacement effect of China's land restoration programs was beyond the scope of this thesis and should be an objective for future research. While datasets on global trade volumes alone are not sufficient for analyzing casual links, integrating remote-sensing derived land use and land cover change information and land-based consumption-production information for modeling would be one option to assess the extent to which China's land use policies shifted external land changes.

References

Alcantara, C., Kuemmerle, T., Prishchepov, A.V., & Radeloff, V.C. (2012). Mapping abandoned agriculture with multi-temporal MODIS satellite data. *Remote Sensing of Environment, 124*, 334-347.

Alcaraz-Segura, D., Liras, E., Tabik, S., Paruelo, J., & Cabello, J. (2010). Evaluating the Consistency of the 1982-1999 NDVI Trends in the Iberian Peninsula across Four Time-series Derived from the AVHRR Sensor: LTDR, GIMMS, FASIR, and PAL-II. *Sensors, 10*, 1291-1314.

An, Y.Q., Qu, Y.H., Cao, H.Y., Duan, X.L., Wu, J.W., & Chen, A.P. (2008). Supervising the salted land distribution of Hetao irrigation area in Inner Mongolia using remote sensing. *Remote Sensing Technology and Application, 23*, 68-74 In Chinese.

Baldi, G., Nosetto, M.D., Aragon, R., Aversa, F., Paruelo, J.M., & Jobbagy, E.G. (2008). Long-term satellite NDVI data sets: Evaluating their ability to detect ecosystem functional changes in south America. *Sensors, 8*, 5397-5425.

Bao, Y.H., Wulantuya, Xiang, B., & Zhao, X.L. (1998). Studies on the movement of farmland gravity and analysis of its driving forces in Inner Mongolia, China. *Progress in Geography, 17*, 47-54 In Chinese.

Barnosky, A.D., Hadly, E.A., Bascompte, J., Berlow, E.L., Brown, J.H., Fortelius, M., Getz, W.M., Harte, J., Hastings, A., Marquet, P.A., Martinez, N.D., Mooers, A., Roopnarine, P., Vermeij, G., Williams, J.W., Gillespie, R., Kitzes, J., Marshall, C., Matzke, N., Mindell, D.P., Revilla, E., & Smith, A.B. (2012). Approaching a state shift in Earth's biosphere. *Nature, 486*, 52-58.

Barsimantov, J., & Antezana, J.N. (2012). Forest cover change and land tenure change in Mexico's avocado region: Is community forestry related to reduced deforestation for high value crops? *Applied Geography, 32*, 844-853.

Barthold, F.K., Wiesmeier, M., Breuer, L., Frede, H.G., Wu, J., & Blank, F.B. (2013). Land use and climate control the spatial distribution of soil types in the grasslands of Inner Mongolia. *Journal of Arid Environments, 88*, 194-205.

Bayaer, Audengaowa, Ma, A.Q., Zhou, Y.M., & Wang, J.H. (2005). Inner Mongolia LUCC time and space process and driving mechanism in the historic times. *Human Geography, 20*, 122-127 In Chinese.

Beck, H.E., McVicar, T.R., van Dijk, A.I.J.M., Schellekens, J., de Jeu, R.A.M., & Bruijnzeel, L.A. (2011). Global evaluation of four AVHRR-NDVI data sets: Intercomparison and assessment against Landsat imagery. *Remote Sensing of Environment, 115*, 2547-2563.

Bégué, A., Vintrou, E., Ruelland, D., Claden, M., & Dessay, N. (2011). Can a 25-year trend in Soudano-Sahelian vegetation dynamics be interpreted in terms of land use change? A remote sensing approach. *Global Environmental Change, 21*, 413-420.

Bennett, M.T. (2008). China's sloping land conversion program: Institutional innovation or business as usual? *Ecological Economics, 65*, 699-711.

Boschetti, L., Flasse, S.P., & Brivio, P.A. (2004). Analysis of the conflict between omission and commission in low spatial resolution dichotomic thematic products: The Pareto Boundary. *Remote Sensing of Environment, 91*, 280-292.

Boschetti, M., Stroppiana, D., Brivio, P.A., & Bocchi, S. (2009). Multi-year monitoring of rice crop phenology through time series analysis of MODIS images. *International Journal of Remote Sensing, 30*, 4643-4662.

Bouza-Deano, R., Ternero-Rodriguez, M., & Fernandez-Espinosa, A.J. (2008). Trend study and assessment of surface water quality in the Ebro River (Spain). *Journal of Hydrology, 361*, 227-239.

Bradley, B.A., & Mustard, J.F. (2008). Comparison of phenology trends by land cover class: a case study in the Great Basin, USA. *Global Change Biology, 14*, 334-346.

Breiman, L. (2001). Random forests. *Machine learning, 45*, 5-32.

Brogaard, S., & Zhao, X.Y. (2002). Rural reforms and changes in land management and attitudes: A case study from Inner Mongolia, China. *Ambio, 31*, 219-225.

Broich, M., Hansen, M.C., Potapov, P., Adusei, B., Lindquist, E., & Stehman, S.V. (2011). Time-series analysis of multi-resolution optical imagery for quantifying forest cover loss in Sumatra and Kalimantan, Indonesia. *International Journal of Applied Earth Observation and Geoinformation, 13*, 277-291.

Brown, J.C., Jepson, W.E., Kastens, J.H., Wardlow, B.D., Lomas, J.M., & Price, K.P. (2007). Multitemporal, moderate-spatial-resolution remote sensing of modern agricultural production and land modification in the Brazilian Amazon. *Giscience & Remote Sensing, 44*, 117-148.

Brown, M.E., Lary, D.J., Vrieling, A., Stathakis, D., & Mussa, H. (2008). Neural networks as a tool for constructing continuous NDVI time series from AVHRR and MODIS. *International Journal of Remote Sensing, 29*, 7141-7158.

Brown, M.E., Pinzon, J.E., Didan, K., Morisette, J.T., & Tucker, C.J. (2006). Evaluation of the consistency of long-term NDVI time series derived from AVHRR, SPOT-Vegetation, SeaWiFS, MODIS, and Landsat ETM+ sensors. *IEEE Transactions on Geoscience and Remote Sensing, 44*, 1787-1793.

Cai, W.H., Yang, J., Liu, Z.H., Hu, Y.M., & Weisberg, P.J. (2013). Post-fire tree recruitment of a boreal larch forest in Northeast China. *Forest Ecology and Management, 307*, 20-29.

Canadell, J.G., Steffen, W.L., & White, P.S. (2002). IGBP/GCTE terrestrial transects: Dynamics of terrestrial ecosystems under environmental change - Introduction. *Journal of Vegetation Science, 13*, 298-300.

Cao, S.X. (2008). Why large-scale afforestation efforts in China have failed to solve the desertification problem. *Environmental Science & Technology, 42*, 1826-1831.

Cao, S.X., Wang, G.S., & Chen, L. (2010a). Assessing effects of afforestation projects in China Reply. *Nature, 466*, 315-315.

Cao, S.X., Wang, G.S., & Chen, L. (2010b). Questionable value of planting thirsty trees in dry regions. *Nature, 465*, 31-31.

Card, D.H. (1982). Using known map category marginal frequencies to improve estimates of thematic map accuracy. *Photogrammetric Engineering and Remote Sensing, 48*, 431-439.

Cardinale, B.J., Duffy, J.E., Gonzalez, A., Hooper, D.U., Perrings, C., Venail, P., Narwani, A., Mace, G.M., Tilman, D., Wardle, D.A., Kinzig, A.P., Daily, G.C., Loreau, M., Grace, J.B., Larigauderie, A., Srivastava, D.S., & Naeem, S. (2012). Biodiversity loss and its impact on humanity. *Nature, 486*, 59-67.

Chan, A.L. (2001). *Mao's crusade : politics and policy implementation in China's great leap forward*. Oxford: Oxford University Press.

Chang, R.Y., Fu, B.J., Liu, G.H., & Liu, S.G. (2011). Soil Carbon Sequestration Potential for "Grain for Green" Project in Loess Plateau, China. *Environmental Management, 48*, 1158-1172.

Chaogemandula (2012). A study on the land issues of Hinggan League area in modern era. Hohhot: Inner Mongolia University.

Charney, J., Stone, P.H., & Quirk, W.J. (1975). Drought in the Sahara: A Biogeophysical Feedback Mechanism. *Science, 187*, 434-435.

Chazdon, R.L. (2008). Beyond deforestation: Restoring forests and ecosystem services on degraded lands. *Science, 320*, 1458-1460.

Chen, J.S., He, D.W., & Cui, S.B. (2003). The response of river water quality and quantity to the development of irrigated agriculture in the last 4 decades in the Yellow River Basin, China. *Water Resources Research, 39*.

Ci, L.J., & Yang, X.H. (2010). *Desertification and its control in China*. Heidelberg: Springer.

Clark, M.L., Aide, T.M., Grau, H.R., & Riner, G. (2010). A scalable approach to mapping annual land cover at 250 m using MODIS time series data: A case study in the Dry Chaco ecoregion of South America. *Remote Sensing of Environment, 114*, 2816-2832.

Clark, M.L., Aide, T.M., & Riner, G. (2012). Land change for all municipalities in Latin America and the Caribbean assessed from 250-m MODIS imagery (2001-2010). *Remote Sensing of Environment, 126*, 84-103.

Cleveland, R.B., Cleveland, W.S., McRae, J.E., & Terpenning, I. (1990). STL: A seasonal-trend decomposition procedure based on Loess. *Journal of Official Statistics, 6*, 3-73.

Cleverland, R.B., Cleveland, W.S., & McRae, J.E. (1990). A seasonal-trend decomposition procedure based on Loess. *Journal of Official Statistics, 6*, 3-73.

Colditz, R.R., Schmidt, M., Conrad, C., Hansen, M.C., & Dech, S. (2011). Land cover classification with coarse spatial resolution data to derive continuous and discrete maps for complex regions. *Remote Sensing of Environment, 115*, 3264-3275.

Cracknell, A.P. (Ed.) (1997). *The advanced very high resolution radiometer (AVHRR)*. London ; Bristol, PA: Taylor & Francis.

Crutzen, P.J. (2002). Geology of mankind. *Nature, 415*, 23-23.

de Beurs, K.M., & Henebry, G.M. (2004). Land surface phenology, climatic variation, and institutional change: Analyzing agricultural land cover change in Kazakhstan. *Remote Sensing of Environment, 89*, 497-509.

de Blas, D.E., & Perez, M.R. (2008). Prospects for Reduced Impact Logging in Central African logging concessions. *Forest Ecology and Management, 256*, 1509-1516.

de Jong, R., Verbesselt, J., Schaepman, M.E., & de Bruin, S. (2012). Trend changes in global greening and browning: contribution of short-term trends to longer-term change. *Global Change Biology, 18*, 642-655.

De Sherbinin, A., Data, S., Use, L., & Change, C. (2002). *A CIESIN thematic guide to land-use and land-cover change (LUCC)*.Center for International Earth Science Information Network, Columbia University.

Dearing, J.A., Braimoh, A.K., Reenberg, A., Turner, B.L., & van der Leeuw, S. (2010). Complex Land Systems: the Need for Long Time Perspectives to Assess their Future. *Ecology and Society, 15*.

DeFries, R.S., Asner, G.P., & Houghton, R.A. (2004a). *Ecosystems and land use change*. Washington, DC: American Geophysical Union.

DeFries, R.S., Foley, J.A., & Asner, G.P. (2004b). Land-use choices: balancing human needs and ecosystem function. *Frontiers in Ecology and the Environment, 2*, 249-257.

DeFries, R.S., Houghton, R.A., Hansen, M.C., Field, C.B., Skole, D., & Townshend, J. (2002). Carbon emissions from tropical deforestation and regrowth based on satellite observations for the 1980s and 1990s. *Proceedings of the National Academy of Sciences of the United States of America, 99*, 14256-14261.

Defries, R.S., & Townshend, J.R.G. (1994). NDVI-derived land-cover classifications at a global scale. *International Journal of Remote Sensing, 15*, 3567-3586.

Deng, L., Liu, G.-b., & Shangguan, Z.-p. (2013). Land use conversion and changing soil carbon stocks in China's ‘Grain-for-Green’ Program: a synthesis. *Global Change Biology*, n/a-n/a.

Deng, L., Shangguan, Z.P., & Li, R. (2012). Effects of the grain-for-green program on soil erosion in China. *International Journal of Sediment Research, 27*, 120-127.

Deng, M., & Di, L. (2001). Solar zenith angle correction of global NDVI time-series from AVHRR. *IEEE Geoscience and Remote Sensing Symposium, 4*, 1838-1840.

Deng, X.Z., Huang, J.K., Rozelle, S., & Uchida, E. (2006). Cultivated land conversion and potential agricultural productivity in China. *Land Use Policy, 23*, 372-384.

Dent, D.L., Bai, Z.G., Olsson, L., & Schaepman, M.E. (2008). Proxy global assessment of land degradation. *Soil Use and Management, 24*, 223-234.

Devasthale, A., Karlsson, K.G., Quaas, J., & Grassl, H. (2012). Correcting orbital drift signal in the time series of AVHRR derived convective cloud fraction using rotated empirical orthogonal function. *Atmospheric Measurement Techniques, 5*, 267-273.

Di Gregorio, A., & Jansen, L.J.M. (1998). *Land Cover Classification System (LCCS): Classification concepts and user manual*, Environment and Natural Resources Service, GCP/RAF/287/ITA Africover - East Africa Project and Soil Resources, Management and Conservation Service. Rome: FAO.

Ding, C.R. (2003). Land policy reform in China: assessment and prospects. *Land Use Policy, 20*, 109-120.

Du, L.T. (2006). Remote sensing technology and application perspectives for monitoring Grain to Green Program. *Monitoring technology of returning farmland to forest project based on remote sensing and its application forecase, 21*, 477-482 In Chinese.

Eckstein, A. (1977). *China's economic revolution*. Cambridge: Cambridge University Press.

Eklundh, L., & Olsson, L. (2003). Vegetation index trends for the African Sahel 1982-1999. *Geophysical Research Letters, 30*.

Ellis, E.A., & Porter-Bolland, L. (2008). Is community-based forest management more effective than protected areas? A comparison of land use/land cover change in two neighboring study areas of the Central Yucatan Peninsula, Mexico. *Forest Ecology and Management, 256*, 1971-1983.

Ellis, E.C., Kaplan, J.O., Fuller, D.Q., Vavrus, S., Goldewijk, K.K., & Verburg, P.H. (2013). Used planet: A global history. *Proceedings of the National Academy of Sciences of the United States of America, 110*, 7978-7985.

Ellis, J.E., Prince, K., & Yu, F. (2002). Dimensions of desertification in the drylands of northern China. In Reynolds, J.F. & Smith, D.M.S. (Eds.), *Global Desertification: Do Humans Cause Deserts?* (pp. 167-180). Berlin: Dahlem Univ. Press.

Enkhee, J. (2000). The Mongolian tradition of legal culture and the grassland management in Inner Mongolia today. *Processings of the International Symposium on "Nomads and use of pasture today"*, (pp. 194-199).

Erb, K.H., Haberl, H., Jepsen, M.R., Kuemmerle, T., Lindner, M., Muller, D., Verburg, P.H., & Reenberg, A. (2013). A conceptual framework for analysing and measuring land-use intensity. *Current Opinion in Environmental Sustainability, 5*, 464-470.

Feng, X.M., Fu, B.J., Lu, N., Zeng, Y., & Wu, B.F. (2013). How ecological restoration alters ecosystem services: an analysis of carbon sequestration in China's Loess Plateau. *Scientific Reports, 3*.

Fensholt, R., & Proud, S.R. (2012). Evaluation of Earth Observation based global long term vegetation trends - Comparing GIMMS and MODIS global NDVI time series. *Remote Sensing of Environment, 119*, 131-147.

Fensholt, R., Rasmussen, K., Nielsen, T.T., & Mbow, C. (2009). Evaluation of earth observation based long term vegetation trends - Intercomparing NDVI time series trend

analysis consistency of Sahel from AVHRR GIMMS, Terra MODIS and SPOT VGT data. *Remote Sensing of Environment, 113*, 1886-1898.

Field, C.B., Behrenfeld, M.J., Randerson, J.T., & Falkowski, P. (1998). Primary production of the biosphere: Integrating terrestrial and oceanic components. *Science, 281*, 237-240.

Foley, J.A., DeFries, R., Asner, G.P., Barford, C., Bonan, G., Carpenter, S.R., Chapin, F.S., Coe, M.T., Daily, G.C., Gibbs, H.K., Helkowski, J.H., Holloway, T., Howard, E.A., Kucharik, C.J., Monfreda, C., Patz, J.A., Prentice, I.C., Ramankutty, N., & Snyder, P.K. (2005). Global consequences of land use. *Science, 309*, 570-574.

Foley, J.A., Ramankutty, N., Brauman, K.A., Cassidy, E.S., Gerber, J.S., Johnston, M., Mueller, N.D., O'Connell, C., Ray, D.K., West, P.C., Balzer, C., Bennett, E.M., Carpenter, S.R., Hill, J., Monfreda, C., Polasky, S., Rockstrom, J., Sheehan, J., Siebert, S., Tilman, D., & Zaks, D.P.M. (2011). Solutions for a cultivated planet. *Nature, 478*, 337-342.

Fontana, F., Rixen, C., Jonas, T., Aberegg, G., & Wunderle, S. (2008). Alpine Grassland Phenology as Seen in AVHRR, VEGETATION, and MODIS NDVI Time Series - a Comparison with In Situ Measurements. *Sensors, 8*, 2833-2853.

Foster, D., Swanson, F., Aber, J., Burke, I., Brokaw, N., Tilman, D., & Knapp, A. (2003). The importance of land-use legacies to ecology and conservation. *Bioscience, 53*, 77-88.

Friedl, M.A., McIver, D.K., Hodges, J.C.F., Zhang, X.Y., Muchoney, D., Strahler, A.H., Woodcock, C.E., Gopal, S., Schneider, A., Cooper, A., Baccini, A., Gao, F., & Schaaf, C. (2002). Global land cover mapping from MODIS: algorithms and early results. *Remote Sensing of Environment, 83*, 287-302.

Friedl, M.A., Sulla-Menashe, D., Tan, B., Schneider, A., Ramankutty, N., Sibley, A., & Huang, X.M. (2010). MODIS Collection 5 global land cover: Algorithm refinements and characterization of new datasets. *Remote Sensing of Environment, 114*, 168-182.

Fritz, S., See, L., McCallum, I., Schill, C., Obersteiner, M., van der Velde, M., Boettcher, H., Havlik, P., & Achard, F. (2011). Highlighting continued uncertainty in global land cover maps for the user community. *Environmental Research Letters, 6*.

Fu, B.J., Liu, Y., Lu, Y.H., He, C.S., Zeng, Y., & Wu, B.F. (2011). Assessing the soil erosion control service of ecosystems change in the Loess Plateau of China. *Ecological Complexity, 8*, 284-293.

Gallo, K., Li, L., Reed, B., Eidenshink, J., & Dwyer, J. (2005). Multi-platform comparisons of MODIS and AVHRR normalized difference vegetation index data. *Remote Sensing of Environment, 99*, 221-231.

Ganguly, S., Friedl, M.A., Tan, B., Zhang, X.Y., & Verma, M. (2010). Land surface phenology from MODIS: Characterization of the Collection 5 global land cover dynamics product. *Remote Sensing of Environment, 114*, 1805-1816.

Gao, J., & Liu, Y.S. (2012). De(re)forestation and climate warming in subarctic China. *Applied Geography, 32*, 281-290.

Gauvin, C., Uchida, E., Rozelle, S., Xu, J.T., & Zhan, J.Y. (2010). Cost-effectiveness of payments for ecosystem services with dual goals of environment and poverty alleviation. *Environmental Management, 45*, 488-501.

Geerken, R., & Ilaiwi, M. (2004). Assessment of rangeland degradation and development of a strategy for rehabilitation. *Remote Sensing of Environment, 90*, 490-504.

Gilbert, R.O. (Ed.) (1987). *Statistical methods for environmental pollution monitoring*. New York: Van Nostrand Reinhold Co.

Gitelson, A.A., & Kaufman, Y.J. (1998). MODIS NDVI optimization to fit the AVHRR data series spectral considerations. *Remote Sensing of Environment, 66*, 343-350.

Gleason, A.C.R., Prince, S.D., Goetz, S.J., & Small, J. (2002). Effects of orbital drift on land surface temperature measured by AVHRR thermal sensors. *Remote Sensing of Environment, 79*, 147-165.

Gobron, N., Pinty, B., Verstraete, M.M., & Widlowski, J.L. (2000). Advanced vegetation indices optimized for up-coming sensors: Design, performance, and applications. *IEEE Transactions on Geoscience and Remote Sensing, 38*, 2489-2505.

Goetz, S.J., Shortle, J.S., & Bergstrom, J.C. (2004). *Land use problems and conflicts: causes, consequences and solutions*. London: Routledge.

Goldewijk, K.K. (2001). Estimating global land use change over the past 300 years: The HYDE Database. *Global Biogeochemical Cycles, 15*, 417-433.

Gong, X.J. (2011). An empirical study of reform and development of Inner Mongolia Forest Industry Group. Beijing: Beijing Forestry University.

Goward, S.N., Dye, D.G., Turner, S., & Yang, J. (1993). Objective assessment of the NOAA global vegetation index data product. *International Journal of Remote Sensing, 14*, 3365-3394.

Gray, J., & Song, C.H. (2013). Consistent classification of image time series with automatic adaptive signature generalization. *Remote Sensing of Environment, 134*, 333-341.

Griffiths, P., Kuemmerle, T., Kennedy, R.E., Abrudan, I.V., Knorn, J., & Hostert, P. (2012). Using annual time-series of Landsat images to assess the effects of forest restitution in post-socialist Romania. *Remote Sensing of Environment, 118*, 199-214.

Griffiths, P., Van der Linden, S., Kuemmerle, T., & Hostert, P. (2013). A pixel-based Landsat compositing algorithm for large area land cover mapping. *IEEE Journal of Selected Topics in Applied Earth Observations and Remote Sensing, 6*, 1-14.

Grosjean, P., & Kontoleon, A. (2009). How sustainable are sustainable development programs? The case of the Sloping Land Conversion Program in China. *World Development, 37*, 268-285.

Gu, Y., Brown, J., Miura, T., Van Leeuwen, W.J., & Reed, B. (2010). Phenological Classification of the United States: A Geographic Framework for Extending Multi-Sensor Time-Series Data. *Remote Sensing, 2*, 526-544.

Guan, W.Q. (2008). A survey of Inner Mongolia returning cropland to forestry and grass situation and its institutional improvement. Lanzhou: Lanzhou University.

Guo, B.Y., & Zhang, G.J. (2009). Land use/cover changes using remote sensing and GIS techniques - taking Duolun, Inner Mongolia for example. *Agricultural Research in the Arid Areas, 27*, 240-244 In Chinese.

Guo, J.J., Liu, S.S., Liu, H.C., & Zhang, X.Y. (2013). The necessity of implementing phase II Natural Forest Conservation Program in Greater Khingan Range of Inner Mongolia. *Inner Mongolia Forestry Investigation and Design, 36*, 9-11 In Chinese.

Gupta, R.K., Prasad, T.S., Rao, P.V.K., & Manikavelu, P.M.B. (2000). Problems in upscaling of high resolution remote sensing data to coarse spatial resolution over land surface. *Remote Sensing for Land Surface Characterisation, 26*, 1111-1121.

Gutman, G., & Ignatov, A. (1997). Satellite-derived green vegetation fraction for the use in numerical weather prediction models. *Satellite Data Applications: Weather and Climate, 19*, 477-480.

Gutman, G., Janetos, A.C., Justice, C.O., Moran, E.F., Mustard, J.F., Rindfuss, R.R., Skole, D., Turner II, B.L., & Cochrane, M.A. (Eds.) (2004). *Land change science: observing, monitoring and understanding trajectories of change on the earth's surface*Springer London.

Hall, F.G., Strebel, D.E., Nickeson, J.E., & Goetz, S.J. (1991). Radiometric Rectification - toward a Common Radiometric Response among Multidate, Multisensor Images. *Remote Sensing of Environment, 35*, 11-27.

Han, J.G., Zhang, Y.J., Wang, C.J., Bai, W.M., Wang, Y.R., Han, G.D., & Li, L.H. (2008). Rangeland degradation and restoration management in China. *Rangeland Journal, 30*, 233-239.

Hao, Q.M. (2011). Research on the government behavior in the process of converting cropland to forest. Shenyang: Liaoning University.

Harding, J.S., Benfield, E.F., Bolstad, P.V., Helfman, G.S., & Jones, E.B.D. (1998). Stream biodiversity: The ghost of land use past. *Proceedings of the National Academy of Sciences of the United States of America, 95*, 14843-14847.

Hasbagen (2009). The dynamic studies on grassland vegetation types and characteristic in Etuokeqian Banner. Huhhot Inner Mongolia Agricultural University.

Helldén, U., & Tottrup, C. (2008). Regional desertification: A global synthesis. *Global and Planetary Change, 64*, 169-176.

Henry, P., & Meygret, A. (2001). Calibration of vegetation cameras on-board SPOT4. In, *Proceedings of the VEGETATION 2000 conference* (pp. 23-32). Belgirate, Italy

Heumann, B.W., Seaquist, J.W., Eklundh, L., & Jonsson, P. (2007). AVHRR derived phenological change in the Sahel and Soudan, Africa, 1982-2005. *Remote Sensing of Environment, 108*, 385-392.

Hilker, T., Natsagdorj, E., Waring, R.H., Lyapustin, A., & Wang, Y.J. (2014). Satellite observed widespread decline in Mongolian grasslands largely due to overgrazing. *Global Change Biology, 20*, 418-428.

Hill, J., Stellmes, M., Udelhoven, T., Roder, A., & Sommer, S. (2008). Mediterranean desertification and land degradation Mapping related land use change syndromes based on satellite observations. *Global and Planetary Change, 64*, 146-157.

Hill, M.J., & Donald, G.E. (2003). Estimating spatio-temporal patterns of agricultural productivity in fragmented landscapes using AVHRR NDVI time series. *Remote Sensing of Environment, 84*, 367-384.

Hird, J.N., & McDermid, G.J. (2009). Noise reduction of NDVI time series: An empirical comparison of selected techniques. *Remote Sensing of Environment, 113*, 248-258.

Hirsch, R.M., & Slack, J.R. (1984). A Nonparametric Trend Test for Seasonal Data with Serial Dependence. *Water Resources Research, 20*, 727-732.

Hirsch, R.M., Slack, J.R., & Smith, R.A. (1982). Techniques of trend analysis for monthly water-quality data. *Water Resources Research, 18*, 107-121.

Holben, B.N. (1986). Characteristics of maximum-value composite images from temporal AVHRR data. *International Journal of Remote Sensing, 7*, 1417-1434.

Hostert, P., Kuemmerle, T., Prishchepov, A., Sieber, A., Lambin, E.F., & Radeloff, V.C. (2011). Rapid land use change after socio-economic disturbances: the collapse of the Soviet Union versus Chernobyl. *Environmental Research Letters, 6*.

Hostert, P., Roder, A., & Hill, J. (2003). Coupling spectral unmixing and trend analysis for monitoring of long-term vegetation dynamics in Mediterranean rangelands. *Remote Sensing of Environment, 87*, 183-197.

Hou, X.C., Huang, L.L., Xing, G.C., Wu, L.N., & Feng, C.F. (2013). Successful experience of forestry ecological engineering construction in Tumotezuoqi. *Inner Mongolia Forestry Investigation and Design, 36*, 10-13 In Chinese.

Hu, X.L., Li, J.R., Xue, B., & Guo, J.Y. (2013). Analysis of dynamic change in wetland landscape in agro-pastoral ecotone - A case study of Duolun county, Inner Monglia. *Research of Soil and Water Conservation, 20*, 120-129 In Chinese.

Hu, Y.F., Liu, J.Y., Qi, Y.Q., & Shi, H.D. (2010). Positivist analysis on the effects of ecological projects in the farming-pastoral transition belt of Inner Mongolia Autonomous Region. *Geographical Research, 29*, 1452-1460 In Chinese.

Huang, C.Q., Coward, S.N., Masek, J.G., Thomas, N., Zhu, Z.L., & Vogelmann, J.E. (2010). An automated approach for reconstructing recent forest disturbance history using dense Landsat time series stacks. *Remote Sensing of Environment, 114*, 183-198.

Huete, A., Didan, K., Miura, T., Rodriguez, E.P., Gao, X., & Ferreira, L.G. (2002). Overview of the radiometric and biophysical performance of the MODIS vegetation indices. *Remote Sensing of Environment, 83*, 195-213.

Hufkens, K., Bogaert, J., Dong, Q.H., Lu, L., Huang, C.L., Ma, M.G., Che, T., Li, X., Veroustraete, F., & Ceulemans, R. (2008). Impacts and uncertainties of upscaling of remote-sensing data validation for a semi-arid woodland. *Journal of Arid Environments, 72*, 1490-1505.

Huttich, C., Herold, M., Wegmann, M., Cord, A., Strohbach, B., Schmullius, C., & Dech, S. (2011). Assessing effects of temporal compositing and varying observation periods for large-area land-cover mapping in semi-arid ecosystems: Implications for global monitoring. *Remote Sensing of Environment, 115*, 2445-2459.

Hyde, W.F., Belcher, B., & Xu, J.T. [CIFORHQ 1282] (2003). *China's forests: global lessons from market reforms*. Washington, DC: Resources for the Future and CIFOR.

IMARBS (2000-2013). *Inner Mongolia statistical yearbook*. Beijing: China Statistics Press. In Chinese.

Jamali, S., Seaquist, J., Eldundh, L., & Ardo, J. (2014). Automated mapping of vegetation trends with polynomials using NDVI imagery over the Sahel. *Remote Sensing of Environment, 141*, 79-89.

James, M.E., & Kalluri, S.N.V. (1994). The Pathfinder Avhrr Land Data Set - an Improved Coarse Resolution Data Set for Terrestrial Monitoring. *International Journal of Remote Sensing, 15*, 3347-3363.

Jelinski, L.W., Graedel, T.E., Laudise, R.A., Mccall, D.W., & Patel, C.K.N. (1992). Industrial Ecology - Concepts and Approaches. *Proceedings of the National Academy of Sciences of the United States of America, 89*, 793-797.

Jiang, H. (2005). Grassland management and views of nature in China since 1949: regional policies and local changes in Uxin Ju, inner Mongolia. *Geoforum, 36*, 641-653.

Jiang, H. (2006). Decentralization, Ecological Construction, and the Environment in Post-Reform China:: Case Study from Uxin Banner, Inner Mongolia. *World Development, 34*, 1907-1921.

Jiang, L., Deng, X.Z., & Seto, K.C. (2013). The impact of urban expansion on agricultural land use intensity in China. *Land Use Policy, 35*, 33-39.

John, R., Chen, J.Q., Lu, N., & Wilske, B. (2009). Land cover/land use change in semi-arid Inner Mongolia: 1992-2004. *Environmental Research Letters, 4*.

Jonsson, P., & Eklundh, L. (2002). Seasonality extraction by function fitting to time-series of satellite sensor data. *IEEE Transactions on Geoscience and Remote Sensing, 40*, 1824-1832.

Jonsson, P., & Eklundh, L. (2004). TIMESAT - a program for analyzing time-series of satellite sensor data. *Computers & Geosciences, 30*, 833-845.

Julien, Y., & Sobrino, J.A. (2010). Comparison of cloud-reconstruction methods for time series of composite NDVI data. *Remote Sensing of Environment, 114*, 618-625.

Kariyeva, J., & Van Leeuwen, W. (2011). Environmental Drivers of NDVI-Based Vegetation Phenology in Central Asia. *Remote Sensing, 3*, 203-246.

Kaufman, Y.J. (1988). Atmospheric effect on spectral signature - measurements and corrections. *IEEE Transactions on Geoscience and Remote Sensing, 26*, 441-450.

Kawada, K., Wuyunna, & Nakamura, T. (2011). Land degradation of abandoned croplands in the Xilingol steppe region, Inner Mongolia, China. *Grassland Science, 57*, 58-64.

Kendall, M.G. (Ed.) (1975). *Rank Correlation Methods*. London: Charles Griffin.

Kennedy, R.E., Yang, Z.G., & Cohen, W.B. (2010). Detecting trends in forest disturbance and recovery using yearly Landsat time series: 1. LandTrendr - Temporal segmentation algorithms. *Remote Sensing of Environment, 114*, 2897-2910.

Kenneny, R., Andréfouët, S., Cohen, W., Gómez, C., Griffiths, P., Hais, M., Healey, S., Helmer, E., Hostert, P., Lyons, M., Meigs, G., Pflugmacher, D., Phinn, S., Powell, S., Scarth, P., Sen, S., Schroeder, T., Schneider, A., Sonnenschein, R., Vogelmann, J.E., Wulder, M., & Zhu, Z. (2014). Bringing an ecological view of change to Landsat-based remote sensing. *Frontiers in Ecology and Environment*, in press.

King, M.D., Kaufman, Y.J., Menzel, W.P., & Tanre, D. (1992). Remote-sensing of cloud, aerosol, and water-vapor properties from the Moderate Resolution Imaging Spectrometer (MODIS). *IEEE Transactions on Geoscience and Remote Sensing, 30*, 2-27.

Kobayashi, H., & Dye, D.G. (2005). Atmospheric conditions for monitoring the long-terrn vegetation dynamics in the Amazon using normalized difference vegetation index. *Remote Sensing of Environment, 97*, 519-525.

Kuemmerle, T., Erb, K., Meyfroidt, P., Müller, D., Verburg, P.H., Estel, S., Haberl, H., Hostert, P., Jepsen, M.R., Kastner, T., Levers, C., Lindner, M., Plutzar, C., Verkerk, P.J., van der Zanden, E.H., & Reenberg, A. (2013). Challenges and opportunities in mapping land use intensity globally. *Current Opinion in Environmental Sustainability, 5*, 484-493.

Kuemmerle, T., Hostert, P., Radeloff, V.C., van der Linden, S., Perzanowski, K., & Kruhlov, I. (2008). Cross-border comparison of post-socialist farmland abandonment in the Carpathians. *Ecosystems, 11*, 614-628.

Labus, M.P., Nielsen, G.A., Lawrence, R.L., Engel, R., & Long, D.S. (2002). Wheat yield estimates using multi-temporal NDVI satellite imagery. *International Journal of Remote Sensing, 23*, 4169-4180.

Lambin, E.F., & Geist, H.J. (2006). *Land use and land cover change: local processes and global impacts*. Berlin: Springer.

Lambin, E.F., Geist, H.J., & Lepers, E. (2003). Dynamics of land-use and land-cover change in tropical regions. *Annual Review of Environment and Resources, 28*, 205-241.

Lambin, E.F., Geist, H.J., & Rindfuss, R.R. (2004). Introduction: Local processess with global impacts. In Lambin, E.F. & Geist, H.J. (Eds.), *Land-use and land-cover change* (p. 4). Berlin Heidelberg New York: Springer.

Lambin, E.F., & Linderman, M. (2006). Time series of remote sensing data for land change science. *IEEE Transactions on Geoscience and Remote Sensing, 44*, 1926-1928.

Lambin, E.F., & Meyfroidt, P. (2010). Land use transitions: Socio-ecological feedback versus socio-economic change. *Land Use Policy, 27*, 108-118.

Lambin, E.F., & Meyfroidt, P. (2011). Global land use change, economic globalization, and the looming land scarcity. *Proceedings of the National Academy of Sciences of the United States of America, 108*, 3465-3472.

Lambin, E.F., Turner, B.L., Geist, H.J., Agbola, S.B., Angelsen, A., Bruce, J.W., Coomes, O.T., Dirzo, R., Fischer, G., Folke, C., George, P.S., Homewood, K., Imbernon, J., Leemans, R., Li, X.B., Moran, E.F., Mortimore, M., Ramakrishnan, P.S., Richards, J.F., Skanes, H., Steffen, W., Stone, G.D., Svedin, U., Veldkamp, T.A., Vogel, C., & Xu, J.C. (2001). The causes of land-use and land-cover change: moving beyond the myths. *Global Environmental Change-Human and Policy Dimensions, 11*, 261-269.

Lasanta, T., & Vicente-Serrano, S.M. (2012). Complex land cover change processes in semiarid Mediterranean regions: An approach using Landsat images in northeast Spain. *Remote Sensing of Environment, 124*, 1-14.

Latifovic, R., & Olthof, I. (2004). Accuracy assessment using sub-pixel fractional error matrices of global land cover products derived from satellite data. *Remote Sensing of Environment, 90*, 153-165.

Latifovic, R., Pouliot, D., & Dillabaugh, C. (2012). Identification and correction of systematic error in NOAA AVHRR long-term satellite data record. *Remote Sensing of Environment, 127*, 84-97.

Lee, R., Yu, F., Price, K.P., Ellis, J., & Shi, P. (2002). Evaluating vegetation phenological patterns in Inner Mongolia using NDVI time-series analysis. *International Journal of Remote Sensing, 23*, 2505-2512.

Li, A., Wu, J.G., & Huang, J.H. (2012a). Distinguishing between human-induced and climate-driven vegetation changes: a critical application of RESTREND in inner Mongolia. *Landscape Ecology, 27*, 969-982.

Li, A.N., Deng, W., Liang, S.L., & Huang, C.Q. (2010a). Investigation on the patterns of global vegetation change using a satellite-sensed vegetation index. *Remote Sensing, 2*, 1530-1548.

Li, C.B., Qi, J.G., Feng, Z.D., Yin, R.S., Guo, B.Y., Zhang, F., & Zou, S.B. (2010b). Quantifying the effect of ecological restoration on soil erosion in China's Loess Plateau region: An application of the MMF approach. *Environmental Management, 45*, 476-487.

Li, H.Y., Wu, Y.N., & Li, X.B. (2012b). Mountain effect and differences in storm floods between northern and southern sources of the Songhua River Basin. *Journal of Mountain Science, 9*, 431-440.

Li, J., Feldman, M.W., Li, S.Z., & Daily, G.C. (2011). Rural household income and inequality under the Sloping Land Conversion Program in western China. *Proceedings of the National Academy of Sciences of the United States of America, 108*, 7721-7726.

Li, M.Z., & Zhang, X.P. (2004). Problems and counter measures in implementing Sandstorm Source Control Project in and around Beijing and Tianjin. *Journal of Beijing Forestry University, 3*, 4.

Li, O., Ma, R., & Simpson, J. (1993). Changes in the nomadic pattern and its impact on the Inner Mongolian steppe grassland ecosystem. *Nomadic Peoples, 33*, 173-192.

Li, S.Y., Huang, M., & Li, S.G. (2014). Forest carbon research in Inner Mongolia: current knowledge, opportunity and challenge. *IOP Conference Series: Earth and Environmental Science, 17*, 012011.

Li, W.J., Ali, S.H., & Zhang, Q. (2007). Property rights and grassland degradation: A study of the Xilingol Pasture, Inner Mongolia, China. *Journal of Environmental Management, 85*, 461-470.

Li, X.B. (1999). Change of arable land area in China during the past 20 years and its policy implications. *Journal of Natural Resources, 14*, 329-333 In Chinese.

Li, Y.H. (1995). Restoration dynamics of degraded grasslands in the typical steppe zone of Inner Mongolia. *Chinese Biodiversity, 3*, 125-130 In Chinese.

Li, Z.Y. (2012). The ecological effects of Natural Forest Conservation Program in Greater Khingan Range of Inner Mongolia. *Inner Mongolia Forestry Investigation and Design, 35*, 12-13 In Chinese.

Lian, J., Zhao, X.Y., Zuo, X.A., & Chang, X.L. (2012). Dynamics of landscape pattern of water areas in Horqin sandy land, China - A case study in Naiman Banner of Inner Mongolia. *Journal of Desert Research, 32*, 210-218 In Chinese.

Lillesand, T.M., Kiefer, R.W., & Chipman, J.W. (Eds.) (2008). *Remote Sensing and Image Interpretation*. Hoboken: NJ.: John Wiley and Sons, Inc.

Lin, G.C.S., & Ho, S.P.S. (2003). China's land resources and land-use change: insights from the 1996 land survey. *Land Use Policy, 20*, 87-107.

Linderman, M., Rowhani, P., Benz, D., Serneels, S., & Lambin, E.F. (2005). Land-cover change and vegetation dynamics across Africa. *Journal of Geophysical Research-Atmospheres, 110*.

Liu, C., Lu, J.Z., & Yin, R.S. (2010a). An estimation of the effects of China's priority forestry programs on farmers' income. *Environmental Management, 45*, 526-540.

Liu, C., & Wu, B. (2010). *'Grain for Green Programme' in china: Policy making and implementation?* University of Nottingham.

Liu, C., & Zhang, W. (2006). Impacts of conversion of farmland to forestland program on household income: Evidence from a sandy control program in the vicinity of Beijing and Tianjin. *China Economic Quarterly, 6*, 273-290 In Chinese.

Liu, D.S., & Cai, S.S. (2012). A spatial-temporal modeling approach to reconstructing land-cover change trajectories from multi-temporal satellite imagery. *Annals of the Association of American Geographers, 102*, 1329-1347.

Liu, H.Y., Cui, H.T., Pott, R., & Speier, M. (1999). The surface pollen of the woodland-steppe ecotone in southeastern Inner Mongolia, China. *Review of Palaeobotany and Palynology, 105*, 237-250.

Liu, H.Y., Cui, H.T., Pott, R., & Speier, M. (2000). Vegetation of the woodland-steppe transition at the southeastern edge of the Inner Mongolian Plateau. *Journal of Vegetation Science, 11*, 525-532.

Liu, J.G., & Diamond, J. (2005). China's environment in a globalizing world. *Nature, 435*, 1179-1186.

Liu, J.G., Li, S.X., Ouyang, Z.Y., Tam, C., & Chen, X.D. (2008). Ecological and socioeconomic effects of China's policies for ecosystem services. *Proceedings of the National Academy of Sciences of the United States of America, 105*, 9477-9482.

Liu, J.Y., Kuang, W.H., Zhang, Z.X., Xu, X.L., Qin, Y.W., Ning, J., Zhou, W.C., Zhang, S.W., Li, R.D., Yan, C.Z., Wu, S.X., Shi, X.Z., Jiang, N., Yu, D.S., Pan, X.Z., & Chi, W.F. (2014). Spatiotemporal characteristics, patterns, and causes of land-use changes in China since the late 1980s. *Journal of Geographical Sciences, 24*, 195-210.

Liu, J.Y., Liu, M.L., Deng, X.Z., Zhuang, D.F., Zhang, Z.X., & Luo, D. (2002). The land-use and land-cover change database and its relative studies in China. *Journal of Geographical Sciences, 12*, 275-282.

Liu, J.Y., Liu, M.L., Tian, H.Q., Zhuang, D.F., Zhang, Z.X., Zhang, W., Tang, X.M., & Deng, X.Z. (2005). Spatial and temporal patterns of China's cropland during 1990-2000: An analysis based on Landsat TM data. *Remote Sensing of Environment, 98*, 442-456.

Liu, J.Y., Liu, M.L., Zhuang, D.F., Zhang, Z.X., & Deng, X.Z. (2003). Study on spatial pattern of land-use change in China during 1995-2000. *Science in China Series D-Earth Sciences, 46*, 373-384.

Liu, J.Y., Zhang, Z.X., Xu, X.L., Kuang, W.H., Zhou, W.C., Zhang, S.W., Li, R.D., Yan, C.Z., Yu, D.S., Wu, S.X., & Jiang, N. (2009). Spatial patterns and driving forces of land use change in China in the early 21st century. *Acta Geographica Sinica, 64*, 1411-1420 In Chinese.

Liu, J.Y., Zhang, Z.X., Xu, X.L., Kuang, W.H., Zhou, W.C., Zhang, S.W., Li, R.D., Yan, C.Z., Yu, D.S., Wu, S.X., & Nan, J. (2010b). Spatial patterns and driving forces of land use change in China during the early 21st century. *Journal of Geographical Sciences, 20*, 483-494.

Liu, Q., He, Y., & Cui, B.S. (2007a). Land use/cover change and its influence on the evapotranspiration in Taoer River basin. *Resources Science, 29*, 121-126 In Chinese.

Liu, X.L., Li, F.M., Zeng, Z.X., & Chen, Q.W. (2007b). Comparisons of water use efficiency under different conversion models of cropland to grassland in the Loess Plateau of China. *Acta Ecological Sinica, 27*, 2847-2855 In Chinese.

Liu, X.Q., Wang, Y.L., Peng, J., Braimoh, A.K., & Yin, H. (2013). Assessing vulnerability to drought based on exposure, sensitivity and adaptive capacity: A case study in middle Inner Mongolia of China. *Chinese Geographical Science, 23*, 13-25.

Liu, Y., Liu, R.G., & Chen, J.M. (2012). Retrospective retrieval of long-term consistent global leaf area index (1981–2011) from combined AVHRR and MODIS data. *Journal of Geophysical Research: Biogeosciences, 117*, G04003.

Longworth, J.W., & Williamson, G.J. (1993). *China's pastoral region : sheep and wool, minority nationalities, rangeland degradation and sustainable development*. Wallingford, UK: CAB International.

Loveland, T.R., & DeFries, R.S. (2004a). Ecosystems and land use change. In DeFries, R.S., Asner, G.P. & Houghton, R.A. (Eds.), *Geophysical monograph,* (pp. viii, 344 p.). Washington, DC: American Geophysical Union.

Loveland, T.R., & Defries, R.S. (2004b). Observing and Monitoring land use and land cover change. In DeFries, R.S., Asner, G.P. & Houghton, R.A. (Eds.), *Ecosystems and land use change* (pp. 231-246). Washington, DC: American Geophysical Union.

Loveland, T.R., Reed, B.C., Brown, J.F., Ohlen, D.O., Zhu, Z., Yang, L., & Merchant, J.W. (2000). Development of a global land cover characteristics database and IGBP DISCover from 1 km AVHRR data. *International Journal of Remote Sensing, 21*, 1303-1330.

Lu, D., Mausel, P., Brondízio, E., & Moran, E. (2004). Change detection techniques. *International Journal of Remote Sensing, 25*, 2365-2401.

Lunetta, R.S., Knight, J.F., Ediriwickrema, J., Lyon, J.G., & Worthy, L.D. (2006). Land-cover change detection using multi-temporal MODIS NDVI data. *Remote Sensing of Environment, 105*, 142-154.

Luo, J.C. (2002). Influence of forest fire disaster on forest ecosystem in Great Xing'anling. *Journal of Beijing Forestry University, 24*, 101-107 In Chinese.

Luo, Z.H., Liu, B.W., Liu, S.T., Jiang, Z.G., & Halbrook, R.S. (2014). Influences of Human and Livestock Density on Winter Habitat Selection of Mongolian Gazelle (Procapra gutturosa). *Zoological Science, 31*, 108-108.

Lv, X.G., & Zhang, W.Z. (1999). The flood of the Nenjiang River and the Songhua River in 1998 and the comprehensive management of the river valley. *Scientia Geographica Sinica, 19*, 11-14 In Chinese.

Ma, Y., Chen, L.D., & Hu, C.X. (2008). Response of farmer households to / Grain-for-Green Project and quantitative analysis of its affecting factors. *Scientia Geographica Sinica, 28*, 34-39 In Chinese.

Main-Knorn, M., Cohen, W.B., Kennedy, R.E., Grodzki, W., Pflugmacher, D., Griffiths, P., & Hostert, P. (2013). Monitoring coniferous forest biomass change using a Landsat trajectory-based approach. *Remote Sensing of Environment, 139*, 277-290.

Mangiarotti, S., Mazzega, P., Hiernaux, P., & Mougin, E. (2010). The vegetation cycle in West Africa from AVHRR-NDVI data: Horizons of predictability versus spatial scales. *Remote Sensing of Environment, 114*, 2036-2047.

Mann, H.B. (1945). Non-parametric test against trend. *Econometrica, 13*, 245-259.

Martinez-Beltran, C., Jochum, M.A.O., Calera, A., & Melia, J. (2009). Multisensor comparison of NDVI for a semi-arid environment in Spain. *International Journal of Remote Sensing, 30*, 1355-1384.

Mas, J.F. (1999). Monitoring land-cover changes: a comparison of change detection techniques. *International Journal of Remote Sensing, 20*, 139-152.

Matson, P.A., Parton, W.J., Power, A.G., & Swift, M.J. (1997). Agricultural intensification and ecosystem properties. *Science, 277*, 504-509.

Mayer, A.L., Kauppi, P.E., Angelstam, P.K., Zhang, Y., & Tikka, P.M. (2005). Importing timber, exporting ecological impact. *Science, 308*, 359-360.

MEA (2005a). Ecosystems and human well-being: Desertification Synthesis. In, *Millennium Ecosystem Assessment*. Washington DC: World Resources Institute.

MEA (2005b). Ecosystems and human well-being: Synthesis. In, *Millenium Ecosystem Assessment* (p. 155). Washington DC, USA: Island Press.

Meigs, G.W., Kennedy, R.E., & Cohen, W.B. (2011). A Landsat time series approach to characterize bark beetle and defoliator impacts on tree mortality and surface fuels in conifer forests. *Remote Sensing of Environment, 115*, 3707-3718.

Meyer, W.B., & Turner, B.L. (1992). Human-population growth and global land-use cover change. *Annual Review of Ecology and Systematics, 23*, 39-61.

Meyer, W.B., & Turner, B.L. (1994). *Changes in land use and land cover : a global perspective*. Cambridge: Cambridge University Press.

Meyfroidt, P., Lambin, E.F., Erb, K.-H., & Hertel, T.W. (2013). Globalization of land use: distant drivers of land change and geographic displacement of land use. *Current Opinion in Environmental Sustainability, 5*, 438-444.

Miao, L.J., Zhu, F., He, B., Ferrat, M., Liu, Q., Cao, X., & Cui, X.F. (2013). Synthesis of China's land use in the past 300 years. *Global and Planetary Change, 100*, 224-233.

Mustard, J.F., DeFries, R.S., Fisher, T., & Moran, E. (2004). Land-use and land-cover change pathways and impacts. In Gutman, G., Janetos, A.C., Justice, C.O., Moran, E.F., Mustard, J.F., Rindfuss, R.R., Skole, D., Turner II, B.L. & Cochrane, M.A. (Eds.), *Land change science: observing, monitoring and understanding trajectories of change on the Earth's surface* (pp. 411-429). Dordrecht Boston London: Kluwer Academic Publishers.

Myneni, R.B., Keeling, C.D., Tucker, C.J., Asrar, G., & Nemani, R.R. (1997). Increased plant growth in the northern high latitudes from 1981 to 1991. *Nature, 386*, 698-702.

Nagol, J.R., Vermote, E.F., & Prince, S.D. (2009). Effects of atmospheric variation on AVHRR NDVI data. *Remote Sensing of Environment, 113*, 392-397.

Nemani, R.R., Keeling, C.D., Hashimoto, H., Jolly, W.M., Piper, S.C., Tucker, C.J., Myneni, R.B., & Running, S.W. (2003). Climate-driven increases in global terrestrial net primary production from 1982 to 1999. *Science, 300*, 1560-1563.

Nesheim, I., Reidsma, P., Bezlepkina, I., Verburg, R., Abdeladhim, M.A., Bursztyn, M., Chen, L., Cissé, Y., Feng, S., Gicheru, P., Jochen König, H., Novira, N., Purushothaman, S., Rodrigues-Filho, S., & Sghaier, M. (2014). Causal chains, policy trade offs and sustainability: Analysing land (mis)use in seven countries in the South. *Land Use Policy, 37*, 60-70.

Ojima, D.S., Chuluun, T., Bolortsetseg, B., Tucker, C.J., & Hicke, J. (2004). Ecosystems and land use change. In DeFries, R.S., Asner, G.P. & Houghton, R.A. (Eds.), *Geophysical monograph,* (pp. viii, 344 p.). Washington, DC: American Geophysical Union.

Olofsson, P., Foody, G.M., Stehman, S.V., & Woodcock, C.E. (2013). Making better use of accuracy data in land change studies: Estimating accuracy and area and quantifying uncertainty using stratified estimation. *Remote Sensing of Environment, 129*, 122-131.

Otterman, J. (1974). Baring high-albedo soils by overgrazing - hypothesized desertification mechanism. *Science, 186*, 531-533.

Ouyang, L., Liu, G.T., & Bao, X.Y. (2008). Analysis on the status quo and dynamic change of Horqin Sandy Land in the semi-arid agro-pastoral interweaving bet - Taking the Muzishan village of Ao Han as an example. *Chinese Agricultural Science Bulletin, 24*, 379-385 In Chinese.

Panda, S.S., Ames, D.P., & Panigrahi, S. (2010). Application of Vegetation Indices for Agricultural Crop Yield Prediction Using Neural Network Techniques. *Remote Sensing, 2*, 673-696.

Peng, D.L. (2010). *Monitoring Technology of the Sandstorm Source Control Project around Beijing and Tianjin*. Beijing: Science Press.

Peng, S.S., Piao, S.L., Zeng, Z.Z., Ciais, P., Zhou, L.M., Li, L.Z.X., Myneni, R.B., Yin, Y., & Zeng, H. (2014). Afforestation in China cools local land surface temperature. *Proceedings of the National Academy of Sciences of the United States of America, 111*, 2915-2919.

Persha, L., Agrawal, A., & Chhatre, A. (2011). Social and ecological synergy: Local rulemaking, forest livelihoods, and biodiversity conservation. *Science, 331*, 1606-1608.

Pettorelli, N., Vik, J.O., Mysterud, A., Gaillard, J.M., Tucker, C.J., & Stenseth, N.C. (2005). Using the satellite-derived NDVI to assess ecological responses to environmental change. *Trends in Ecology & Evolution, 20*, 503-510.

Pflugmacher, D., Cohen, W.B., & Kennedy, R.E. (2012). Using Landsat-derived disturbance history (1972-2010) to predict current forest structure. *Remote Sensing of Environment, 122*, 146-165.

Piao, S.L., Fang, J.Y., Ciais, P., Peylin, P., Huang, Y., Sitch, S., & Wang, T. (2009). The carbon balance of terrestrial ecosystems in China. *Nature, 458*, 1009-U1082.

Pinzon, J. (2002). Using HHT to successfully uncouple seasonal and interannual components in remotely sensed data. In, *SCI 2002 Conference Proceedings*. Orlando, Florida: SCI International.

Pinzon, J., Brown, M.E., & Tucker, C.J. (2004). Satellite time series correction of orbital drift artifacts using empirical mode decomposition. In Huang, N.E. & Shen, S.P. (Eds.), *Hilbert-Huang Transform: Introduction and Applications*.

Pinzon, J., & Tucker, C.J. (2014). A non-stationary 1981–2012 AVHRR GIMMS3g time series. *Remote Sensing*, in press.

Pinzon, J.E., Brown, M.E., & Tucker, C.J. (2007). *Monitoring seasonal and interannual variations in land-surface vegetation from 1981-2006 using GIMMS NDVI*. University of Maryland Global Land Cover Facility Data Distribution.

POES (U.S.), & NCDC (U.S.) (1997). Technical documentation with imagery and digital data NOAA polar orbiter data user's guide (August 1997) and NOAA global vegetation index user's guide (July 1997). In (p. 1 computer optical laser disc). Asheville, N.C.: The Center : Satellite Services Group,.

Potapov, P., Turubanova, S., & Hansen, M.C. (2011). Regional-scale boreal forest cover and change mapping using Landsat data composites for European Russia. *Remote Sensing of Environment, 115*, 548-561.

Pouliot, D., Latifovic, R., Zabcic, N., Guindon, L., & Olthof, I. (2014). Development and assessment of a 250 m spatial resolution MODIS annual land cover time series (2000-2011) for the forest region of Canada derived from change-based updating. *Remote Sensing of Environment, 140*, 731-743.

Powell, S.L., Cohen, W.B., Healey, S.P., Kennedy, R.E., Moisen, G.G., Pierce, K.B., & Ohmann, J.L. (2010). Quantification of live aboveground forest biomass dynamics with Landsat time-series and field inventory data: A comparison of empirical modeling approaches. *Remote Sensing of Environment, 114*, 1053-1068.

Price, J.C. (1991). Timing of NOAA Afternoon Passes. *International Journal of Remote Sensing, 12*, 193-198.

Qiao, G.H., Zhao, L.J., & Klein, K.K. (2009). Water user associations in Inner Mongolia: Factors that influence farmers to join. *Agricultural Water Management, 96*, 822-830.

Qinggeletu (1998). Land reforms in Eastern Inner Mongolia. *Journal o f Inner Mongolia University, 1*, 13-19 In Chinese.

Qiu, G.Y., Xie, F., Feng, Y.C., & Tian, F. (2011). Experimental studies on the effects of the "Conversion of Cropland to Grassland Program" on the water budget and evapotranspiration in a semi-arid steppe in Inner Mongolia, China. *Journal of Hydrology, 411*, 120-129.

Qu, Z., Wang, J., Almøy, T., & Bakken, L.R. (2014). Excessive use of nitrogen in Chinese agriculture results in high N2O/(N2O+N2) product ratio of denitrification, primarily due to acidification of the soils. *Global Change Biology, 20*, 1685-1698.

Rabe, A., Jakimow, B., Held, M., van der Linden, S., & Hostert, P. (2014). EnMAP-Box Manual, Version 2.0. In (p. software available at www.enmap.org)

Ramankutty, N., & Foley, J.A. (1999). Estimating historical changes in global land cover: Croplands from 1700 to 1992. *Global Biogeochemical Cycles, 13*, 997-1027.

Ramankutty, N., Graumlich, L., Achard, F., Alves, D., Chhabra, A., DeFries, R.S., Foley, J.A., Geist, H., Houghton, R.A., Goldewijk, K., Lambin, E.F., Millington, A., Rasmussen, K., Reid, R.S., & Turner, B. (2006). Global land-cover change: Recent progress, remaining challenges. In Lambin, E.F. & Geist, H. (Eds.), *Land-use and land-cover change* (pp. 9-39). Springer Berlin Heidelberg.

Ran, Y.H., Li, X., & Lu, L. (2009). China land cover classification at 1 km spatial resolution based on a multi-source data fusion approach. *Advances in earth science, 24*, 192-203.

Rasmussen, P.E., Goulding, K.W.T., Brown, J.R., Grace, P.R., Janzen, H.H., & Korschens, M. (1998). Agroecosystem - Long-term agroecosystem experiments: Assessing agricultural sustainability and global change. *Science, 282*, 893-896.

Redo, D.J., & Millington, A.C. (2011). A hybrid approach to mapping land-use modification and land-cover transition from MODIS time-series data: A case study from the Bolivian seasonal tropics. *Remote Sensing of Environment, 115*, 353-372.

Reed, B.C., & Brown, J.F. (2005). Trend analysis of time-series phenology derived from satellite data. *Analysis of Multi-Temporal Remote Sensing Images, 2005 International Workshop on the*, 16-18 May 2005, (pp. 166-168).

Reid, R.S., Tomich, T.P., Xu, J.C., Geist, H.J., Mather, A., DeFries, R.S., Liu, J.G., Alves, D., Agbola, B., Lambin, E.F., Chabbra, A., Veldkamp, T.A., Kok, K., Noordwijk, M., Thomas, D., Palm, C.A., & Verburg, P.H. (2006). Linking land-change science and policy: Current lessons and future integration. In Lambin, E.F. & Geist, H.J. (Eds.), *Land-use and land-cover change* (pp. 157-171). Springer Berlin Heidelberg.

Renwick, A., Jansson, T., Verburg, P.H., Revoredo-Giha, C., Britz, W., Gocht, A., & McCracken, D. (2013). Policy reform and agricultural land abandonment in the EU. *Land Use Policy, 30*, 446-457.

Reynolds, J.F., & Stafford Smith, D.M. (2002). *Global desertification: Do humans cause deserts?* , Dahlem Workshop Report 88. Berlin:

Richardson, S.D. (1990). *Forests and forestry in China : changing patterns of resource development*. Washington, D.C.: Island Press.

Roy, D.P., Ju, J.C., Kline, K., Scaramuzza, P.L., Kovalskyy, V., Hansen, M., Loveland, T.R., Vermote, E., & Zhang, C.S. (2010). Web-enabled Landsat Data (WELD): Landsat ETM plus composited mosaics of the conterminous United States. *Remote Sensing of Environment, 114*, 35-49.

Ruddiman, W.F. (2003). The anthropogenic greenhouse era began thousands of years ago. *Climatic Change, 61*, 261-293.

Sala, O.E., Chapin, F.S., Armesto, J.J., Berlow, E., Bloomfield, J., Dirzo, R., Huber-Sanwald, E., Huenneke, L.F., Jackson, R.B., Kinzig, A., Leemans, R., Lodge, D.M., Mooney, H.A., Oesterheld, M., Poff, N.L., Sykes, M.T., Walker, B.H., Walker, M., & Wall, D.H. (2000). Biodiversity - Global biodiversity scenarios for the year 2100. *Science, 287*, 1770-1774.

Samanta, A., Costa, M.H., Nunes, E.L., Vieira, S.A., Xu, L., & Myneni, R.B. (2011). Comment on "Drought-induced reduction in global terrestrial net primary production from 2000 through 2009". *Science, 333*.

Schwartz, M.D. (Ed.) (2003). *Phenology: An integrative environmental science - Introduction*. PO Box 17/3300 AA Dordrecht/Netherlands: Kluwer Academic Publ.

Sen, P.K. (1968). Estimates of regression coefficient based on Kendall's tau. *Journal of the American Statistical Association, 63*, 1379-1389.

SFA (2000-2013). *China Forestry Statistics Yearbook*. Beijing:

SFA (2008). Technical regulation of classifying ecological forest and economic forest in project of conversion of cropland to forest. In

SFA (2013). 2012 Annual Report of National Forestry In (p. 4)

Shi, Z.H., Li, L., Yin, W., Ai, L., Fang, N.F., & Song, Y.T. (2011). Use of multi-temporal Landsat images for analyzing forest transition in relation to socioeconomic factors and the environment. *International Journal of Applied Earth Observation and Geoinformation, 13*, 468-476.

Sieber, A., Kuemmerle, T., Prishchepov, A.V., Wendland, K.J., Baumann, M., Radeloff, V.C., Baskin, L.M., & Hostert, P. (2013). Landsat-based mapping of post-Soviet land-use change to assess the effectiveness of the Oksky and Mordovsky protected areas in European Russia. *Remote Sensing of Environment, 133*, 38-51.

Singh, A. (1989). Digital change detection techniques using remotely-sensed data. *International Journal of Remote Sensing, 10*, 989-1003.

Sneath, D. (1998). State policy and pasture degradation in inner Asia. *Science, 281*, 1147-1148.

Sobrino, J.A., Julien, Y., Atitar, M., & Nerry, F. (2008). NOAA-AVHRR orbital drift correction from solar zenithal angle data *IEEE Geoscience and Remote Sensing, 46*, 4014-4019.

Song, C.H., Zhang, Y.L., Mei, Y., Liu, H., Zhang, Z.Q., Zhang, Q.F., Zha, T.G., Zhang, K.R., Huang, C.L., Xu, X.N., Jagger, P., Chen, X.D., & Bilsborrow, R. (2014). Sustainability of forests created by China's Sloping Land Conversion Program: A comparison among three sites in Anhui, Hubei and Shanxi. *Forest Policy and Economics, 38*, 161-167.

Song, J. (1985). Reforms and Open Policy in China. *Science, 229*, 525-527.

Song, N.P., & Zhang, F.R. (2006). Re-evaluation of the "Food for the program" policy and its impact on environment. *Economic Geography, 26*, 628-631 In Chinese.

Song, W., & Pijanowski, B.C. (2014). The effects of China's cultivated land balance program on potential land productivity at a national scale. *Applied Geography, 46*, 158-170.

Song, Y., Ma, M.G., & Veroustraete, F. (2010). Comparison and conversion of AVHRR GIMMS and SPOT VEGETATION NDVI data in China. *International Journal of Remote Sensing, 31*, 2377-2392.

Sorgog, K., Saito, M., Hironaka, K., Higashiura, Y., & Matsuda, H. (2013). Influence of agricultural activities on grassland arthropods in Inner Mongolia. *Environment and Natural Resources Research, 3*, 33-41.

SPOT Vegetation user's guide (2012). In. http://www.spot-vegetation.com/userguide/userguide.htm (assessed June 2011)

Stahls, M.H., Mayer, A.L., Tikka, P.M., & Kauppi, P.E. (2010). Disparate Geography of Consumption, Production, and Environmental Impacts. *Journal of Industrial Ecology, 14*, 576-585.

Steffen, W.L. (2005). *Global change and the Earth system: A planet under pressure*. Berlin Heidelberg and New York: Springer.

Steffen, W.L., Walker, B.H., Ingram, J.S.I., & Koch, G.W. (1992). *Global change and terrestrial ecosystems: The operational plan*. The International Geosphere-Biosphere Programme, Report no. 21, Stockholm:

Stellmes, M., Roder, A., Udelhoven, T., & Hill, J. (2013). Mapping syndromes of land change in Spain with remote sensing time series, demographic and climatic data. *Land Use Policy, 30*, 685-702.

Stellmes, M., Udelhoven, T., Roder, A., Sonnenschein, R., & Hill, J. (2010). Dryland observation at local and regional scale - Comparison of Landsat TM/ETM plus and NOAA AVHRR time series. *Remote Sensing of Environment, 114*, 2111-2125.

Steven, M.D., Malthus, T.J., Baret, F., Xu, H., & Chopping, M.J. (2003). Intercalibration of vegetation indices from different sensor systems. *Remote Sensing of Environment, 88*, 412-422.

Su, Y.X., Peng, D.L., Xie, C., & Huang, D. (2011). Achievements and trends of Grain for Green Program in Northwest China - Analysis based on surveying 793 rural households in 5 provinces in Northwest China and Inner Mongolia Autonomous Region. *Bulletin of Soil and Water Conservation, 31*, 56-61 In Chinese.

Su, Y.Z., Li, Y.L., Cui, H.Y., & Zhao, W.Z. (2005). Influences of continuous grazing and livestock exclusion on soil properties in a degraded sandy grassland, Inner Mongolia, northern China. *Catena, 59*, 267-278.

Sulla-Menashe, D., Kennedy, R., Yang, Z., Braaten, J., Krankina, O., & Friedl, M. (2014). Detecting forest disturbance in the Pacific Northwest from MODIS time series using temporal segmentation. *Remote Sensing of Environment*, http://dx.doi.org/10.1016/j.rse.2013.1007.1042.

Swinnen, E., & Veroustraete, F. (2008). Extending the SPOT-VEGETATION NDVI time series (1998-2006) back in time with NOAA-AVHRR data (1985-1998) for southern Africa. *IEEE Transactions on Geoscience and Remote Sensing, 46*, 558-572.

Symeonakis, E., & Drake, N. (2004). Monitoring desertification and land degradation over sub-Saharan Africa. *International Journal of Remote Sensing, 25*, 573-592.

Tan, B., Woodcock, C.E., Hu, J., Zhang, P., Ozdogan, M., Huang, D., Yang, W., Knyazikhin, Y., & Myneni, R.B. (2006). The impact of gridding artifacts on the local spatial properties of MODIS data: Implications for validation, compositing, and band-to-band registration across resolutions. *Remote Sensing of Environment, 105*, 98-114.

Tan, K., Piao, S.L., Peng, C.H., & Fang, J.Y. (2007). Satellite-based estimation of biomass carbon stocks for northeast China's forests between 1982 and 1999. *Forest Ecology and Management, 240*, 114-121.

Tang, J.M., Bu, K., Yang, J.C., Zhang, S.W., & Chang, L.P. (2012). Multitemporal analysis of forest fragmentation in the upstream region of the Nenjiang River Basin, Northeast China. *Ecological Indicators, 23*, 597-607.

Tao, F.L., Yokozawa, M., Zhang, Z., Xu, Y.L., & Hayashi, Y. (2005). Remote sensing of crop production in China by production efficiency models: models comparisons, estimates and uncertainties. *Ecological Modelling, 183*, 385-396.

Tao, J., Zhang, Y.J., Yuan, X.Y., Wang, J.S., & Zhang, X.Z. (2013). Analysis of forest fires in Northeast China from 2003 to 2011. *International Journal of Remote Sensing, 34*, 8235-8251.

Tao, R., Xu, Z.G., & Xu, J.T. (2004). Grain for Green, food production and sustainable development. *Social Science in China, 6*, 25-38 In Chinese.

Tardin, A.T., dos Santos, A.P., Lee, D.C., Maia, F.C.S., Mendoncza, F.J., Assunczio, G.V., Rodrigues, J.E., de Moura Abdon, M., Novacs, R.A., Chen, S.C., Duarte, V., & Shimabukuro, Y.E. (1979). *Levantamento de areas do desmatamento na Amazonia Lefal atraves de imagens do satellite Landsat. Report 411-NTE/142*. San Jose dos Campos, Brazil: Instituto Nacional de Pesquisas Espaciais.

Tardin, A.T., Lee, D.C.L., Santos, R.J.R., Ossis, O.R., Barbosa, M.P.S., Moreira, M.L., Pereira, M.T., Silva, D., & Santos Filho, C.P. (1980). *Subprojecto desmatamento: Convenio IBDF/CNP-INPE,*. Sao Jose dos Campos, Brazil: Instituto de Pesquisas Espaciais.

Tarnavsky, E., Garrigues, S., & Brown, M.E. (2008). Multiscale geostatistical analysis of AVHRR, SPOT-VGT, and MODIS global NDVI products. *Remote Sensing of Environment, 112*, 535-549.

Thornthwaite, C.W., & Mather, J.R. (1955). *The water balance*. Centerton, N.J.,.

Thwaites, R., De Lacy, T., Hong, L.Y., & Hua, L.X. (1998). Property rights, social change, and grassland degradation in Xilingol Biosphere Reserve, Inner Mongolia, China. *Society & Natural Resources, 11*, 319-338.

Tian, Y., Wu, J.G., Kou, X.J., Li, Z.W., Wang, T.M., Mou, P., & Ge, J.P. (2009). Spatiotemporal pattern and major causes of the Amur tiger population dynamics *Biodiversity Science, 17*, 211-225 In Chinese.

Tilman, D., & Lehman, C. (2001). Human-caused environmental change: Impacts on plant diversity and evolution. *Proceedings of the National Academy of Sciences of the United States of America, 98*, 5433-5440.

Tong, C., Wu, J., Yong, S., Yang, J., & Yong, W. (2004). A landscape-scale assessment of steppe degradation in the Xilin River Basin, Inner Mongolia, China. *Journal of Arid Environments, 59*, 133-149.

Townshend, J., Justice, C., Li, W., Gurney, C., & McManus, J. (1991). Global land cover classification by remote sensing: present capabilities and future possibilities. *Remote Sensing of Environment, 35*, 243-255.

Townshend, J.R.G. (1994). Global data sets for land applications from the advanced very high-resolution radiometer - an introduction. *International Journal of Remote Sensing, 15*, 3319-3332.

Tucker, C.J. (1979). Red and photographic infrared linear combinations for monitoring vegetation. *Remote Sensing of Environment, 8*, 127-150.

Tucker, C.J., Dregne, H.E., & Newcomb, W.W. (1991). Expansion and Contraction of the Sahara Desert from 1980 to 1990. *Science, 253*, 299-301.

Tucker, C.J., Pinzon, J.E., Brown, M.E., Slayback, D.A., Pak, E.W., Mahoney, R., Vermote, E.F., & El Saleous, N. (2005). An extended AVHRR 8-km NDVI dataset compatible with MODIS and SPOT vegetation NDVI data. *International Journal of Remote Sensing, 26*, 4485-4498.

Tucker, C.J., Townshend, J.R.G., & Goff, T.E. (1985). African land-cover classification using satellite data. *Science, 227*, 369-375.

Turner, B.L., Lambin, E.F., & Reenberg, A. (2007). The emergence of land change science for global environmental change and sustainability. *Proceedings of the National Academy of Sciences, 104*, 20666-20671.

Turner, B.L., Lambin, E.F., & Reenberg, A. (2008). Land Change Science Special Feature: The emergence of land change science for global environmental change and sustainability (vol 104, pg 20666, 2007). *Proceedings of the National Academy of Sciences of the United States of America, 105*, 2751-2751.

Turner, B.L., Meyer, W.B., & Skole, D.L. (1994). Global land-use land-cover change - towards an integrated study. *Ambio, 23*, 91-95.

Uchida, E., Xu, J.T., & Rozelle, S. (2005). Grain for green: Cost-effectiveness and sustainability of China's conservation set-aside program. *Land Economics, 81*, 247-264.

Udelhoven, T. (2011). TimeStats: A Software Tool for the Retrieval of Temporal Patterns From Global Satellite Archives. *IEEE Journal of Selected Topics in Applied Earth Observations and Remote Sensing, 4*, 310-317.

Udelhoven, T., Stellmes, M., Del Barrio, G., & Hill, J. (2009). Assessment of rainfall and NDVI anomalies in Spain (1989-1999) using distributed lag models. *International Journal of Remote Sensing, 30*, 1961-1976.

UN (1996). *Land administration guideline. With special reference to countries in transition*. Geneva.

UN (2013). *World Population Prospects: The 2012 Revision. Volume II: Demographic Profiles* New York:

US Census Bureau (2014). Historical estimates of world population. In (p. https://www.census.gov/population/international/data/worldpop/table_history.php (accessed in 05 May 2014))

Van Den Hoek, J., Ozdogan, M., Burnicki, A., & Zhu, A.X. (2014). Evaluating forest policy implementation effectiveness with a cross-scale remote sensing analysis in a priority conservation area of Southwest China. *Applied Geography, 47*, 177-189.

van Leeuwen, W.J.D., Huete, A.R., & Laing, T.W. (1999). MODIS vegetation index compositing approach: A prototype with AVHRR data. *Remote Sensing of Environment, 69*, 264-280.

van Leeuwen, W.J.D., Orr, B.J., Marsh, S.E., & Herrmann, S.M. (2006). Multi-sensor NDVI data continuity: Uncertainties and implications for vegetation monitoring applications. *Remote Sensing of Environment, 100*, 67-81.

Verbesselt, J., Hyndman, R., Newnham, G., & Culvenor, D. (2010a). Detecting trend and seasonal changes in satellite image time series. *Remote Sensing of Environment, 114*, 106-115.

Verbesselt, J., Hyndman, R., Zeileis, A., & Culvenor, D. (2010b). Phenological change detection while accounting for abrupt and gradual trends in satellite image time series. *Remote Sensing of Environment, 114*, 2970-2980.

Vermote, E.F., El Saleous, N.Z., & Justice, C.O. (2002). Atmospheric correction of MODIS data in the visible to middle infrared: first results. *Remote Sensing of Environment, 83*, 97-111.

Vitousek, P.M., Mooney, H.A., Lubchenco, J., & Melillo, J.M. (1997). Human domination of Earth's ecosystems. *Science, 277*, 494-499.

Vogelmann, J.E., Xian, G., Homer, C., & Tolk, B. (2012). Monitoring gradual ecosystem change using Landsat time series analyses: Case studies in selected forest and rangeland ecosystems. *Remote Sensing of Environment, 122*, 92-105.

Vörösmarty, C., Lettenmaier, D., Leveque, C., Meybeck, M., Pahl-Wostl, C., Alcamo, J., Cosgrove, W., Grassl, H., Hoff, H., Kabat, P., Lansigan, F., Lawford, R., & Naiman, R. (2004). Humans transforming the global water system. *Eos, Transactions American Geophysical Union, 85*, 509-514.

Wang, F., Pan, X.B., Wang, D.F., Shen, C.Y., & Lu, Q. (2013). Combating desertification in China: Past, present and future. *Land Use Policy, 31*, 311-313.

Wang, G., Han, L., & Zhang, Y. (2012a). Temporal variation and spatial distribution of NDVI in northeastern China. *Journal of Beijing Forestry University, 34*, 86-91 In Chinese.

Wang, G.Y., Innes, J.L., Lei, J.F., Dai, S.Y., & Wu, S.W. (2007a). China's forestry reforms. *Science, 318*, 1556-1557.

Wang, J. (2009). Study on adjustment and mechanism of the industrial structure of agriculture in Inner Mongolia Hohhoy: Inner Mongolia Agricultural University. In Chinese.

Wang, J., Chen, Y.Q., Shao, X.M., Zhang, Y.Y., & Cao, Y.G. (2012b). Land-use changes and policy dimension driving forces in China: Present, trend and future. *Land Use Policy, 29*, 737-749.

Wang, J., Xia, X.G., Wang, P.C., & Christopher, S.A. (2004a). Diurnal variability of dust aerosol optical thickness and Angstrom exponent over dust source regions in China. *Geophysical Research Letters, 31*.

Wang, L.Z. (2005). The change analysis of the forest resource in Daxinganling. *Forest By-Product and Speciality in China, 3*, 61-62 In Chinese.

Wang, Q.S., Feng, Z.W., & Luo, J.C. (2000). Biodiversity of a forest-steppe ecotone in Northern Hebei Province and Eastern Inner Mongolia. *Acta Phytoecologica Sinica, 24*, 141-146 In Chinese.

Wang, S., van Kooten, G.C., & Wilson, B. (2004b). Mosaic of reform: forest policy in post-1978 China. *Forest Policy and Economics, 6*, 71-83.

Wang, S.H., Zhao, Y.W., Yin, X.A., Yu, L., & Xu, F. (2010a). Land use and landscape pattern changes in Nenjiang River basin during 1988-2002. *Frontiers of Earth Science, 4*, 33-41.

Wang, W., Maruyama, N., Liu, B.W., Morimoto, H., & Gao, Z.X. (2002). Relationships between bird communities and vegetation structure in Honghua'erji, northern inner Mongolia. *Journal of Forestry Research, 13*, 294-298.

Wang, X.H., Lu, C.H., Fang, J.F., & Shen, Y.C. (2007b). Implications for development of grain-for-green policy based on cropland suitability evaluation in desertification-affected north China. *Land Use Policy, 24*, 417-424.

Wang, X.M., Sheng, H.L., Bi, J.H., & Li, M. (1997). Recent history and status of the mongolian gazelle in Inner Mongolia, China. *Oryx, 31*, 120-126.

Wang, X.M., Zhang, C.X., Hasi, E., & Dong, Z.B. (2010b). Has the Three Norths Forest Shelterbelt Program solved the desertification and dust storm problems in arid and semiarid China? *Journal of Arid Environments, 74*, 13-22.

Wang, Y. (2013). The study on the reform of forest management and forest resources system in China key state owned forest region. Beijing: Beijing Forestry University.

Wang, Y.C. (2006). Research on Inner Mongolia Forest Industry Co., Ltd. corporate governance issues. Hohhot: Inner Mongolia University.

Wang, Z.G., & Shen, P. (2008). Reform and development of Inner Mongolia Forest Industry Group. *Journal of Inner Mongolia Forestry, 5*, 18-23. In Chinese.

WCED (1987). *Our common future*. Oxford ; New York: Oxford University Press.

Wessels, K.J., Prince, S.D., Malherbe, J., Small, J., Frost, P.E., & VanZyl, D. (2007). Can human-induced land degradation be distinguished from the effects of rainfall variability? A case study in South Africa. *Journal of Arid Environments, 68*, 271-297.

Wessels, K.J., van den Bergh, F., & Scholes, R.J. (2012). Limits to detectability of land degradation by trend analysis of vegetation index data. *Remote Sensing of Environment, 125*, 10-22.

White, M.A., de Beurs, K.M., Didan, K., Inouye, D.W., Richardson, A.D., Jensen, O.P., O'Keefe, J., Zhang, G., Nemani, R.R., van Leeuwen, W.J.D., Brown, J.F., de Wit, A., Schaepman, M., Lin, X.M., Dettinger, M., Bailey, A.S., Kimball, J., Schwartz, M.D., Baldocchi, D.D., Lee, J.T., & Lauenroth, W.K. (2009). Intercomparison, interpretation, and assessment of spring phenology in North America estimated from remote sensing for 1982-2006. *Global Change Biology, 15*, 2335-2359.

Wickham, J.D., Stehman, S.V., Gass, L., Dewitz, J., Fry, J.A., & Wade, T.G. (2013). Accuracy assessment of NLCD 2006 land cover and impervious surface. *Remote Sensing of Environment, 130*, 294-304.

Woodwell, G.M., Hobbie, J.E., Houghton, R.A., Melillo, J.M., Moore, B., Peterson, B.J., & Shaver, G.R. (1983). Global deforestation - Contribution to atmospheric Carbon-dioxide. *Science, 222*, 1081-1086.

Wu, B., & Ci, L.J. (2002). Landscape change and desertification development in the Mu Us Sandland, northern China. *Journal of Arid Environments, 50*, 429-444.

Xia, B.C., & Hu, J.M. (2004). Analysis of land-use change in Taoerhe catchment during last 15 years. *Journal of Soil Water Conservation, 11*, 5-8. In Chinese.

Xiao, L. (2012). China's farm produce trade deficit: general pattern, factors and solutions. Changsha: Hunan Agricultural University.

Xin, J., Yu, Z., van Leeuwen, L., & Driessen, P.M. (2002). Mapping crop key phenological stages in the North China Plain using NOAA time series images. *International Journal of Applied Earth Observation and Geoinformation, 4*, 109-117.

Xu, J.T., Yin, R.S., Li, Z., & Liu, C. (2006a). China's ecological rehabilitation: Unprecedented efforts, dramatic impacts, and requisite policies. *Ecological Economics, 57*, 595-607.

Xu, J.X. (2006). Sand-dust storms in and around the Ordos Plateau of China as influenced by land use change and desertification. *Catena, 65*, 279-284.

Xu, Z.G., Xu, J.T., Deng, X.Z., Huang, J.K., Uchida, E., & Rozelle, S. (2006b). Grain for green versus grain: Conflict between food security and conservation set-aside in China. *World Development, 34*, 130-148.

Yan, H.M., Liu, J.Y., Huang, H.Q., Dong, J.W., Xu, X.L., & Wang, J.B. (2012). Impacts of cropland transformation on agricultural production under urbanization and Grain for Green Project in China. *Acta Geographica Sinica, 67*, 579-588. In Chinese.

Yan, L.Z., & Yan, Q.W. (2004). Discussion on concept and proportion of economic forest and ecologic forest in returning cultivated land to forest. *Research of Soil and Water Conservation, 11*, 50-53. In Chinese.

Yan, Y. (2010). The investigation and rational speculation about implementation of the policy of returning farmland to forest in Chifeng. Dalian: Dalian University of Technology.

Yang, G.M., & Min, Q.W. (2006). Pressures of urbanization on ecology and environment in Inner Mongolia. *Arid land geography, 30*, 141-148. In Chinese.

Yang, S., Wen, Y.J., & Liu, H.Y. (2006). Ecological effects of mandatory conversion of marginal farmland to forestland and grassland in Central Inner Mongolia. *Research of Soil and Water Conservation, 13*, 143-149. In Chinese.

Yang, X.H., Jia, Z.Q., & Ci, L.J. (2010). Assessing effects of afforestation projects in China. *Nature, 466*, 315-315.

Yao, S.B., Guo, Y.J., & Huo, X.X. (2010). An empirical analysis of the effects of China's Land Conversion Program on farmers' income growth and labor transfer. *Environmental Management, 45*, 502-512.

Ye, Y., & Fang, X.Q. (2014). Land Reclamation in the Farming–Grazing Transitional Zone of Northeast China: 1644–1930. *The Professional Geographer*, 1-9.

Yin, H., Li, Z.G., Wang, Y.L., & Cai, F. (2011). Assessment of desertification using time series analysis of hyper-temporal vegetation indicator in Inner Mongolia. *Acta Geographica Sinica, 66*, 653-661. In Chinese.

Yin, H., Pflugmacher, D., Kennedy, E.K., Sulla-Menashe, D., & Hostert, P. (under review). Mapping annual land cover changes using MODIS time series. *IEEE Journal of Selected Topics in Applied Earth Observation and Remote Sensing*.

Yin, H., Udelhoven, T., Fensholt, R., Pflugmacher, D., & Hostert, P. (2012). How Normalized Difference Vegetation Index (NDVI) trends from Advanced Very High Resolution Radiometer (AVHRR) and Système Probatoire d'Observation de la Terre VEGETATION (SPOT VGT) time series differ in agricultural areas: An Inner Mongolian case study. *Remote Sensing, 4*, 3364-3389.

Yu, F.F., Price, K.P., Ellis, J., & Shi, P.J. (2003). Response of seasonal vegetation development to climatic variations in eastern central Asia. *Remote Sensing of Environment, 87*, 42-54.

Yu, H.Y., Luedeling, E., & Xu, J.C. (2010). Winter and spring warming result in delayed spring phenology on the Tibetan Plateau. *Proceedings of the National Academy of Sciences of the United States of America, 107*, 22151-22156.

Yu, M., Ellis, J.E., & Epstein, H.E. (2004). Regional analysis of climate, primary production, and livestock density in inner Mongolia. *Journal of Environmental Quality, 33*, 1675-1681.

Yu, W.Y., Zhou, G.S., Zhao, X.L., Xie, Y.B., & Jia, Q.Y. (2009). Characteristics of forest fire and its controls in Daxing'anling Mountains, Heilongjiang province. *Journal of Meteorology and Environment, 25*, 1-5. In Chinese.

Yu, Z., Wang, J.X., Liu, S.R., Sun, P.S., & Liu, W.G. (2013). Inconsistent NDVI trends from AVHRR, MODIS, and SPOT sensors in the Tibetan Plateau. In, *The Second International Conference on Agro-Geoinformatics* (pp. 97-101). Fairfax, VA USA

Zalasiewicz, J., Williams, M., Haywood, A., & Ellis, M. (2011). The Anthropocene: a new epoch of geological time? INTRODUCTION. *Philosophical Transactions of the Royal Society a-Mathematical Physical and Engineering Sciences, 369*, 835-841.

Zhan, J.Y., Deng, X.Z., Yue, T.X., Bao, Y.H., Zhao, T., & Ma, S.N. (2004). Land use change and its environmental effects in the farming-pasturing interlocked areas of Inner Mongolia. *Resources Science, 26*, 80-88. In Chinese.

Zhang, B.P., Zhang, X.Q., Yao, Y., H., & Han, F. (2009). Desertification and strategic policies in the Alxa region of Inner Mongolia. *Arid Zone Research, 26*, 453-459. In Chinese.

Zhang, D.P. (2011a). Analysis on the Current Status and the Changes of Land Use in Hulunbuir, Inner Mongolia. *China Land Science, 25*, 43-48 In Chinese.

Zhang, F., Wang, Q., Wang, W.J., Shen, W.M., Luo, H.J., & Liu, X.M. (2006). Analyzing land use change in ecotone between forest and grass in Inner Mongolia. *Resources Science, 28*, 52-58. In Chinese.

Zhang, G.L., Dong, J.W., Xiao, X.M., Hu, Z.M., & Sheldon, S. (2012). Effectiveness of ecological restoration projects in Horqin Sandy Land, China based on SPOT-VGT NDVI data. *Ecological Engineering, 38*, 20-29.

Zhang, G.Z., Gai, Z.Y., & Gao, W. (2008). Inspiration of Ulanhu's "Protecting grassland and prohibiting land reclamation". *Inner Mongolia Prataculture, 20*, 5-10. In Chinese.

Zhang, M.H., Liu, Q.X., Piao, R.Z., & Jiang, G.S. (2007a). The wolverine Gulo gulo population and its distribution in the Great Khingan Mountains, northeastern China. *Wildlife Biology, 13*, 83-88.

Zhang, P.C., Shao, G.F., Zhao, G., Le Master, D.C., Parker, G.R., Dunning, J.B., & Li, Q.L. (2000). China's forest policy for the 21st century. *Science, 288*, 2135-2136.

Zhang, W.L., Chen, S.P., Chen, J., Wei, L., Han, X.G., & Lin, G.H. (2007b). Biophysical regulations of carbon fluxes of a steppe and a cultivated cropland in semiarid Inner Mongolia. *Agricultural and Forest Meteorology, 146*, 216-229.

Zhang, X.Y., Friedl, M.A., Schaaf, C.B., Strahler, A.H., Hodges, J.C.F., Gao, F., Reed, B.C., & Huete, A. (2003). Monitoring vegetation phenology using MODIS. *Remote Sensing of Environment, 84*, 471-475.

Zhang, Y.X., & Song, C.H. (2006). Impacts of afforestation, deforestation, and reforestation on forest cover in China from 1949 to 2003. *Journal of Forestry, 104*, 383-387.

Zhang, Y.Y. (2011b). Study on vegetation succession in converting the land for forestry in Inner Mongolia Ordos. Beijing: Beijing Forestry University.

Zhao, H.L., Zhao, X.Y., Zhou, R.L., Zhang, T.H., & Drake, S. (2005). Desertification processes due to heavy grazing in sandy rangeland, Inner Mongolia. *Journal of Arid Environments, 62*, 309-319.

Zhao, M., Han, G., & Mei, H. (2006). Grassland resource and its situation in Inner Mongolia, China. *Bulletin of the Faculty of Agriculture at Niigata University, 58*, 129-132.

Zhou, D.C., Zhao, S.Q., & Zhu, C. (2011). Impacts of the Sloping Land Conversion Program on the land use/cover change in the Loess Plateau: A case study in Ansai county of Shaanxi Province, China. *Journal of Natural Resources, 26*, 1866-1878. In Chinese.

Zhou, D.C., Zhao, S.Q., & Zhu, C. (2012). The Grain for Green Project induced land cover change in the Loess Plateau: A case study with Ansai County, Shanxi Province, China. *Ecological Indicators, 23*, 88-94.

Zhou, Z., Sun, O.J., Huang, J., Gao, Y., & Han, X. (2006). Land use affects the relationship between species diversity and productivity at the local scale in a semi-arid steppe ecosystem. *Functional Ecology, 20*, 753-762.

Zhu, H.G. (2008). Forecast of timber supply and demand in the Northeast and Inner Mongolia region. *Forest Engineering, 24*, 84-91. In Chinese.

Zhu, Z.H., Yin, X.R., Zang, H.B., Liu, H.M., Dong, J.L., Liu, Q.Q., Li, J.R., & Ruan, X.P. (2008). Dynamic monitoring on forestry resources in Etuoke Qianqi based on the interpretation of TM image. *Journal of Inner Mongolia Forestry Science & Technology, 34*, 45-48. In Chinese.

Publikationen

PEER-REVIEWED ARTICLES

Yin, H., Pflugmacher, D., Li, A., Li, Z.G., Hostert, P., Land use and land cover change in Inner Mongolia - understanding the effects of China's re-vegetation programs *(in preparation).*

Wang, R., Zhang, Y.Z., Wünnemann, B., Yin, H., Xia, F., Zhou, L.F., Diekmann, B., Grain size distribution patterns in core H7 from Hala Lake, Tibetan Plateau, China: Evidence of climate signatures during the last 24 ka. *Palaeogeography, Palaeoclimatology, Palaeoecology (under review).*

Yin, H., Pflugmacher, D., Kennedy, R.E., Sulla-Menashe, D. Hostert, P., Mapping annual land cover changes using MODIS time series. *IEEE Journal of Selected Topics in Applied Earth Observations and Remote Sensing (in revision)*.

Li, Z.G., Yang, P., Tang, H.J., Wu, W.B., Yin, H., Liu, Z.H., Zhang, Li. (2014): Response of maize phenology to climate warming in Northeast China between 1990 and 2012. *Regional Environmental Change*. 14, 39-48.

Liu, X.Q., Wang, Y.L., Peng, J., Ademola, K.B., Yin, H. (2013): Assessing vulnerability to drought based on exposure, sensitivity and adaptive capacity: A case study in middle Inner Mongolia of China. *Chinese Geographical Science*, 1, 13-25.

Yin, H., Udelhoven, T., Fensholt, R., Pflugmacher, D., Hostert, P. (2012): How Normalized Difference Vegetation Index (NDVI) trends from Advanced Very High Resolution Radiometer (AVHRR) and Système Probatoire d'Observation de la Terre VEGETATION (SPOT VGT) time series differ in agricultural areas: An Inner Mongolian case study. *Remote Sensing*, 4, 3364-3389.

Yin, H., Li, Z.G., Wang, Y.L., Cai, F. (2011): Assessment of desertification using time series analysis of hyper-temporal vegetation indicator in Inner Mongolia. *Acta Geographica Sinica*, 66, 653-661 (in Chinese).

Li, Z.G., Tang, H.J., Yang, P., Zhou, QB., Wang, Y.L., Wu, W.B., Yin. H., Zhang, L. (2011): Identification and application of seasonality parameters of crop growing season in Northeast China based on NDVI time series data. *Acta Scientiarum Naturalium Universitatis Pekinensis*, 47, 882-892 (in Chinese).

Yin, H., Li, Z.G., Wang, Y.L. (2011): A review on the research progress of desertification

assessment. *Chinese Journal of Plant Ecology*, 35, 345–352 (in Chinese).

Cai, J.L., Yin. H., Huang, Yi. (2010): Ecological function regionalization: a review. *Acta Ecologica Sinica*, 30, 3018-3027 (in Chinese).

Yin, H., Wang, Y.L., Peng, J. (2009): Variation analysis on precipitation and temperature in middle and upper reach of Yellow River Basin during 1956 to 2006. *Research of Soil and Water Conservation*, 16, 35-39 (in Chinese).

Huang, Y., Cai, J.L., Yin, H., Cai, M.T. (2009): Correlation of precipitation to temperature variation in the Huanghe River (Yellow River) basin during 1957-2006. *Journal of Hydrology*, 372, 1-8.

Peng, J., Wu, J.S., Yin, H., Li, Z.G., Chang, Q., Mu, T.L. (2008): Rural land use change during 1986-2002 and its ecological effects in Lijiang, China, based on remote sensing and GIS. *Sensors*, 8, 8201-8223.

CONFERENCE PRESENTATIONS

Yin, H., Pflugmacher, D. Li, Z.G., and Hostert, P. (2014): Land use and land cover change in Inner Mongolia – understanding the effects of China's re-vegetation programs. *2nd Global Land Project Open Science Meeting*. March 2014, Berlin, Germany. Oral presentation.

Li, Z.G., Yin, H., Yang, P., Tang, H.J., Wu, W.B., Chen, Z.X., Liu, Z.H., Tan, J.Y., and Zhang, L. (2014): Response of maize cropping system to climate warming in Northeast China in the past 30 years. *2nd Global Land Project Open Science Meeting*. March 2014, Berlin, Germany. Oral presentation.

Yin, H., Pflugmacher, D., and Hostert, P. (2014): Mapping annual land cover changes using MODIS time series. *Joint workshop of the EARSeL 5th Land Use & Land Cover Workshop and NASA LCLUC Science Team*. March 2014, Berlin, Germany. Poster presentation.

Yin, H., Pflugmacher, D. Li, Z.G., and Hostert, P. (2013): Assessing land degradation in Inner Mongolia using MODIS time series. *7th International Workshop on the Analysis of Multi-temporal Remote Sensing Images*. June 2013, Banff, Canada. Oral presentation.

Yin, H., Wang, Y.L., and Chang Q. (2007): A study on multi-scale effect of urban landscape pattern based on wavelet transform in Shenzhen. *The Xth China Landscape Ecology Congress*. September 2007, Beijing, China.

Eidesstattliche Erklärung

Hiermit erkläre ich, die vorliegende Dissertation selbstständig und ohne Verwendung unerlaubter Hilfe angefertigt zu haben. Die aus fremden Quellen direkt oder indirekt übernommenen Inhalte sind als solche kenntlich gemacht. Die Dissertation wird erstmalig und nur an der Humboldt-Universität zu Berlin eingereicht. Weiterhin erkläre ich, nicht bereits einen Doktortitel im Fach Geographie zu besitzen. Die dem Verfahren zu Grunde liegende Promotionsordnung ist mir bekannt.

He Yin

Berlin, den 06. Juni 2014